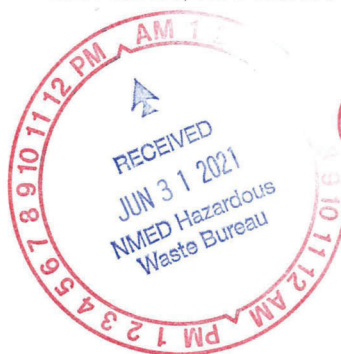




**DEPARTMENT OF ENERGY**  
 Environmental Management Los Alamos Field Office (EM-LA)  
 Los Alamos, New Mexico 87544

EMLA-2021-BF125-02-001

Mr. Ricardo Maestas  
 Acting Bureau Chief  
 Hazardous Waste Bureau  
 New Mexico Environment Department  
 2905 Rodeo Park Drive East, Building 1  
 Santa Fe, NM 87505-6313



*June 30th CN*  
 JUN 30 2021

Subject: Submittal of the Assessment Report for the Evaluation of Conditions in the Regional Aquifer Around Well R-70

Dear Mr. Maestas:

Enclosed please find two hard copies with electronic files of the "Assessment Report for the Evaluation of Conditions in the Regional Aquifer Around Well R-70." This report presents the results of an assessment that was conducted to evaluate the hydrologic and geochemical conditions in the chromium monitoring well R-70 area. The driver for this assessment was the early chromium data obtained from the first round of groundwater samples collected from R-70 (screens 1 and 2). Those data, which were reproduced in subsequent sampling, revealed higher concentrations of chromium in the lower screen than in the upper screen. The objective of this assessment report is to evaluate the hydrologic and geochemical conditions in the R-70 area to determine if an additional monitoring well is necessary to ensure protection of Los Alamos County production well PM-3 and/or necessary to define the lateral and vertical extent of chromium contamination in the northeastern portion of the chromium plume and provide long-term interim measure performance monitoring. This report is being submitted to fulfill a proposed fiscal year 2021 milestone in Appendix B of the 2016 Compliance Order on Consent.

If you have any questions, please contact Danny Katzman at (505) 309-1371 (danny.katzman@em-la.doe.gov) or Cheryl Rodriguez at (505) 414-0450 (cheryl.rodriguez@em.doe.gov).

Sincerely,

**M Lee**  
**Bishop for**

Arturo Q. Duran  
 Compliance and Permitting Manager  
 Environmental Management  
 Los Alamos Field Office

Digitally signed by M Lee  
 Bishop for  
 Date: 2021.06.29  
 16:56:50 -06'00'

Enclosure(s):

1. Two hard copies with electronic files – Assessment Report for the Evaluation of Conditions in the Regional Aquifer Around Well R-70 (EM2021-0321)

cc (letter and enclosure[s] emailed):

Laurie King, EPA Region 6, Dallas, TX

Raymond Martinez, San Ildefonso Pueblo, NM

Dino Chavarria, Santa Clara Pueblo, NM

Chris Catechis, NMED-DOE-OB/-RPD

Steve Yanicak, NMED-DOE-OB

Jennifer Payne, LANL

Felicia Aguilar, N3B

William Alexander, N3B

Emily Day, N3B

Sherry Gaddy, N3B

Jeff Holland, N3B

Danny Katzman, N3B

Kim Lebak, N3B

Joseph Legare, N3B

Dana Lindsay, N3B

Pamela Maestas, N3B

Christian Maupin, N3B

Joseph Murdock, N3B

Troy Thomson, N3B

Steve Veenis, N3B

Peter Maggiore, NA-LA

M. Lee Bishop, EM-LA

John Evans, EM-LA

Stephen Hoffman, EM-LA

David Nickless, EM-LA

Cheryl Rodriguez, EM-LA

Hai Shen, EM-LA

[emla.docs@em.doe.gov](mailto:emla.docs@em.doe.gov)

[n3brecords@em-la.doe.gov](mailto:n3brecords@em-la.doe.gov)

Public Reading Room (EPRR)

PRS website

June 2021  
EM2021-0321

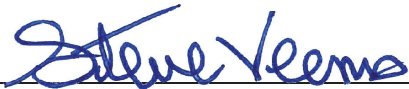
# **Assessment Report for the Evaluation of Conditions in the Regional Aquifer Around Well R-70**

Newport News Nuclear BWXT-Los Alamos, LLC (N3B), under the U.S. Department of Energy Office of Environmental Management Contract No. 89303318CEM000007 (the Los Alamos Legacy Cleanup Contract), has prepared this document pursuant to the Compliance Order on Consent, signed June 24, 2016. The Compliance Order on Consent contains requirements for the investigation and cleanup, including corrective action, of contamination at Los Alamos National Laboratory. The U.S. government has rights to use, reproduce, and distribute this document. The public may copy and use this document without charge, provided that this notice and any statement of authorship are reproduced on all copies.

# Assessment Report for the Evaluation of Conditions in the Regional Aquifer Around Well R-70

June 2021

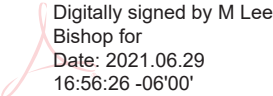
Responsible program director:

Steve Veenis		T2S Program Director	Water Program	6/22/2021
Printed Name	Signature	Title	Organization	Date

Responsible N3B representative:

Troy Thomson		Acting Program Manager	N3B Environmental Remediation Program	6/22/2021
Printed Name	Signature	Title	Organization	Date

Responsible DOE EM-LA representative:

Arturo Q. Duran	M Lee Bishop for 	Compliance and Permitting Manager	Office of Quality and Regulatory Compliance	
Printed Name	Signature	Title	Organization	Date

Digitally signed by M Lee Bishop for  
Date: 2021.06.29 16:56:26 -06'00'



## EXECUTIVE SUMMARY

This report presents the results of an assessment that was conducted to evaluate the hydrologic and geochemical conditions in the chromium monitoring well R-70 area. The driver for this assessment was the early chromium data obtained from the first round of groundwater samples collected from R-70 (screens 1 and 2). Those data, which were reproduced in subsequent sampling, revealed higher concentrations of chromium in the lower screen than in the upper screen. A series of letters originating initially from the New Mexico Environment Department (NMED) and from the U.S. Department of Energy (DOE) Environmental Management Los Alamos Field Office (EM-LA) that discuss the implications for the chromium concentrations at R-70 was exchanged, leading to an agreement of the designated agency managers that an assessment work plan would be prepared and submitted to NMED by December 17, 2019, in lieu of the direction NMED provided in the letter dated July 12, 2019. The “Assessment Work Plan for the Evaluation of Conditions in the Regional Aquifer Around Well R-70” was submitted to NMED on December 16, 2019, and subsequently approved by NMED on April 14, 2020. NMED and EM-LA also agreed to the June 30, 2021, submittal date for this report as part of the fiscal year 2021 Appendix B negotiations.

The objective of this assessment report is to evaluate the hydrologic and geochemical conditions in the R-70 area (northeastern portion of the chromium plume in Figure 1.0-1) to determine if an additional monitoring well is necessary to ensure protection of Los Alamos County production well PM-3 and/or necessary to define the lateral and vertical extent of chromium contamination in the northeastern portion of the chromium plume and provide long-term interim measure (IM) performance monitoring.

This report provides an analysis of key aspects of a conceptual model for the R-70 area, including (1) a detailed analysis of the hydrostratigraphic framework for the sedimentary deposits that compose the portion of the aquifer where the plume is located, (2) an analysis of the hydraulic characteristics of the aquifer in the R-70 area derived from intentional and opportunistic aquifer tests and corresponding responses in nearby wells, and (3) an evaluation of the geochemistry of R-70 and surrounding wells, including perspectives that incorporate data collected from wells before installation of R-70, and potential effects on the spatial variability in chromium concentrations that may relate to IM operations conducted to date. The R-70 assessment work plan indicated that numerical modeling would also be incorporated into the assessment report as one of the methods used to evaluate data gaps in the monitoring network and to predict IM performance in the northeastern portion of the plume. However, the relatively short data set and high variability in chromium concentrations in R-70 screen 1 made its model validation very challenging, with the likelihood of producing unreliable and highly uncertain results, and therefore not supportive of meeting the objective of the report. As presented to NMED in a pre-submission meeting held on April 22, 2021, numerical modeling will not be included in this report, and the conclusions and recommendations derived from the other assessment lines of inquiry will not be affected.

The high-resolution stratigraphy combined with estimated hydraulic conductivity (K) from particle-size distributions provide a detailed characterization of the hydraulic structure of the regional aquifer. Permeable beds are distributed throughout the stratigraphic sequence regardless of geologic unit, and the regional aquifer where the plume is located is effectively a single highly heterogeneous hydrogeologic unit. The high-resolution stratigraphic information is supplemented by an assessment of mass flux distributions that uses order-of-magnitude differences in hydraulic conductivity to identify flow regimes in the aquifer. Mass flux distributions suggest large portions of the aquifer are characterized by advective flow. Preferential flow paths do not appear to be associated with particular geologic units, but rather regimes of higher groundwater flow likely occur where networks of interconnected high-K beds form in heterogeneous alluvial deposits.

Utilizing the full period of record for monitoring wells in the R-70 area and coupling that data with historical data on the transient geochemistry of water from sources including the sanitary wastewater treatment facility, an assessment of source water to R-70 is explained. The geochemical data are coupled with transients in effluent discharge rates to explain the observed evolution of chromium (and other constituent) concentrations and vertical distribution in the R-70 area. The structure (orientation and dip) of prominent geosurfaces in the vadose zone is also factored into the analysis. A case is made that the vertical distribution of chromium at R-70 is not driven by vertical spreading caused by pumping at PM-3 or local downward gradients. Instead, it is likely caused by one or more of the following:

- the migration of early arrival chromium plume-front contamination mixed with clean ambient groundwater,
- mixing of young post-chromate effluent water with some fraction of ambient groundwater, and
- the origin of contamination at R-70 screen 1 being from some unknown source.

The deep contamination at R-70 possibly originates as far upgradient as the CrEX-4 area and remains at that approximate depth in the R-70 area.

R-70 screen 1 and screen 2 consistently show no apparent response to PM-3 activity. A hypothesis is that chromium-area monitoring wells are isolated from pressure responses generated by PM-3 pumping because most water production at PM-3 is generated from Miocene sedimentary deposits beneath a layer of Miocene basalt in the upper portion of the PM-3 screen, so the chromium contamination is effectively isolated from the high-production zones in PM-3. Sentinel wells R-35a and R-35b, completed above the basalt, show no increase in chromium contamination to date.

The operation of the IM system in the eastern portion of the plume demonstrates the following:

- R-70 screen 1 and screen 2 are clearly within the hydraulic zone of influence of CrEX-5, with R-70 screen 2 showing greater drawdown in response to CrEX-5 pumping than screen 1.
- Both screens at R-70 show response to CrIN-1, with screen 2 slightly more elevated than screen 1.
- The effects of the next nearest pumping and injection wells (CrIN-2; CrEX-3 and -1) on R-70 are difficult to discern from the noise in the hydraulic head data.

The impact of the R-70 screen 1 and screen 2 pumping tests were reflected in drawdowns at observed various wells at least as far away as R-44. Consistent with the observations above, that R-70 screen 2 responds with greater drawdown to IM pumping and injection, the corollary is also seen that pumping at R-70 screen 2 appears to elicit greater drawdown at wells around the site than pumping at R-70 screen 1 at approximately the same rate.

The analysis of data in the R-70 area (geochemical, stratigraphic, hydraulic) leads to the recommendation that a new well, R-73, be drilled in the vicinity of R-70. A drilling work plan is proposed for submittal with a primary objective of characterizing the vertical extent of chromium contamination in the portion of the plume near R-70. R-73 should provide important information on the extent of chromium in this portion of the plume.

The recommendation is also made at this time that well R-35c is not necessary to provide for protective monitoring of PM-3 beyond that already provided by sentinel wells R-35b and R35a. There is no evidence from existing data for hydraulic influence of PM-3 on R-70 screen 2 on the scale that would be necessary to influence groundwater migration at the depth of R-70 screen 2.

## CONTENTS

<b>1.0</b>	<b>INTRODUCTION .....</b>	<b>1</b>
<b>2.0</b>	<b>HIGH-RESOLUTION STRATIGRAPHY IN THE CHROMIUM INVESTIGATION AREA .....</b>	<b>1</b>
2.1	Lithologic Characteristics of the Upper Regional Aquifer .....	2
2.2	Estimated Hydraulic Conductivity from Particle Size Data .....	3
2.3	Partitioning of Hydraulic Conductivity into High-, Medium-, and Low-Flow Regimes .....	4
2.4	Flow Networks that Cross Stratigraphic Boundaries .....	6
<b>3.0</b>	<b>Hydrogeochemistry.....</b>	<b>6</b>
3.1	Groundwater Geochemistry at Well R-70 Screen 1 and R-70 Screen 2.....	7
3.2	Comparison of R-70 Screen 1 and Screen 2 Geochemistry with That of Nearby Wells.....	8
3.3	Conceptual Models that Describe the Vertical Chromium Distributions at Well R-70.....	9
<b>4.0</b>	<b>OBSERVATIONS OF IM PERFORMANCE AND HYDRAULIC ANALYSIS.....</b>	<b>10</b>
4.1	Hydraulic Analysis .....	10
4.1.1	Effect of PM-3 on R-70.....	11
4.1.2	Effect of IM Pumping and Injection on R-70.....	13
4.1.3	Effect of Pumping Tests at R-70 on Other Monitoring Wells .....	16
<b>5.0</b>	<b>MODELING .....</b>	<b>17</b>
<b>6.0</b>	<b>SUMMARY OF OBSERVATIONS .....</b>	<b>17</b>
<b>7.0</b>	<b>CONCLUSIONS AND RECOMMENDATIONS .....</b>	<b>18</b>
<b>8.0</b>	<b>REFERENCES AND MAP DATA SOURCES .....</b>	<b>19</b>
8.1	References .....	19
8.2	Map Data Sources.....	21

### Figures

Figure 1.0-1	Chromium plume site location and area discussed in this report .....	23
Figure 2.0-1	Geologic map at the top of the regional aquifer and geologic cross-section for the upper part of the regional aquifer in the chromium plume at Los Alamos National Laboratory.....	24
Figure 2.1-1	Clastic rock classification of Pliocene and Miocene geologic units at the top of the regional aquifer beneath Mortandad Canyon based on particle-size data for cores collected from CrCH-1, CrCH-2, CrCH-3, CrCH-4, and CrCH-5 .....	25
Figure 2.2-1	Histograms of K for four of the K estimation methods used in this study .....	26
Figure 2.2-2	Histograms comparing Ks by geologic unit for four of the K estimation methods .....	27
Figure 2.2-3	High-resolution vertical profiles of Ks in the regional aquifer at core hole CrCH-2 by various K estimation methods.....	28
Figure 2.3-1	Cumulative flow distribution plots for core holes based on Ks determined from particle-size data .....	29
Figure 2.3-2	Cumulative flow distribution plots for the Puye Formation (Tpf), pumiceous subunit of the Puye Formation [Tpf(p)], and Miocene pumiceous unit (Tjfp) .....	30
Figure 2.3-3	High-resolution stratigraphy for core hole CrCH-3 showing distribution of Q90 beds.....	31
Figure 2.4-1	Conceptual geologic block diagram showing potential groundwater flow paths in heterogeneous alluvial fan deposits.....	32

Figure 2.4-2	Geologic cross-section between wells CrEX-4 and PM-3 showing potential groundwater flow paths that cross geologic units .....	32
Figure 3.1-1	R-70 screen 1 trends in chromium and other solutes .....	33
Figure 3.1-2	R-70 screen 2 trends in chromium and other solutes .....	33
Figure 3.2-1	R-70 screen 1 Piper diagram illustrating the geochemical evolution of plume migration from the plume centroid near R-42 towards R-70 screen 2.....	34
Figure 3.2-2	R-11 trends in chromium and other constituents .....	35
Figure 3.2-3	R-45 screen 1 trends in chromium and other constituents .....	35
Figure 4.1-1	Hydrograph for R-70 screen 1 and screen 2 from installation to December 31, 2020 .....	36
Figure 4.1-2	Hydrograph for R-70 screen 2 from March 9 to 14, 2020 .....	37
Figure 4.1-3	Hydrograph for R-70 screen 2 from May 1 to 31, 2020 .....	38
Figure 4.1-4	Hydrograph for R-70 screen 2 from May 1 to 31, 2020, showing all nearby pumping .....	39
Figure 4.1-5	Hydrograph for R-70 screen 1 and screen 2 showing all nearby pumping.....	40
Figure 4.1-6	Hydrograph for R-70 screen 1 and screen 2 showing all nearby pumping from November 20 to December 16, 2020.....	41
Figure 4.1-7	Geophysical logs for well PM-3.....	42
Figure 4.1-8	West-southwest/east-northeast regional geologic cross-section.....	43
Figure 4.1-9	Hydrograph for R-70 screen 1 and screen 2 from September 26 to October 8, 2020 .....	44
Figure 4.1-10	Hydrograph for R-70 screen 1 and screen 2 from August 1 to 31, 2020.....	45
Figure 4.1-11	Hydrograph for R-70 screen 1 and screen 2 from July 10 to August 1, 2020 .....	46
Figure 4.1-12	Hydraulic head difference between R-70 screen 1 and screen 2, along with CrEX-5 and CrIN-1 pumping rates.....	47
Figure 4.1-13	Hydrograph for R-45 screen 1 and screen 2 from June 26, 2019, to March 31, 2020 .....	48
Figure 4.1-14	Chromium concentrations at R-70 screen 1 and screen 2 along with pumping rates at CrEX-5 and CrIN-1 and -2 .....	49
Figure 4.1-15	IM and PM-3 activity before and during the 24-hr R-70 pumping tests (vertical dashed lines).....	50
Figure 4.1-16	Hydrograph for CrEX-5 during the R-70 screen 1 and screen 2 pumping tests.....	51
Figure 4.1-17	Hydrographs for CrIN-1 and R-13 during the R-70 screen 1 and screen 2 pumping tests.....	51
Figure 4.1-18	Hydrographs for R-45 screen 1 and screen 2 during the R-70 screen 1 and screen 2 pumping tests.....	52
Figure 4.1-19	Hydrograph for R-35b during the R-70 screen 1 and screen 2 pumping tests .....	52
Figure 4.1-20	Hydrographs for R-11 and R-28 during the R-70 screen 1 and screen 2 pumping tests.....	53
Figure 4.1-21	Hydrograph for CrIN-2 during the R-70 screen 1 and screen 2 pumping tests .....	53
Figure 4.1-22	Hydrographs for R-44 screen 1 and screen 2 during the R-70 screen 1 and screen 2 pumping tests.....	54
Figure 4.1-23	Hydrograph for R-36 during the R-70 screen 1 and screen 2 pumping tests.....	54
Figure 4.1-24	Hydrograph for SIMR-2 during the R-70 screen 1 and screen 2 pumping tests .....	55
Figure 4.1-25	Approximate hydraulic zone of influence of pumping at R-70 S1 and S2 .....	56

**Table**

Table 2.0-1	Sieve Mesh-Sizes, Particle Size Distributions, and Particle-Size Classification for Analysis of Cores from CrCH-1 through CrCH-5 .....	57
-------------	--	----



## 1.0 INTRODUCTION

This report presents the results of an assessment that was conducted to evaluate the hydrologic and geochemical conditions in the chromium monitoring well R-70 area. Figure 1.0-1 shows the area of the chromium plume. The driver for this assessment was the early chromium data obtained from the first round of samples collected from R-70 (screens 1 and 2). Screens 1 and 2 are located approximately 30 ft and 100 ft below the water table, respectively. Those data, which were reproduced in subsequent sampling, revealed a higher concentration of chromium in the lower screen than in the upper screen. A series of letters originating initially from the New Mexico Environment Department (NMED) and from the U.S. Department of Energy (DOE) Environmental Management Los Alamos Field Office (EM-LA) that discuss the implications for the chromium concentrations at R-70 was exchanged (DOE 2019, 700531; DOE 2019, 700650; NMED 2019, 700508; NMED 2019, 700549), leading to an agreement of the designated agency managers that an assessment work plan would be prepared and submitted to NMED by December 17, 2019, in lieu of the direction NMED provided in the letter dated July 12, 2019 (NMED 2019, 700508). The "Assessment Work Plan for the Evaluation of Conditions in the Regional Aquifer Around Well R-70" was submitted to NMED on December 16, 2019, and subsequently approved by NMED on April 14, 2020 (N3B 2019, 700715; NMED 2020, 700852). NMED and EM-LA also agreed to the June 30, 2021, submittal date for this report as part of the fiscal year 2021 Appendix B negotiations.

The objective of this assessment report is to evaluate the hydrologic and geochemical conditions in the R-70 area (northeastern portion of the plume in Figure 1.0-1) to determine if an additional monitoring well is necessary to ensure protection of Los Alamos County production well PM-3 and/or necessary to define the lateral and vertical extent of chromium contamination in the northeastern portion of the chromium plume and provide long-term interim measure (IM) performance monitoring.

This report fulfills the objective through an analysis of key aspects of a conceptual model for the R-70 area, including (1) a detailed analysis of the hydrostratigraphic framework for the sedimentary deposits comprising the portion of aquifer where the plume is located, (2) an analysis of the hydraulic characteristics of the aquifer in the R-70 area derived from intentional and opportunistic aquifer tests and corresponding responses in nearby wells, and (3) an evaluation of the geochemistry of R-70 and surrounding wells, including perspectives that incorporate data collected from wells before installation of R-70, and potential effects on the spatial variability in chromium concentrations that may relate to IM operations conducted to date. The R-70 assessment work plan indicated that numerical modeling would also be incorporated into the assessment report as one of the methods used to evaluate data gaps in the monitoring network and to predict IM performance in the northeastern portion of the plume. However, the relatively short data set and high variability in chromium concentrations in R-70 screen 1 made its model validation very challenging, with the likelihood of producing unreliable and highly uncertain results, and therefore not supportive of meeting the objective of the report. As presented to NMED in a pre-submission meeting held on April 22, 2021, numerical modeling will not be included in this report, and the conclusions and recommendations derived from the other assessment lines of inquiry will not be affected.

## 2.0 HIGH-RESOLUTION STRATIGRAPHY IN THE CHROMIUM INVESTIGATION AREA

This section presents an analysis of the aquifer based on core collected during sonic drilling of core holes CrCH-1 through CrCH-5 in 2014 and 2015 to collect sediments from the regional aquifer for tests including bench-scale tests for natural attenuation (LANL 2018, 602964). Figure 2.0-1 shows the locations of the core holes. The analysis provides information on particle-size distribution and uses that information to estimate the proportional hydraulic characteristics of beds within each of the three geologic units that compose the aquifer in the chromium plume area. The section also describes the spatially

variable vertical distribution of beds within these geologic units that are likely responsible for the dominant chromium mass flux. A case is presented that the three subunits are effectively a single hydrogeologic unit. Information on the potential role of the Puye pumiceous subunit as a fast or preferential flow path in the R-70 area is also presented.

Using particle-size data from the five drill cores, hydraulic conductivity (K) is estimated on a bed-by-bed basis for the three geologic units that make up the upper regional aquifer in the vicinity of the chromium plume. These units include (1) the lower part of Pliocene Puye Formation, (2) gravels and pumice-rich sands at the base of the Puye Formation called the Puye pumiceous subunit, and (3) pumiceous sands that are informally called the Miocene pumiceous unit (Figure 2.0-1). These geologic units were deposited as alluvial fans shed from the eastern Jemez Mountains volcanic highlands into the western part of the Española basin of the Rio Grande rift. The geologic units were later structurally rotated and dip approximately 2 degrees to the southeast and south.

Core collection, lithologic characterization, sampling, and particle-size analyses by sieving are previously reported (LANL 2015, 600457; LANL 2018, 602964; Broxton et al. 2021, 701441) and are not discussed here. Discrete depositional beds within each core run were identified and sampled for particle-size distribution. A total of 371 depositional beds were sampled in the 5 core holes. Samples were dried and sieved into 7 particle-size fractions (Table 2.0-1). K estimates were calculated using HydrogeoSieveXL, an Excel-based spreadsheet program that estimates K from particle-size distribution analysis using 15 different calculation methods

([https://www.researchgate.net/publication/277632694\\_HydrogeoSieveXL\\_an\\_Excel-based\\_tool\\_to\\_estimate\\_hydraulic\\_conductivity\\_from\\_grain-size\\_analysis](https://www.researchgate.net/publication/277632694_HydrogeoSieveXL_an_Excel-based_tool_to_estimate_hydraulic_conductivity_from_grain-size_analysis)). Additional discussion of the particle-size data and estimated Ks can be found in the “Compendium of Technical Reports Conducted Under the Work Plan for Chromium Plume Center Characterization,” (LANL 2018, 602964) and “Using High-Resolution Stratigraphic Characterization to Inform Remediation Strategies for a Hexavalent Chromium Plume at Los Alamos National Laboratory,” (Broxton et al. 2021, 701441).

## 2.1 Lithologic Characteristics of the Upper Regional Aquifer

Lithologic differences among the geologic units of the regional aquifer are highlighted by clastic rock classification diagrams that reclassify the seven particle-size classes into gravels, sands, and clays/silts (Figure 2.1-1). CrCH-2 particle-size data are used to calculate the mean particle size (as arithmetic mean) and to evaluate sorting for the geologic units following the methodology of Folk (1980, 701455). Histograms of bed thickness are presented by geologic unit in Figure 2.1-1.

The Puye Formation in the chromium investigation area is an alluvial fan deposit made up of muddy sandy gravel with subordinate gravelly muddy sand. The mean particle size of these deposits is coarse to very coarse sand and sorting is very poor. On average gravel makes up 40% by weight of the deposit, and subangular to subrounded gravel clasts are 0.6 to 5 cm in diameter. Mineralogically, the gravel and lithic sand are composed of rhyodacitic and dacitic rock fragments dominated by quartzo-feldspathic minerals with subordinate smectite-clinoptilolite and iron-bearing minerals (e.g., amphibole and pyroxene), which are concentrated in the finer particle-size fractions (LANL 2018, 602964). Volcanic glass is a common constituent of the Puye matrix (10–20% by weight), but it is far less abundant than in underlying pumiceous Puye subunit and Miocene pumiceous deposits. The mean thickness of beds is 0.97 ft (Figure 2.1-1).

The Miocene pumiceous unit is a medial to distal alluvial fan deposit made up of reworked rhyolitic detritus derived from the Bearhead Rhyolite (7.1-6.5 millions of years). It is a gravelly muddy sand with subordinate muddy sand and muddy sandy gravel (Figure 2.1-1). The mean particle size is medium sand

and sorting is poor. Deposits are primarily made up of pumiceous sand and gravel, and their mineralogy is dominated by volcanic glass (60–80% by weight) with subordinate abundances of quartzo-feldspathic minerals. Like in the Puye Formation, smectite-clinoptilolite and iron-bearing minerals are concentrated in the finer particle-size fractions (LANL 2018, 602964). The mean bed thickness is 0.74 ft (Figure 2.1-1).

The Puye pumiceous subunit is a transitional alluvial fan deposit, containing rock types found in both the Puye Formation and the Miocene pumiceous unit. The Puye pumiceous subunit includes beds classified as muddy sandy gravel and gravelly muddy sand (Figure 2.1-1). Mean particle sizes and sorting overlap those in the Puye Formation and the Miocene pumiceous unit. These deposits include rhyodacitic and dacitic gravels and lithic sands mineralogically similar to the Puye Formation and rhyolitic pumiceous sands similar to the Miocene pumiceous unit. Many individual beds include mixtures of these two endmembers. The mean thickness of beds in the Puye pumiceous subunit is 0.88 ft (Figure 2.1-1).

The hybrid nature of the Puye pumiceous subunit indicates the Puye alluvial fan complex received detritus from two distinct sources during the early stages of fan deposition. One source was older Miocene pumiceous unit fan deposits exposed on the western margin of the Española basin that were eroded and redeposited during the early Pliocene. The reworked pumiceous deposits alternate with, and are sometimes mixed with, detritus shed from dacitic volcanic centers that began to form along the Pajarito fault zone during the Pliocene. The transition from the Puye pumiceous subunit to the Puye Formation occurred when increasing sediment supply from the growing dacitic volcanoes caused the rapidly accumulating alluvial fans to expand over the western Española basin, burying the Miocene source rocks.

## 2.2 Estimated Hydraulic Conductivity from Particle Size Data

Figure 2.2-1 presents histograms and summary statistics of Ks produced by 4 of the 15 estimation methods used in this study. These 4 estimation methods capture the range of K distributions found in the set of 15 estimation methods. For comparison, the histograms include 2 Kozeny Carmen K estimations (LANL K-C and HydrogeoSieveXL) to show the effect of varying parameters on K calculations [see discussion in Broxton et al. (2021, 701441)]. K values by all methods have a log-normal distribution. Each estimation method produces a range of Ks that spans an order of magnitude. Similar order-of-magnitude ranges in Ks are characteristic of aquifer tests performed in nearby monitoring wells in the chromium investigation area for the geologic units under investigation (shown as blue shading in Figure 2.2-1). It should be noted that absolute Ks estimated from particle-size data and aquifer tests are not expected to be directly comparable. Ks estimated using particle-size data represent the fine-scale structure of the aquifer on a bed-by-bed basis, whereas aquifer tests interrogate thicker integrated sections of the strata adjacent to well screens and measure the aquifer's bulk properties. As expected, aquifer testing produces Ks that fall on the upper end of the range provided from the bed-by-bed estimates based on particle-size distribution.

K values estimated by multiple methods for the same sample can differ by an order of magnitude or more, and it is generally not possible to identify the best estimate for a given sample. Each of the K estimation methods in HydrogeoSieveXL comes with guidelines for sediment grain-size characteristics to which the methods best apply, but the criteria for establishing a preference for one K estimate over another are generally nonquantitative and subjective. Despite these limitations, use of multiple K estimation methods provides a range of values that are more likely to encompass the actual K than is possible by a single method. Use of multiple methods also provides a better appreciation of the uncertainties associated with the resulting K values.

Figure 2.2-2 presents histograms and summary statistics of Ks for the three geologic units that make up the upper regional aquifer. Ks for the three geologic units show relatively minor differences. Median Ks in the Puye pumiceous subunit are slightly greater (generally less than a factor of 2 greater) than those in the Puye Formation and Miocene pumiceous unit (Figure 2.2-2). Similar comparisons using the mean Ks generally indicate even closer correspondence among the three geologic units. These differences in median or mean Ks are small compared with the order-of-magnitude ranges of K distributions, and histograms of K distributions for the three geologic units strongly overlap for a given estimation method (Figure 2.2-2). The overlap in Ks suggests there is little difference in the bulk hydraulic properties at the scale of geologic units, and the regional aquifer where the chromium plume is located is effectively a single heterogeneous hydrogeologic unit.

A more refined depiction of the hydraulic structure of the regional aquifer is provided by combining the high-resolution stratigraphy with Ks estimated from particle-size data (Figure 2.2-3, the depiction for core hole CrCH-2). The sampling of continuous core provides the ability to evaluate relative Ks at the scale of individual beds. Although absolute values of K vary substantially among the estimation methods, relative comparisons of K versus depth distributions show many similarities, especially in identifying high-K beds. The most permeable beds occur as single beds 0.06–1.2 m thick or as groups of beds up to 3 m thick. All three geologic units are characterized by hydraulic heterogeneity, and high-K beds are widely distributed throughout the stratigraphic sequence regardless of geologic unit (Figure 2.2-3).

Figure 2.2-3 includes vertical profiles for geometric mean and uniformity coefficient, which are additional outputs of HydrogeoSieveXL. The geometric mean combines Ks from the 15 estimation methods in HydrogeoSieveXL to produce average value of K for each sample. The uniformity coefficient is a measure of particle-size sorting. The uniformity coefficient indicates the Puye Formation is very poorly sorted and the Miocene pumiceous unit is poorly sorted.

### **2.3 Partitioning of Hydraulic Conductivity into High-, Medium-, and Low-Flow Regimes**

Cumulative flow distributions are useful in quantifying the volumes where most groundwater is flowing, and they support the interpretation that the regional aquifer is effectively a single hydrogeologic unit. Five of the K estimation methods (K-C LANL, K-C HydrogeoSieve, Hazen, US Bureau of Reclamation, and Geometric Mean) are used to compare cumulative flow distribution in the core hole material (Figure 2.3-1) and in the three geologic units making up the regional aquifer (Figure 2.3-2). These plots represent Ks that are sorted from high to low values, converted to fractional K values, and then plotted against cumulative bed thicknesses.

The cumulative flow distribution plots show the partitioning of groundwater flow in the regional aquifer in three bins: 90% of flow (Q90), 9% of flow (Q9), and 1% of flow (Q1). These bins correspond to the three-compartment model where groundwater flow in a heterogeneous aquifer is partitioned into high-, medium-, and low-flow regimes based on order-of-magnitude differences in Ks (Horst et al. 2017, 701456). This approach emphasizes the importance of relative differences of K within aquifer media rather than absolute K values to differentiate flow regimes. Q90 is used to define the most permeable aquifer media and is dominated by advective flow. Q9 are less permeable strata characterized by slow advection and storage, with low diffusion assumed to occur into and out of the units. The Q1 bin includes the least permeable strata (clays and silts) dominated by both diffusion and storage. The analysis assumes there is a uniform hydraulic gradient across the aquifer and that the total aquifer thickness is approximated by the core hole depths (Horst et al. 2017, 701456). Although the selection of Q90, Q9, and Q1 for purposes of partitioning the flow is arbitrary, it provides a convenient way to assess the effect of heterogeneity on water flow through the aquifer material.

The cumulative flow distributions in the five core holes are shown in Figure 2.3-1. Four of the five K estimation methods (K-C LANL, K-C HydrogeoSieve, Hazen, and Geometric Mean) produce similar Q90, Q9, and Q1 distributions, with the following ranges representing differences in estimates from these four methods:

CrCH-1: Q90 = 44–58%, Q9 = 37–47%, and Q1 = 3–10%

CrCH-2: Q90 = 57–63%, Q9 = 27–34%, and Q1 = 8–10%

CrCH-3: Q90 = 60–65%, Q9 = 29–31%, and Q1 = 6–9%

CrCH-4: Q90 = 61–66%, Q9 = 24–33%, and Q1 = 1–15%

CrCH-5: Q90 = 45–66%, Q9 = 26–43%, and Q1 = 8–12%

The U.S. Bureau of Reclamation K estimation method generally produces lower flow percentages for the Q90 bin and greater percentages for the Q9 and Q1 bins than the other estimation methods (Figure 2.3-1):

CrCH-1: Q90 = 23%, Q9 = 35%, and Q1 = 42%

CrCH-2: Q90 = 38%, Q9 = 42%, and Q1 = 20%

CrCH-3: Q90 = 39%, Q9 = 47%, and Q1 = 14%

CrCH-4: Q90 = 53%, Q9 = 31%, and Q1 = 16%

CrCH-5: Q90 = 21%, Q9 = 37%, and Q1 = 43%

The U.S. Bureau of Reclamation estimation method produces extremely high Ks in a few beds (Figure 2.2-3) resulting in lower Q90 flow estimations (Figure 2.3-1). The remaining flow is distributed between the Q9 and Q1 bins, increasing their proportion relative to the other K estimation methods. This method would be expected to yield representative results in systems in which well-connected, high-K pathways exist over significant distances, which is not likely to be the case in these units because alluvial fan deposits are largely made up of beds with limited lateral extent. Therefore, the other four estimation methods are favored as providing a more representative depiction of the degree of heterogeneity of flow through the porous medium.

The cumulative flow distributions within the three geologic units are shown in Figure 2.3-2. Using the same four estimation methods (K-C LANL, K-C HydrogeoSieve, Hazen, and Geometric Mean) to produce Q90, Q9, and Q1 values, the analysis suggests that groundwater flux in the regional aquifer is similar in the three units:

Puye Formation                      Q90 = 54–65%, Q9 = 29–37%, and Q1 = 6–12%

pumiceous Puye subunit        Q90 = 47–60%, Q9 = 29–39%, and Q1 = 11–15%

Miocene pumiceous unit        Q90 = 61–65%, Q9 = 28–31%, and Q1 = 7–8%

The cumulative flow distribution plots indicate that about 90% of groundwater flux in the regional aquifer takes place in approximately 55–62% of the aquifer (Figure 2.3-2, all units combined). The U.S. Bureau of Reclamation data yield Q90 fluxes as low as 14%, but these estimates are anomalous compared with other methods and considered to be outliers. The cumulative flow distribution plots suggest that groundwater and chromium flux in primary advective transport zones is widely distributed in the aquifer.

High-resolution stratigraphy combined with estimated Ks (Figure 2.3-3) show that Q90 beds are widely and randomly distributed throughout the aquifer in the plume area. Slow advection and diffusion in beds within the Q9 bin represent approximately 31–36% of the aquifer (Figure 2.3-2, all units combined). Matrix

diffusion and storage within the Q1 bin represent approximately 7–12% of the aquifer (Figure 2.3-2, all units combined). Groundwater in the Q1 strata is essentially static and matrix diffusion may be responsible for some chromium to be stored in those units. Q9 and Q1 strata with chromium inventory may function as a long-term source of slow chromium release to the advective strata during remediation.

The lateral extent of individual high-K beds is uncertain. In core hole CrCH-2, a group of prominent high-K beds occurs within the pumiceous Puye subunit (Figure 2.2-3). However, in core hole CrCH-3, the most prominent high-K beds occur in the Puye Formation and the Miocene pumiceous unit (Figure 2.3-3). Correlating individual high-K beds between core holes was attempted, but not possible because of the heterogeneity of geologic units making up the regional aquifer and the lack of unique marker beds that can be used for correlation. In alluvial fan deposits, individual or sets of strata are commonly not very laterally extensive because of initial aerially limited depositional geometry or erosional truncation by younger deposits. Targeting only the highest K (Q90) beds at any given location for remediation is probably impractical because of their limited lateral distribution in the aquifer and the thin nature of the beds.

## **2.4 Flow Networks that Cross Stratigraphic Boundaries**

Although laterally discontinuous, high-K beds are juxtaposed to other permeable deposits by depositional and erosional processes. Regimes of higher groundwater flow likely occur where networks of laterally interconnected high-K beds form preferred pathways for groundwater flow (Figure 2.4-1). Networks of high-K beds likely span the contacts of gently dipping geologic units at some locales and may be important lateral flow paths in the aquifer. Such networks might explain how groundwater in the Miocene pumiceous unit near CrEX-4 flows eastward into the pumiceous Puye subunit and the Puye Formation at CrEX-3, CrEX-5, and R-70 (Figure 2.4-2). In this interpretation, high concentrations of chromium in R-70 screen 2 are not due to the pumiceous Puye subunit being a preferential pathway. Instead, flow is controlled by networks of interconnected high-K beds that cross the primary geologic unit contacts and form complete lateral pathways between Miocene aquifer sediments in the vicinity of CrEX-4 to Pliocene aquifer sediments in the R-70 area.

## **3.0 Hydrogeochemistry**

This section presents data collected from wells in the R-70 area to develop one or more conceptual models for the observed geochemical structure near the northeast portion of the chromium plume. Analytical data collected at R-70 screen 1 and screen 2 are presented and evaluated in the context of determining the type and timing of source(s) that would produce the observed geochemical signatures and by comparing spatial variations in these signatures between wells in the vicinity of R-70. Then, the temporal variations in potential sources and associated geochemical tracers are examined with respect to the spatial distributions of the geochemical signature at and near R-70. Lastly, several preliminary conceptual models are presented that may explain the unique differences in vertical chromium distributions between R-70 screen 1 and screen 2.

The principal source that dominates the geochemical signature in the plume is the early releases that occurred in association with power plant operations between 1956 and 1972. These early releases into Sandia Canyon occurred as cooling tower blowdown and are generally characterized by elevated chromium and sulfate and generally heavier water related to evaporation in the cooling towers. Later releases are primarily characterized by elevated sewage-related nitrate and low concentrations of pharmaceuticals as the Laboratory's treated sanitary effluent was consolidated and discharged into Sandia Canyon through an outfall in upper Sandia Canyon. A short period of releases that may have

included nontreated industrial wastewater also occurred, which may manifest as measurable tritium concentrations. These distinct geochemical signatures are superimposed on the background geochemistry of the aquifer.

### 3.1 Groundwater Geochemistry at Well R-70 Screen 1 and R-70 Screen 2

The geochemical signature in R-70 screen 1 reflects a mixture of sewage and cooling-tower effluent. Evidence for the sewage signature includes elevated nitrate as nitrogen ( $\text{NO}_3$  as N) at 2.65 mg/L with a slightly enriched  $^{15}\text{N}$  ( $\text{NO}_3$ ) isotope composition at 4.99 and 6.60 per mil, and chloride at 6.03 mg/L. A single J-flagged value of the compound sulfamethoxazole, an antibiotic that dates to circa 1961, at the detection limit of 0.54 ng/L may also indicate a partial sewage signal in R-70 screen 1. The key constituents that are associated with the cooling tower source include sulfate at 7.70 mg/L and dissolved chromium at 18.4  $\mu\text{g/L}$ .

The period of monitoring data for chromium, major ions, and tritium at R-70 screen 1 is provided in Figure 3.1-1. The period of record at R-70 is relatively short, thus limiting the ability to observe longer-term trends that may represent evolution in the plume at that location, but the concentrations measured so far can be examined to develop preliminary conceptual models. Tritium concentrations range from 4.41 to 6.62 pCi/L, suggesting an anthropogenic source whether it be releases from the Laboratory or associated with global fallout. Stable-isotope compositions for deuterium ( $^2\text{H}$ ) and  $^{18}\text{O}$  ( $\text{H}_2\text{O}$ ) are  $-76.58$  per mil and  $-10.60$  per mil, respectively. These isotope compositions are near equal to regional-aquifer background compositions, which may indicate mixing of the plume with ambient groundwater or sewage since the sewage signal is superimposed on pumped regional aquifer groundwater used for potable purposes. Additional constituents elevated above regional-aquifer background concentrations include arsenic at 3.14  $\mu\text{g/L}$ , boron at 24.7  $\mu\text{g/L}$ , calcium at 23.2 mg/L, fluoride at 0.47 mg/L, magnesium at 5.23 mg/L, and perchlorate at 0.56  $\mu\text{g/L}$ . With the exception of  $\text{NO}_3$  as N, the low concentrations of other dominant solutes such as chloride and sulfate, and relatively light water-isotope compositions, indicate that the geochemistry of groundwater at the R-70 screen 1 represents power-plant effluent mixed with noncontaminated groundwater from the regional aquifer. The 2.65 mg/L  $\text{NO}_3$  as N concentration at R-70 screen 1 is about half the concentration measured near the centroid of the chromium plume at R-42 where  $\text{NO}_3$  as N concentrations have been consistently measured within a range of 5–6 mg/L since 2008. The proportion of nitrate concentrations between the centroid and the R-70 area also suggests dilution of the plume with ambient groundwater.

The groundwater geochemistry at R-70 screen 2, set approximately 80 ft below the regional water table, indicates a source of mixed sewage, industrial-radionuclide, and cooling-tower effluent. The sewage components include nitrate as nitrogen at 3.75 mg/L, enriched  $^{15}\text{N}$  ( $\text{NO}_3$ ) at 8.59 per mil, elevated chloride at 17.50 mg/L, and sulfamethoxazole at 4.7 and 4.8 ng/L.

Monitoring data for chromium and other constituents at R-70 screen 2 is shown in Figure 3.1-2. The dominant cooling-tower constituents include elevated sulfate at 30.3 mg/L and dissolved chromium at 246  $\mu\text{g/L}$ . The industrial-radionuclide source component is represented by tritium at 56.9 pCi/L. Several trace elements are detected above the regional aquifer background such as nickel at 3.24  $\mu\text{g/L}$ , barium at 68.6  $\mu\text{g/L}$ , and boron at 27.9  $\mu\text{g/L}$ . The  $^2\text{H}$  and  $^{18}\text{O}$  ( $\text{H}_2\text{O}$ ) compositions are  $-74.76$  and  $-10.20$  per mil, respectively. These isotope compositions are slightly heavier than regional aquifer values, likely reflecting evaporation processes at the power-plant cooling towers.

In general, R-70 screen 2 contaminant concentrations compared with concentrations found near the centroid of the plume at R-42 suggest a mixed signal containing plume water and ambient groundwater.

### 3.2 Comparison of R-70 Screen 1 and Screen 2 Geochemistry with That of Nearby Wells

In this section, the geochemistry at R-70 screen 1 and screen 2 is compared with the geochemistry at nearby wells and well screens representing different depths in the aquifer, taking into consideration past effluent discharges into Sandia Canyon. For the R-70 screen 1, the most definitive effluent-linked constituent is chromium. Other tracers may be present but are not detectable. As reflected in the Piper diagram in Figure 3.2-1, other wells in the vicinity of R-70 screen 1 that produce similar geochemical signatures are R-11, located approximately 1100 ft to the northwest, and R-45 screen 1, located about 900 ft southwest of R-70 screen 2. Concentrations of chromium, common solutes, and tritium at R-11 have varied significantly over time and are shown in Figure 3.2-2. Concentrations of chromium at R-11 have ranged from about 5 to 35 µg/L; sulfate has ranged from 6 to 15 mg/L; chloride has ranged from 4 to 6 mg/L; NO<sub>3</sub> as N has shown relatively stable concentrations at about 5 mg/L; and tritium concentrations have ranged from approximately 5 to 10 pCi/L. Nitrogen-isotope compositions for <sup>15</sup>N (NO<sub>3</sub>) average 4.60 per mil. Stable-isotope compositions for deuterium (<sup>2</sup>H) and <sup>18</sup>O (H<sub>2</sub>O) are -76.58 per mil and -10.60 per mil, respectively. As with R-70 screen 1, the common pharmaceutical sulfamethoxazole is not detectable at R-11. Sulfate to chloride ratios at R-11 are higher than the ~1.0 ratio measured at the R-70 screen 1, ranging from a low of 1.3 in 2005 to a more recent maximum at 1.7 in 2020.

R-45 screen 1 chromium concentrations are higher than at R-70 screen 1, with levels ranging from a low of 8 µg/L in early 2009 to a peak high of 50 µg/L in late 2017. Concentrations then steadily declined up to late 2019, when injection at nearby wells CrIN-1 and -2 also began to decrease the chromium concentration at an even faster pace (Figure 3.2-3). Nitrogen-isotope compositions for <sup>15</sup>N (NO<sub>3</sub>) at R-45 screen 1 average approximately 4.80 per mil and the stable-isotope compositions for deuterium (<sup>2</sup>H) and <sup>18</sup>O (H<sub>2</sub>O) average approximately -74.50 per mil and -10.54 per mil, respectively. Data from R-45 screen 1 show sulfamethoxazole at low concentrations ranging from 1.1 to 2.3 ng/L, indicating some fraction of post-1961 effluent recharge. The SO<sub>4</sub>/Cl ratio at R-45 screen 1 is relatively stable at about 1.1, near equal to the 1.0 ratio observed at R-70 screen 1.

Comparing the geochemistry in R-70 screen 1, R-11, and R-45 screen 1, which are all screened near the top of the aquifer, shows significant similarity and may reflect the advancement of chromium-era (1956–1972) releases mixed with differing amounts of clean ambient groundwater that may either pre-date or post-date the chromium-era releases.

Effluent-related constituents present at R-70 screen 2 include dissolved chromium at 246 µg/L and sulfamethoxazole at 4.7 ng/L. For comparison, the nearest well in proximity to R-70 screen 2 is extraction well CrEX-5, located approximately 750 ft upgradient to the west. CrEX-5 is screened from near the regional water table to a depth of approximately 60 ft below the water table. Before continuous extraction pumping at CrEX-5 in late 2019, chromium concentrations at CrEX-5 averaged about 240 µg/L with sulfamethoxazole in the 8.9 and 9.5 ng/L range, similar to that found at R-70 screen 2. In addition, the major-ion geochemistry at CrEX-5 corresponds closely to R-70 screen 2. Although at higher concentrations, the upgradient wells R-28, R-42, and CrEX-4 show the same type of effluent-related constituents and similar geochemical signatures as R-70 screen 2. This is best depicted in the Piper diagram (Figure 3.2-1), which shows a cluster of points associated with R-70 screen 2, R-28, R-42, CrEX-4, and CrEX-5, as distinct from the cluster of shallow monitoring points in the vicinity of R-70, including R-70 screen 1, R-11, and R-45 screen 1. The geochemical signatures at R-70 screen 2 likely reflect plume migration from the R-28, R-42, and CrEX-4 area where contaminants are relatively deep beneath the water-table.

Figure 3.2-1 illustrates the geochemical evolution of plume migration from the plume centroid near R-42 towards R-70 screen 2. Geochemically, the R-70 screen 1 groundwater is very similar to other neighboring wells positioned at the water table along the northeastern plume-front margin including R-11 and R-45.

### 3.3 Conceptual Models that Describe the Vertical Chromium Distributions at Well R-70

The contrast in chromium concentrations in the two screens at well R-70 and the presence of significantly higher concentrations in the deeper of paired screens is unique to the chromium plume. Other chemical constituent concentrations also differ between screen 1 and screen 2. For example, chloride, nitrate as nitrogen, sulfate, and tritium are about 3, 1.5, 4, and 10 times higher, respectively, at screen 2 versus screen 1. Broadening the focus to the nearby wells, R-70 screen 1 chemistry appears similar to nearby water-table screens in R-11 and R-45 screen 1; the geochemical signature of R-70 screen 2 is similar to that of R-28, R-42, CrEX-4, and CrEX-5. The geochemistry in the R-70 area appears to be somewhat stratified, with distinct characteristics shallow and deeper in the aquifer in the R-70 area. The signature at depths close to 100 ft below the water table (at the depth of R-70 screen 2) appears to be overlain by a geochemical signature that includes the characteristic of early chromium releases, but at lower concentrations.

Conceptually, there are several potential explanations for the geochemical stratification observed at R-70 and nearby wells. First, contamination at R-70 screen 1 may represent the same source of contamination as that observed at R-70 screen 2, but mixed with sources of effluent released from a different time period. The suspect subnanogram detection of the pharmaceutical sulfamethoxazole and the absence of carbamazepine (a pharmaceutical compound), also introduced in the 1960s, and lack of younger effluent tracers, may indicate that the signature at R-70 screen 1 represents older pre-1956 chromium-era sources. Alternatively, the geochemistry in R-70 screen 1 may be related to recharge from more recent and relatively noncontaminated sources (power-plant effluent) or infiltration from Los Alamos Canyon, which recharge the aquifer upgradient of R-11, R-45, and R-70. The young recharge signature may be mixing with the predominant geochemical signature in the plume and modifying the geochemistry near the water table in the R-70 area. Further investigations into the sources of fluids and mixing will be required to distinguish between these possibilities. This task is made more difficult by the fact that the effluent releases into Sandia Canyon are likely to have different infiltration points into the vadose zone, and the vadose zone itself leads to a significant travel time and uncertainty in the direction of the flow pathways to the regional aquifer.

Despite the uncertainty concerning a conceptual model, vertical distribution of chromium at R-70 does not appear to be driven by vertical spreading due to pumping at PM-3 or local downward gradients. Instead, it is likely caused by the migration of early-arrival chromium plume-front contamination mixed with clean ambient groundwater. Alternatively, mixing of young post-chromate effluent water with some fraction of ambient groundwater is possible. The deep contamination at R-70 possibly originates as far upgradient as the CrEX-4 area and remains at that approximate depth in the R-70 area.

As it relates to the purpose of this study, the information collected to date suggests that stratified geochemical zones exist near the water table and to depths of at least 100 ft below. There appear to be relatively simple fluid mixing processes within a region of relatively flat water table with minimal vertical head gradients. These observations are inconsistent with a situation in which contamination is being drawn deeper into the aquifer by pumping at water supply well PM-3. Nevertheless, there remain uncertainties in terms of the depth of the contaminant plume in the R-70 region. These uncertainties are important to resolve in order to design an effective remediation plan for this portion of the plume. A

deeper well (R-73) is proposed to provide additional information on the geochemistry and vertical extent of contamination in the R-70 area.

#### **4.0 OBSERVATIONS OF IM PERFORMANCE AND HYDRAULIC ANALYSIS**

This section documents the geochemical and hydraulic information observed to date in the R-70 area. The eastern portion of the IM has been operating in a steady-state manner for only a limited duration. Therefore, the relatively short period of record for eastern area IM operations is not considered sufficient for a conclusive assessment of the relation of changes in chromium concentrations to IM extraction and injection.

This section will include a detailed hydraulic analysis of cross-hole pressure responses in wells located in the R-70 area to pumping and injection associated with the IM and pumping at Los Alamos County water-supply wells. This analysis provides for an understanding of the large-scale hydraulics in the R-70 area and assists in estimations of the likelihood of plume response to the IM.

This section also includes a geologic framework for explaining the negligible or lack of pressure response in R-70 area wells to pumping at Los Alamos County water-supply well PM-3.

The analysis in this section recognized the data gap in the existing monitoring network, namely the characterization and monitoring that would be addressed by R-73.

#### **4.1 Hydraulic Analysis**

Hydraulic response data from intentional and opportunistic aquifer tests in the R-70 area of the regional aquifer are evaluated in order to address three primary questions:

- Does pumping at PM-3 (and other municipal water-supply wells) influence hydraulic heads measured at R-70 screen 1 and screen 2?
- What is the effect of IM pumping and injection on hydraulic heads in R-70 screen 1 and screen 2?
- Where are the effects of pumping conducted at R-70 screen 1 and screen 2 observed at other nearby wells?

The first two questions relate to whether R-70 is located within the zone of influence of neighboring wells, whether water-supply pumping at PM-3 causes any change in the apparent vertical gradient at R-70, and what is likely to be the effect of sustained IM operations on hydraulic heads and gradients in the eastern area of the plume. The final question demonstrates a hypothetical zone of influence of R-70 screen 1 and screen 2.

Water-level data from the site are processed to remove unwanted barometric pressure signals from the raw transducer measurements. In many of the monitoring wells in the chromium area at Los Alamos National Laboratory (LANL), the data show an immediate and opposite change in water level in response to barometric pressure. This is the direct effect of atmospheric pressure on water in the wellbore, as compared to effects of barometric pressure change on the aquifer, which show a time lag and attenuation that are related to vadose zone pneumatic diffusivity, aquifer properties, and wellbore skin effects (Rasmussen and Crawford 1997, 094014; Spane 2002, 602105).

A “basic” barometric correction is applied by adding the barometric pressure—converted to feet of water and interpolated to the same time measurements as the water levels—to the raw water levels and then subtracting a constant value of the average barometric pressure, which removes the effects of barometric

pressure change. More advanced methods of removing delayed, attenuated effects of barometric pressure change on the aquifer were also tested, including the graphical and Clark methods described in (Gonthier 2007, 701330) and the LANL open-source CHiPBETA software, which uses an iterative deconvolution regression approach for separating barometric and earth tide effects (<https://gitlab.com/zem/chipbeta>). Whenever the “basic” method fails to remove undesired signals adequately, impeding the ability to observe signals of interest on the hydrographs, other methods will be considered.

The hydrographs are shown here alongside pumping at infrastructure (CrIN and CrEX) wells and municipal water-supply wells. CrIN and CrEX pumping rates are smoothed in order to show major changes in behavior rather than sub-minute scale variability in pumping rate. The smoothing algorithm has adjustable parameters including the minimum duration of a pumping “event” (on, off, or change in pumping rate) and percent change in rate. The parameters are currently set to 2 hr and 10% change with a minimum of 5 gallons per minute (gpm). This helps keep the pumping rate plots visually clean enough for inspection of major changes and their effects on water levels; however, some events that are smoothed over may be causing some of the variability in hydrographs and will be discussed below as needed.

The following sections are organized according to the list of questions above.

#### **4.1.1 Effect of PM-3 on R-70**

In this section, the effect of PM-3 on R-70 screen 1 and screen 2 are evaluated, and geologic factors contributing to a lack of water-level responses at the chromium-area monitoring wells are discussed.

R-70 has been operational since November 2019, allowing only a relatively short period of observation for longer-term or seasonal trends. Older wells at the chromium site show both cyclic seasonal variability and a long-term declining trend in elevation (N3B 2021, 701366). The seasonal trends appear to be well correlated with water-supply pumping; quantitative inverse analyses have been used to connect these changes to particular municipal wells (LANL 2018, 603032). The Theis analysis presented in the “Evaluation of Chromium Plume Control Interim Measure Operational Alternatives for Injection Well CrIN-6” (LANL 2018, 603032) showed estimated drawdowns from water-supply pumping, with the largest influences typically coming from O-4, PM-2, PM-4, and PM-5, and not PM-3. (Faint influences of PM-3 were possibly detected at R-35a, R-35b, and R-44 screen 2, but even at these locations, the effect was dwarfed by the influence of PM-2 and PM-4, particularly, and in some cases may be of questionable significance.) The stronger effect of drawdown at lower screens of chromium-area monitoring wells has been shown to slightly increase downward vertical gradients at some locations, in some cases reversing a slight upward gradient to a slight downward gradient, such as at R-44 (N3B 2021, 701366).

Figure 4.1-1 shows water-level data for R-70 screen 1 and R-70 screen 2, which have been barometrically compensated using the “basic” method described above. Pumping rates are shown on the lower panels. Of the infrastructure wells, only CrEX-5 and CrIN-1 are shown in order to see whether visible changes in R-70 water levels are due to IM operations (the effects of other IM wells on R-70 are more muted, as discussed in section 4.1.2). Where there are gaps in water-level records, these data are excluded from the plot for clarity because there is either a problem with the transducer data or in the barometric pressure record.

Figures 4.1-2 to Figure 4.1-4 show zoomed-in time periods of interest for R-70 screen 2 to further visually evaluate the impact of municipal water-supply well pumping. Time periods are selected that include the largest changes in PM-3 pumping during R-70’s period of record, especially ones that are isolated from other pumping activities that would confound the signal. These hydrographs include both unprocessed

and barometrically compensated water-level elevations (using the “basic” method described above), as well as barometric pressure, to help the viewer evaluate whether small changes in the hydrograph may be due to uncompensated barometric signals.

Figure 4.1-2 shows a time period in March 2020 when an isolated PM-3 pumping event took place (period “B”). During that time, CrEX-5 and CrIN-1 were operational, but relatively steady. A spike in the R-70 screen 2 water level at point A occurs close to the same time as the PM-3 pumping; however, (1) it precedes the pumping, (2) it is a rise in water levels rather than a decline, and (3) a closer examination of the raw CrEX-5 pumping data shows that a cycle occurred where the pumping rate dropped from 90 to 0 gpm for a period of just over 1 hr on March 11, 2021, at 9:39 a.m. This cycle in CrEX-5 pumping rate is not shown on the figure because it does not meet the 2-hr minimum duration for the smoothing algorithm, described above. Therefore, this change in the R-70 screen 2 water level is clearly not related to the isolated PM-3 pumping event on March 12, 2020, and there is no visible change in R-70 water level caused by the PM-3 event in period B.

In Figure 4.1-3, a time period in May 2020 with no activity at IM wells is shown, along with periods representing a change in PM-3 pumping (point C and period D). As before, no sudden changes are observed at R-70 screen 2 due to the onset of PM-3 pumping, although larger-scale variability is observed throughout the visible period. For example, water levels reach a minimum around May 27, 2020, at which point PM-3 pumping has been off for several days but resumes, while R-70 screen 2 water levels climb slightly until the end of the period shown, while PM-3 pumping rates rise. This figure also demonstrates an apparent lack of influence by PM-3 on R-70 screen 2.

To see whether variability in R-70 screen 2 may be caused by pumping at municipal wells other than PM-3, Figure 4.1-4 shows the same time period as Figure 4.1-3, but with all Los Alamos County pumping on the bottom panel. During this period, pumping at O-4, PM-1, and PM-2 are relatively consistent, with some exceptions. PM-3, PM-4, and PM-5 show greater variability. The gentle decline with a minimum around May 27, 2020, may be related to PM-4 pumping, which would be consistent with other observations around the site (N3B 2021, 701366), while the overall decline to date is also consistent with other wells.

Figure 4.1-5 shows the entire period of record to date at R-70 screen 1 and screen 2 along with all municipal water-supply pumping. A longer period of record at R-70 will likely confirm whether the observed pattern at other chromium-area wells holds at this location, that O-4, PM-2, and PM-4 pumping is capable of generating larger drawdown at R-70 screen 2 than PM-3 pumping.

Hydraulic heads in R-70 screen 2 are higher than screen 1 under ambient conditions, as observed during well installation and seen in Figure 4.1-5 during the spring 2020 shutdown in IM pumping, resulting in an apparent slight upward gradient at this location. This caused cross-flow during well installation and testing when the two screens were not isolated, as evidenced by early geochemical sampling results. R-70 is an angled well, so the small horizontal hydraulic head gradients in the area introduce some uncertainty into the physical vertical gradient at that location. However, upward vertical gradients are also present in several other dual-screened chromium-area wells that are not angled (e.g., R-61 and R-44), particularly during ambient periods in pumping (N3B 2021, 701366).

The effect of IM pumping (discussed in section 4.1.2) is to reduce the magnitude of the vertical gradient, although it is still typically slightly upward. Figure 4.1-6 shows a time period during IM pumping, along with PM well activity, to further evaluate the question of whether PM-3 effects are apparent at R-70. A period of “reversal” of the gradient (to slightly downward) is shown in Figure 4.1-6, period E; while the timing of the reversal suggests that PM-3 *could* have been responsible, evidence against this hypothesis is that a slight reversal occurs again in period F, while PM-3 is not pumping. These two events do not

have a clear explanation based on changes in IM pumping, as the IM pumping during that time was consistent, until the end of period F. Additional data collection at R-70 and proposed well R-73 will further refine our understanding of PM-3 effects on the chromium plume's eastern area; to date, evidence suggests that if PM-3 has an effect at the existing screen depths, it is small and is expected to have little impact on plume hydraulics. On the other hand, IM pumping is clearly seen in Figure 4.1-6 to have a strong effect on the vertical gradient at R-70, as discussed next in section 4.1.2, along with estimated magnitudes of the effect.

A geologic explanation for lack of water-level responses at the chromium-area monitoring wells (including R-70) due to pumping at PM-3 is proposed. The upper part of the PM-3 well screen penetrates thick Miocene basalt flows that are intercalated in the aquifer's sedimentary sequence. These basalts appear to be widespread beneath the Pajarito Plateau and likely are confining or semi-confining beds in the regional aquifer. Chromium-area monitoring wells are apparently isolated from pressure responses generated by PM-3 pumping because most water production at PM-3 is likely from Miocene sedimentary deposits beneath the basalts.

The Miocene basalts in PM-3 occur in the upper part of the well screen and are at least 255 ft thick (~16% of total screen length of 1576 ft) (Figure 4.1-7). Based on geophysical logs, these basalts have low porosities and are likely to be relatively impermeable, especially when compared with the Miocene sedimentary deposits that make up most of the well screen. A spinner log conducted in well PM-4 (McLin 2006, 092218, Figure 14) showed that Miocene basalts are not important contributors of groundwater entering the well screen. At PM-3, Miocene sedimentary rocks (Tcar) above the Miocene basalts make up only 75 ft (~5%) of the well screen, so it is reasonable to assume that most of the water production comes from Miocene sedimentary rocks in the lower part of the well (79% of the well screen). The relatively high stratigraphic position of the Miocene basalts at PM-3 largely isolates shallow portions of the regional aquifer from pressure responses due to pumping of productive sedimentary deposits in the lower part of the well. This may explain why nearby well R-35a, screened at the elevation of the top of the PM-3 screen and located a short distance (~343 ft) from PM-3, is the only monitoring well in the chromium investigation that shows a response to PM-3.

It is notable that water levels in the shallow chromium-area monitoring wells respond to pumping at municipal water supply wells PM-2, PM-4, and PM-5, which are located to the south and southwest. Because of regional dips, the Miocene basalts become progressively deeper in the aquifer southward and occur in the lower portions of the PM-2 and PM-4 well screens (Figure 4.1-8). Consequently, most of the water production comes from sediments above the basalts. At PM-4, 93% of the total production comes from sedimentary deposits above the Miocene basalts (McLin 2006, 092218). Miocene basalts are widely distributed in the middle of the PM-5 well screen (Purtymun 1995, 045344), and significant water production likely occurs in the upper part of the well screen. Because of regional dips, pressure responses from these municipal wells propagate north and northeast along bedding to shallower portions of the regional aquifer beneath the chromium investigation area. In contrast, municipal wells O-1, O-2, and PM-1, located to the north and east, generally do not produce pumping responses in the chromium-area monitoring wells despite the fact they are similar distances from the chromium investigation area (LANL 2009, 107453; LANL 2018, 603032). Like PM-3, Miocene basalts occupy high positions in these wells (Figure 4.1-7), and most of the water production comes from sediments beneath the basalts.

#### **4.1.2 Effect of IM Pumping and Injection on R-70**

Figure 4.1-5 shows R-70 water-level data for the entire period of operation for both screens on the top panel, corrected using the "basic" method described above, with pumping at the CrEX and CrIN wells and municipal water-supply wells for the same time period on the bottom two panels. Additional zoomed-in

plots are shown in Figures 4.1-9 through Figure 4.1-11, some with annotated points for discussion. As before, gaps in the water-level records on these plots indicate missing or erratic transducer data, or that the barometric pressure record was compromised and could not be used to correct the raw data.

While this report focuses on R-70 and the eastern area of the plume, similar figures for the other dual-screened wells at the site are presented in the “Semiannual Progress Report on Chromium Plume Control Interim Measure Performance, July through December 2020” (N3B 2021, 701366), and together, they demonstrate the typical vertical gradients seen at the site and how they change under the influence of water-supply pumping and IM operations.

In the fall of 2020, eastern area IM operations began while pumping and injection in the central and southern portions remained mostly consistent (i.e., CrEX-1 and -2; CrIN-4 and -5). Figure 4.1-9 shows this time period. A reversal in the R-70 vertical gradient occurs when CrEX-5 pumping is initiated at point A (CrEX-1 pumping also increases in rate from approximately 60 to 80 gpm at this time, but as discussed below, CrEX-1 is not observed to have a significant effect on R-70). The reversal occurs because the drawdown at R-70 screen 2 from CrEX-5 is significantly greater than the drawdown at screen 1. CrIN-1 and -2 begin injection shortly after point A, along with a slight increase in CrEX-5 pumping rate, but this event is not observed to have much effect on R-70 other than a potential increase in the screen 2 water level. It is likely the superposition of several events is obscuring the effects of the CrIN wells in isolation.

At point B in Figure 4.1-9, the gradient reverses back to slightly upward. (An earlier spike is caused by a short drop in CrEX-5 pumping that is not reflected on the pumping panel because of the parameters of the smoothing algorithm.) This reversal is likely primarily caused by the decrease in the pumping rate at CrEX-5, from approximately 90 to 60 gpm, although several other events occur at the same time: CrIN-1 injection rate increases from approximately 64 to 75 gpm, CrEX-4 turns on, and CrEX-1 decreases in rate.

There are few substantial isolated events at CrIN-1 during the period of operation at R-70 to clearly see its effects, independent of CrEX-5. Figure 4.1-10, point C, shows a moment at which CrIN-1 shuts off, while CrEX-5 has not been operational. (CrEX-1 and -2 also shut off at the same time but are not expected to have a strong impact, as seen shortly after when they turn back on. CrIN-3 also shuts off at the same time as CrIN-1 and does not turn back on.) With a greater drop at R-70 screen 2 than screen 1 at point C, this indicates that CrIN-1 has been elevating the screen 2 water level more than the screen 1 water level. Therefore, at R-70, it appears that both CrEX-5 and CrIN-1 cause larger effects at screen 2 than screen 1, which is a different pattern of hydraulic response than that seen at several other dual-screened chromium-area wells. As discussed in the “Semiannual Progress Report on Chromium Plume Control Interim Measure Performance, July through December 2020” (N3B 2021, 701366), at R-44, R-45, and R-50, the nearest injection well appears to generate larger hydraulic head change in screen 1 than screen 2, while the nearest extraction well generates larger hydraulic head change in screen 2 than screen 1.

Point D in Figure 4.1-10 is used to demonstrate whether CrIN-2 has any effect on R-70 when operating in isolation, but no clear response is seen to the spike of injection in CrIN-2. Additional intentional and opportunistic cycling of the infrastructure wells will be examined in the future to help isolate the effect of CrIN-1 and -2 injection at R-70.

The next three closest infrastructure wells to R-70 are CrEX-3, CrIN-3, and CrEX-1. There is only one short extraction event at CrEX-3 to analyze, on November 5, 2020, and it coincided too closely with the beginning of operations at CrEX-5 and -4 and CrIN-1 and -3 to be of use for seeing if CrEX-3 drawdown can be observed at R-70.

Figure 4.1-11 shows R-70 screen 1 and screen 2 during the phased start-up of CrEX-1, CrIN-4 and -5, CrEX-2, and CrIN-3. Point E, when CrEX-1 begins, does not show an obvious change, and the slight decline that follows may be associated with other variability at the site. Point F shows the onset of injection at CrIN-3. Note that the sharp dip in hydraulic head in both screens shortly after point F in Figure 4.1-11 was caused by purging of cross-flow from the two screens on July 17, 2020, following electrical work. In summary, the only wells that appear to have significant impact on R-70 screen 1 and screen 2 hydraulic heads are the two nearest IM wells, CrEX-5 and CrIN-1. The effect of IM operation to date at typical pumping rates appears to be a decrease of the upward vertical gradient at R-70, in some cases becoming a slight reversal, depending on pumping rates. This is due primarily to the larger drawdown at R-70 screen 2 than screen 1 resulting from pumping at CrEX-5.

To quantify the magnitude of the reversals of the apparent hydraulic gradient in R-70, Figure 4.1-12 shows the hydraulic head difference between screen 1 and screen 2 during periods of no activity and with CrEX-5 and CrIN-1 pumping and injection at various rates. As discussed above, the actual vertical gradient at R-70 is difficult to quantify precisely due to the angled construction of the well in the presence of horizontal hydraulic gradients in the area. The discussion that follows refers to the gradient observed along the wellbore angle and is intended to illustrate the magnitude of the effects of the IM on this gradient.

During a period of no IM activity (May 2020), the hydraulic head difference averaged  $-0.13$  ft (when the difference is negative, the direction is upward); given the screen center vertical separation of  $67.7$  ft (including correction for the angle of the well), this implies an upward hydraulic gradient of  $0.0019$  ft. During a period of reversal in October 2020 when CrEX-5 was pumping at a high rate, the hydraulic head difference averaged  $0.018$  ft, for a slight downward vertical gradient of  $0.0003$  ft. These magnitudes compare similarly in size (or are smaller than) both ambient (non-pumping) and IM pumping periods in other dual-screened wells at the site. For example, at R-45, during May 2020 (no pumping) the average downward vertical gradient was estimated at  $0.0016$  ft.

Injection along the eastern portion of the plume at CrIN-1, -2, and -3 modifies the water table by generally raising upper screen hydraulic heads. R-45 is strongly affected by CrIN-1 and -2, with the net effect of IM operation in the eastern area being a rise at both screen 1 and screen 2. R-45 shown in Figure 4.1-13, point A, demonstrates the effect of turning on CrIN-1 and -2 in the absence of CrEX-5 (both screen 1 and screen 2 rise sharply, with screen 1 greater than screen 2). When CrEX-5 is turned on along with CrIN-1 and -2 (point B), the injection wells still act to raise the water levels in screen 1 and screen 2 for the pumping rates at point B in Figure 4.1-13 (CrEX-5,  $89$  gpm; CrIN-1,  $49$  gpm; CrIN-2,  $48$  gpm). That is, CrEX-5 pumping somewhat counteracts the effects of injection at CrIN-1 and -2 at R-45, since the rise at point B is smaller than at point A. The impact of CrEX-5 alone is seen at point C, when CrEX-5 turns on with only minimal change in CrIN-1 (along with turning off CrIN-3, CrEX-4, and some other activity that is not expected to have a significant impact). At point C, the effect is that CrEX-5 appears to generate slightly larger and faster drawdown at screen 2 than screen 1.

The effects of eastern area IM operation on chromium concentrations in R-70 and other nearby wells will be further evaluated as additional data are collected. An early look at chromium concentrations at R-70 screen 1 and screen 2 in relation to nearby IM pumping is shown in Figure 4.1-14 (through March 2021). A steep drop in chromium concentrations in the January 2021 sample at R-70 screen 2 may be related to extraction-only operations in the area in late 2020. During the February 2021 sampling at R-70 screen 2, extraction at CrEX-5 is paused while injection occurs in CrIN-1 and -2, and the chromium concentrations appear to rebound. Before and during the March 2021 sampling, both extraction and injection are occurring. Additional data will help confirm the direct effects of IM operation on R-70 chromium

concentrations; the analysis so far is speculative in the absence of more months of consistent IM operation and sampling at R-70.

#### 4.1.3 Effect of Pumping Tests at R-70 on Other Monitoring Wells

Pumping tests were performed from May 20–28, 2019, following the installation of R-70 (N3B 2019, 700721). Activities included development testing and 24-hr tests at both screens. This section focuses on the effects of the R-70 aquifer tests on other nearby wells.

Figure 4.1-15 shows IM pumping and PM-3 activity before and during the time of the R-70 pumping tests. PM-3 was active, but the IM had paused operations on May 9, 2019. As discussed in section 4.1-1, any effect of PM-3 activity on R-70 screen 1 and screen 2 is not apparent. Therefore, PM-3 activity is not thought to affect any of the following analyses of the pumping tests.

Wells evaluated for the zone of influence of R-70's 24-hr pumping tests included CrEX-5, R-45, CrIN-1, R-11, R-35a/b, CrIN-2, R-13, R-44, R-28, R-36, and SIMR-2. Of these, response to the R-70 screen 1 and/or screen 2 pumping tests was clearly observed at CrEX-5, R-45 screen 1 and screen 2, CrIN-1, R-11, R-13, and R-44 screen 2. As discussed below, at CrIN-2 and R-44 screen 1, the response is less clear. There is no apparent response at R-35a or b, R-28, R-36, or SIMR-2.

Figure 4.1-16 shows the barometrically compensated water levels at CrEX-5 during the two pumping tests. CrEX-5 was collecting data on an hourly frequency. The R-70 screen 2 pumping test generated larger drawdown at CrEX-5 than the R-70 screen 1 pumping test, despite nearly identical pumping rates.

Figure 4.1-17 shows barometrically compensated water levels at CrIN-1 and R-13. Like CrEX-5, CrIN-1 shows an apparently greater drawdown due to the R-70 screen 2 pumping test than the screen 1 pumping test. R-13 shows a clear response, similar to that of CrIN-1.

Figure 4.1-18 shows barometrically compensated water levels at R-45 screen 1 and screen 2. R-45 screen 1 does not show a clear response to the R-70 screen 1 pumping test. Both screens appear to respond to the R-70 screen 2 test, but the effect is especially apparent at R-45 screen 2, which shows greater drawdown when R-70 screen 2 is pumped than when R-70 screen 1 is pumped.

Figure 4.1-19 shows R-35b water levels, both raw and barometrically compensated, along with the barometric pressure. The R-35b signal shows a high degree of variability, and the effect of the R-70 pumping tests (dashed vertical lines) is not discernable. The hydrograph for R-35a is not shown. R-35a was collecting data every 2 hr during the R-70 pumping tests, and PM-3 was active, which dominates the R-35a signal; any potential effects of the R-70 pumping tests on drawdown R-35a are not apparent.

Figure 4.1-20 shows barometrically compensated water levels at R-28 and R-11. It is unclear whether R-28 shows a discernable response, while R-11, as at the other wells, shows a larger drawdown in response to R-70 screen 2 pumping.

Figure 4.1-21 shows barometrically compensated water levels at CrIN-2. While the drawdown effect is minimal, it appears to follow the same pattern as the other wells, with a slightly greater response to the R-70 screen 2 pumping test.

Figure 4.1-22 shows barometrically compensated water levels at R-44 screen 1 and screen 2. The effect of the pumping tests on screen 1 is not discernable. At R-44 screen 2, there may be drawdown from the tests, particularly the R-70 screen 2 pumping test, but the effect is muted.

Figure 4.1-23 shows barometrically compensated water levels at R-36. The effect of the pumping tests is not discernable.

Figure 4.1-24 shows barometrically compensated water levels at SIMR-2. At SIMR-2, the effects of the R-70 pumping tests are likewise not visible.

Figure 4.1-25 illustrates the approximate hydraulic zone of influence at surrounding locations due to pumping at R-70 screen 1 and screen 2. Notably, the influence of pumping is felt a significant distance from R-70, but not at R-35a or R-35b, indicating that R-70 is either isolated from or too distant from PM-3 to be hydraulically connected. In all cases with an apparent drawdown caused by the R-70 screen 2 test is greater.

## 5.0 MODELING

The “Assessment Work Plan for the Evaluation of Conditions in the Regional Aquifer Around Well R-70” (N3B 2019, 700715) indicated that numerical modeling would be conducted as one of the methods used to evaluate data gaps in the monitoring network and to predict IM performance in the northeastern portion of the plume. In order to produce reliable modeling results useful for the objectives of this report, relatively steady-state chromium concentrations or a clear trend for chromium and water-level data from R-70 were necessary for robust calibration.

However, the data collected between August 2020 and March 2021 at R-70 screen 1 show significant variability in chromium concentrations, which may be related to the transient nature of IM operations in the area (e.g., pumping at CrEX-5) (Figure 4.1-14), plume variability, or the continued settling of geochemical conditions in the relatively new well. The temporal behavior of the calibration targets at R-70 would have had a considerable impact on model behavior in that area. In order for the model calibration to recognize and connect concentration targets to real processes, there needs to be enough data to correlate chromium concentration variability to physical processes such as IM pumping and injection or source-term characteristics.

Any model runs conducted without adequate calibration would have been considered too preliminary for supporting recommendations in this report.

Ongoing modeling will be conducted to incorporate data from R-70 (and other existing and planned wells, including R-73) for future applications, but the absence of modeling for this report did not adversely affect the recommendations in this report.

## 6.0 SUMMARY OF OBSERVATIONS

The high-resolution stratigraphy combined with estimated Ks from particle-size distributions provide a detailed characterization of the hydraulic structure of the regional aquifer. Permeable beds are distributed throughout the stratigraphic sequence regardless of geologic unit, and the regional aquifer where the plume is located is effectively a single highly heterogeneous hydrogeologic unit. The high-resolution stratigraphic information is supplemented by an assessment of mass flux distributions that uses order-of-magnitude differences in K to identify flow regimes in the aquifer. Mass flux distributions suggest large portions of the aquifer are characterized by advective flow. Preferential flow paths do not appear to be associated with particular geologic units, but rather regimes of higher groundwater flow likely occur where networks of interconnected high-K beds form in heterogeneous alluvial deposits.

The geochemical signature at R-70 screen 1 tends to corresponded closely to other northeastern plume-front wells such as R-11 and R-45 screen 1, but is not equivalent to the nearby extraction well CrEX-5, located approximately 750 feet upgradient and screened along the similar horizon as R-70 screen 1. The R-70 screen 2 geochemical signature is similar to upgradient wells CrEX-4, CrEX-5, R-28, and R-42. The contrast in chromium distribution between the two screens is significant, and could be related to the timing of effluent releases, and mixing of plume groundwater with clean ambient groundwater. Additional data (i.e., R-73 sample data) are needed to determine the origin and geochemical evolution of contamination at R-70 screen 1.

The potentiometric surface elevations in R-70 screen 1 and screen 2 exhibit no apparent response to pumping activity at PM-3. A hypothesis is that chromium-area monitoring wells are isolated from pressure responses generated by PM-3 pumping because most water production at PM-3 is generated from Miocene sedimentary deposits beneath a layer of Miocene basalt in the upper portion of the PM-3 screen. In this conceptual model, these basalts prevent or significantly limit pressure responses from transmitting from above or below.

The IM in the eastern portion of the plume is accomplishing the following:

- R-70 screen 1 and screen 2 are clearly within the hydraulic zone of influence of CrEX-5, with R-70 screen 2 showing greater drawdown in response to CrEX-5 pumping than screen 1,
- both screens at R-70 show response to CrIN-1, with screen 2 slightly more elevated than screen-1, and
- the effects of the next nearest pumping and injection wells (CrIN-2; CrEX-3 and -1) on R-70 are difficult to discern from the noise in the hydraulic head data.

The impact of the R-70 screen 1 and screen 2 pumping tests were reflected in drawdowns measured at various wells at least as far away as R-44. Consistent with the observations above, that R-70 screen 2 responds with greater drawdown to IM pumping and injection, the corollary is also seen that pumping at R-70 screen 2 appears to elicit greater drawdown at wells around the site than pumping at R-70 screen 1 at approximately the same rate.

## **7.0 CONCLUSIONS AND RECOMMENDATIONS**

The analysis of data in the R-70 area (geochemical, stratigraphic, hydraulic) leads to the recommendation that a new well, R-73, be drilled in the vicinity of R-70. A drilling work plan is proposed for submittal with a primary objective of characterizing the vertical extent of chromium contamination in the portion of the plume near R-70. Additional objectives for the well will be included in the drilling work plan.

The recommendation is also made at this time that well R-35c is not necessary to monitor the depth interval between R-35a and R-35b as a means to ensure protection of Los Alamos County water-supply well PM-3. The concern raised by NMED in correspondence submitted to EM-LA in September 2019 is that chromium contamination observed at R-70 screen 2 travels on a preferential pathway affected by the presence of the Puye pumiceous unit and/or by water-supply pumping at PM-3. While it is possible that PM-3 exerts a hydraulic influence at depths between lower monitoring screens in the R-70 area and the top of the louvers at PM-3, there is no evidence that at the depth of R-70 screen 2 there are significant hydraulic influences that would influence chromium migration at depths between R-35a and R-35b. Further, the Puye pumiceous unit pinches out significantly upgradient of the PM-3 area. There is no apparent evidence from existing data for hydraulic influence of PM-3 on R-70 screen 2 on the scale that would be necessary to influence groundwater migration at the depth of R-70 screen 2, which is discussed

in the context of stratigraphy and comparison with the different observed influence of PM-2 (section 4.1.1).

Information gleaned from the recommended well, R-73, is expected to provide additional insights into the potential need for additional monitoring in the R-70 area. The recommendation with respect to R-35c is that it is unnecessary to provide for protective monitoring of PM-3 beyond that already provided by sentinel wells R-35b and R-35a.

## 8.0 REFERENCES AND MAP DATA SOURCES

### 8.1 References

*The following reference list includes documents cited in this report. Parenthetical information following each reference provides the author(s), publication date, and ERID, ESHID, or EMID. This information is also included in text citations. ERIDs were assigned by the Laboratory's Associate Directorate for Environmental Management (IDs through 599999); ESHIDs were assigned by the Laboratory's Associate Directorate for Environment, Safety, and Health (IDs 600000 through 699999); and EMIDs are assigned by Newport News Nuclear BWXT-Los Alamos, LLC (N3B) (IDs 700000 and above). IDs are used to locate documents in N3B's Records Management System and in the Master Reference Set. The NMED Hazardous Waste Bureau and N3B maintain copies of the Master Reference Set. The set ensures that NMED has the references to review documents. The set is updated when new references are cited in documents.*

Broxton, D., G. WoldeGabriel, D. Katzman, and R. Harris, March 8–12, 2021. "Using High-Resolution Stratigraphic Characterization to Inform Remediation Strategies for a Hexavalent Chromium Plume at Los Alamos National Laboratory," Waste Management 2021 Conference, March 8–12, 2021, Phoenix, Arizona. (Broxton et al. 2021, 701441)

DOE (U.S. Department of Energy), August 7, 2019. "Extension Request for Submittal of Two Drilling Work Plans for Monitoring Wells R-35c and R-73," U.S. Department of Energy letter (EM-LA-40DH-00491) to J.E. Kieling (NMED-HWB) from D. Hintze (EM-LA), Los Alamos, New Mexico. (DOE 2019, 700531)

DOE (U.S. Department of Energy), October 28, 2019. "Response to NMED's Letter Dated August 21, 2019; Approval Extension Request for Submittal of Two Drilling Work Plans for Monitoring Well R-35c and R-73," U.S. Department of Energy letter (EMLA-2020-1001-00-001) to J.E. Kieling (NMED-HWB) from D. Hintze (EM-LA), Los Alamos, New Mexico. (DOE 2019, 700650)

Folk, R.L., 1980. *Petrology of Sedimentary Rocks*, Hemphill Publishing Company, Austin, Texas. (Folk 1980, 701455)

Gonthier, G.J., 2007. "A Graphical Method for Estimation of Barometric Efficiency from Continuous Data—Concepts and Application to a Site in the Piedmont, Air Force Plant 6, Marietta, Georgia," prepared in cooperation with U.S. Air Force Aeronautical Systems Center, Marietta, Georgia, U.S. Geological Survey Scientific Investigations Report 2007-5111. (Gonthier 2007, 701330)

Horst, J., S. Potter, M. Schnobrich, N. Welty, A. Gupta, and J. Quinnan, "Advancing Contaminant Mass Flux Analysis to Focus Remediation: The Three-Compartment Model," *Groundwater Monitoring and Remediation*, Vol. 37, No. 4, pp. 15-22. (Horst et al. 2017, 701456)

- LANL (Los Alamos National Laboratory), October 2009. "Investigation Report for Sandia Canyon," Los Alamos National Laboratory document LA-UR-09-6450, Los Alamos, New Mexico. (LANL 2009, 107453)
- LANL (Los Alamos National Laboratory), May 2015. "Completion Report for Chromium Project Coreholes 1 through 5," Los Alamos National Laboratory document LA-UR-15-23197, Los Alamos, New Mexico. (LANL 2015, 600457)
- LANL (Los Alamos National Laboratory), March 2018. "Compendium of Technical Reports Conducted Under the Work Plan for Chromium Plume Center Characterization," Los Alamos National Laboratory document LA-UR-18-21450, Los Alamos, New Mexico. (LANL 2018, 602964)
- LANL (Los Alamos National Laboratory), April 2018. "Evaluation of Chromium Plume Control Interim Measure Operational Alternatives for Injection Well CrIN-6," Los Alamos National Laboratory document LA-UR-18-23385, Los Alamos, New Mexico. (LANL 2018, 603032)
- McLin, S., January 2006. "Analyses of the PM-4 Aquifer Test Using Multiple Observation Wells," Los Alamos National Laboratory report LA-14252-MS, Los Alamos, New Mexico. (McLin 2006, 092218)
- N3B (Newport News Nuclear BWXT-Los Alamos, LLC), December 2019. "Assessment Work Plan for the Evaluation of Conditions in the Regional Aquifer Around Well R-70," Newport News Nuclear BWXT-Los Alamos, LLC, document EM2019-0458, Los Alamos, New Mexico. (N3B 2019, 700715)
- N3B (Newport News Nuclear BWXT-Los Alamos, LLC), December 2019. "Completion Report for Regional Aquifer Well R-70," Newport News Nuclear BWXT-Los Alamos, LLC, document EM2019-0365, Los Alamos, New Mexico. (N3B 2019, 700721)
- N3B (Newport News Nuclear BWXT-Los Alamos, LLC), March 2021. "Semiannual Progress Report on Chromium Plume Control Interim Measure Performance, July through December 2020," Newport News Nuclear BWXT-Los Alamos, LLC, document EM2021-0110, Los Alamos, New Mexico. (N3B 2021, 701366)
- NMED (New Mexico Environment Department), July 12, 2019. "Results from Regional Groundwater Monitoring Well R-70," New Mexico Environment Department letter to D. Hintze (EM-LA) from J.E. Kielling (NMED-HWB), Santa Fe, New Mexico. (NMED 2019, 700508)
- NMED (New Mexico Environment Department), August 21, 2019. "Approval Extension Request for Submittal of Two Drilling Work Plans for Monitoring Wells R-35c and R-73," New Mexico Environment Department letter to D. Hintze (EM-LA) from J.E. Kielling (NMED-HWB), Santa Fe, New Mexico. (NMED 2019, 700549)
- NMED (New Mexico Environment Department), April 14, 2020. "Approval, Submittal of the Assessment Work Plan for the Evaluation of Conditions in the Regional Aquifer Around Well R-70," New Mexico Environment Department letter to A. Duran (EM-LA) from K. Pierard (NMED-HWB), Santa Fe, New Mexico. (NMED 2020, 700852)

Purtymun, W.D., January 1995. "Geologic and Hydrologic Records of Observation Wells, Test Holes, Test Wells, Supply Wells, Springs, and Surface Water Stations in the Los Alamos Area," Los Alamos National Laboratory report LA-12883-MS, Los Alamos, New Mexico. (Purtymun 1995, 045344)

Rasmussen, T.C., and L.A. Crawford, 1997. "Identifying and Removing Barometric Pressure Effects in Confined and Unconfined Aquifers," *Ground Water*, Vol. 35, No. 3, pp. 502-511. (Rasmussen and Crawford 1997, 094014)

Spane, F.A., 2002. "Considering Barometric Pressure in Groundwater Flow Investigations," *Water Resources Research*, Vol. 38, No. 6, pp. 1-18. (Spane 2002, 602105)

## 8.2 Map Data Sources

Hillshade; Los Alamos National Laboratory, ER-ES, As published;  
\\slip\gis\Data\HYP\LiDAR\2014\Bare\_Earth\BareEarth\_DEM\_Mosaic.gdb; 2014.

Unpaved roads; Los Alamos National Laboratory, ER-ES, As published, GIS projects folder;  
\\slip\gis\GIS\Projects\14-Projects\14-0062\project\_data.gdb\digitized\_site\_features\digitized\_roads; 2017.

Drainage channel; Los Alamos National Laboratory, ER-ES, As published, GIS projects folder;  
\\slip\gis\GIS\Projects\15-Projects\15-0080\project\_data.gdb\correct\_drainage; 2017.

Structures; Los Alamos National Laboratory, KSL Site Support Services, Planning, Locating and Mapping Section; 06 January 2004; as published 29 November 2010.

Paved Road Arcs; Los Alamos National Laboratory, FWO Site Support Services, Planning, Locating and Mapping Section; 06 January 2004; as published 29 November 2010.

Chromium plume > 50 ppb; Los Alamos National Laboratory, ER-ES, As published;  
\\slip\gis\GIS\Projects\13-Projects\13-0065\shp\chromium\_plume\_2.shp; 2018.

Regional groundwater contour May 2017, 4-ft interval; Los Alamos National Laboratory, ER-ES, As published; \\slip\gis\GIS\Projects\16-Projects\16-0027\project\_data.gdb\line\contour\_wl2017may\_2ft; 2017.

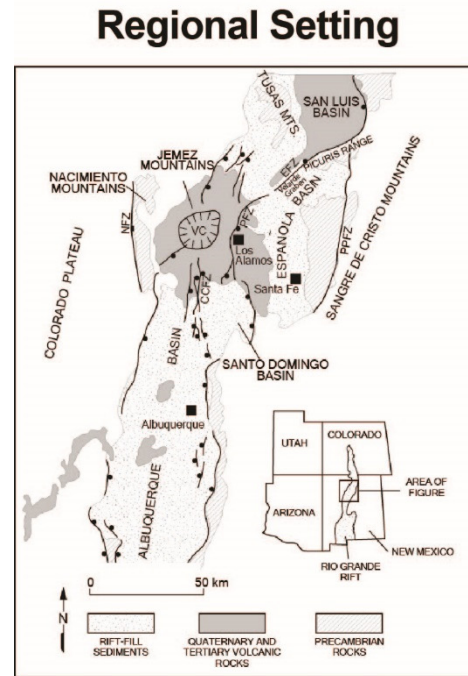
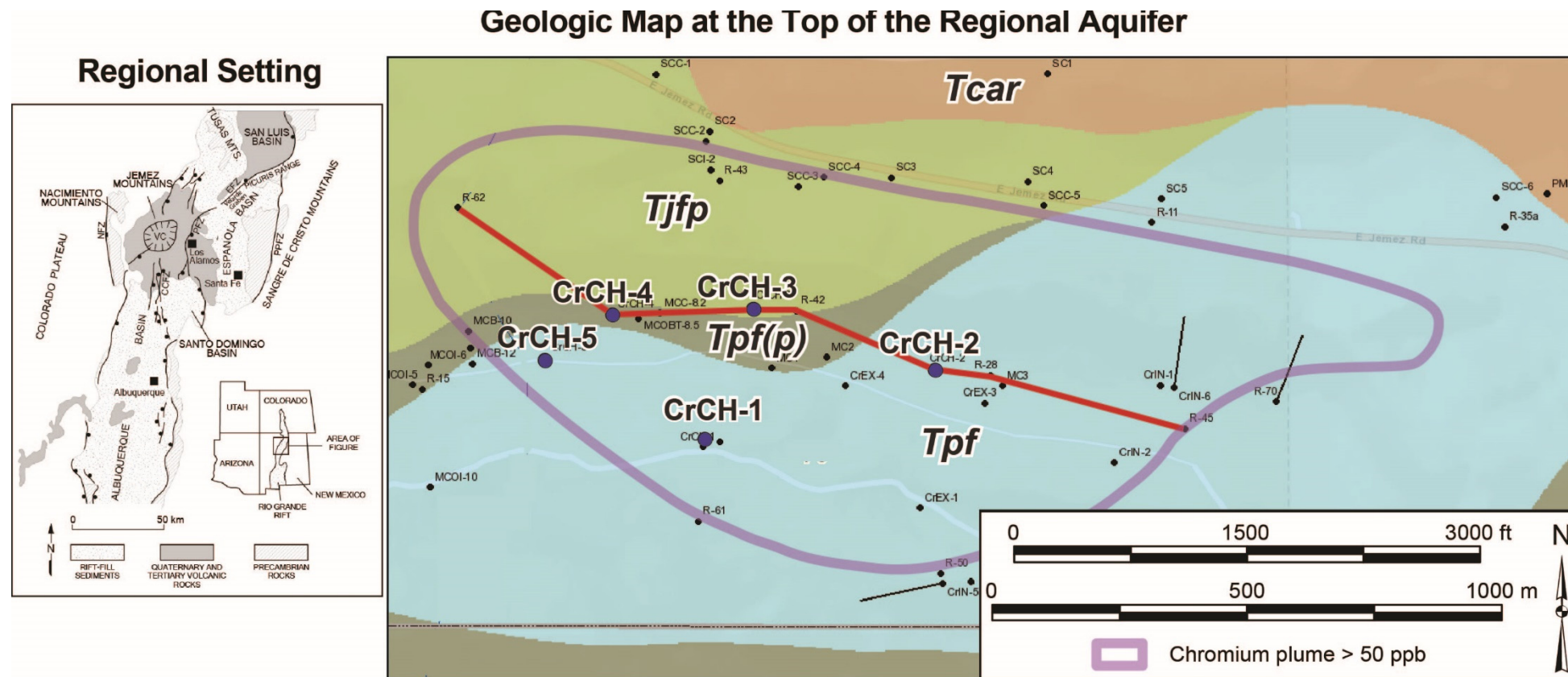
Regional groundwater contour November 2017, 2-ft interval; Los Alamos National Laboratory, ER-ES, As published; \\slip\gis\GIS\Projects\16-Projects\16-0027\project\_data.gdb\line\contour\_wl2017nov\_2ft; 2017.

Point features; As published; EIM data pull; 2017.

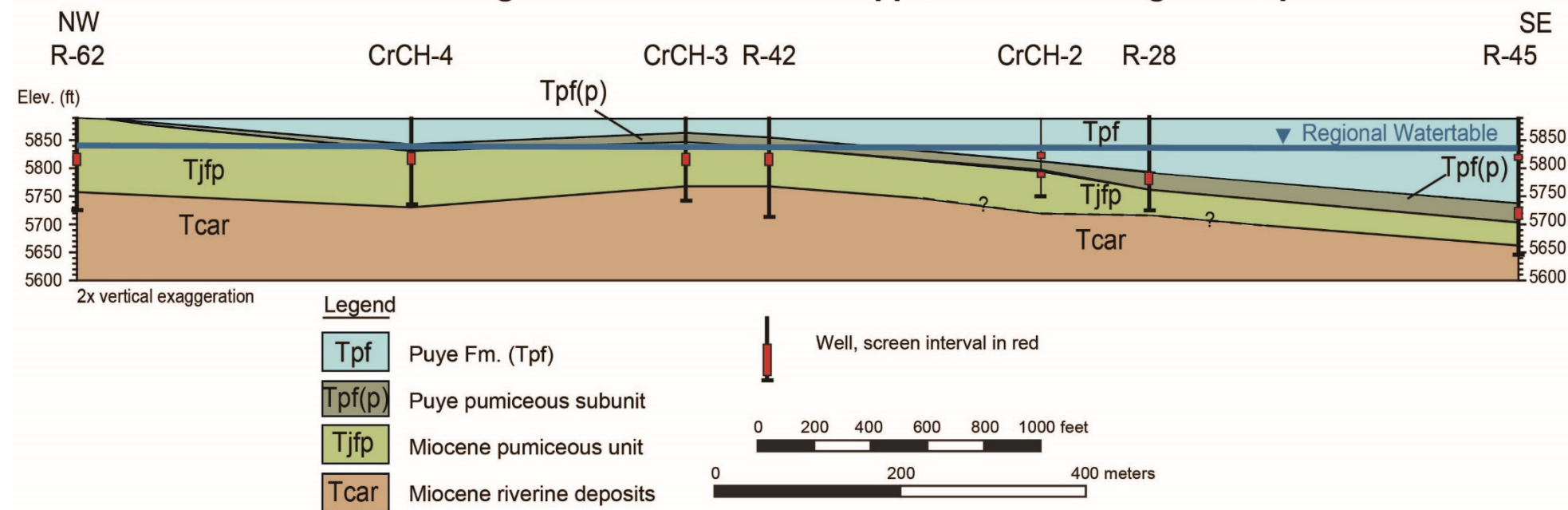
Technical Area Boundaries; Los Alamos National Laboratory, Site Planning & Project Initiation Group, Infrastructure Planning Office; September 2007; as published 13 August 2010.





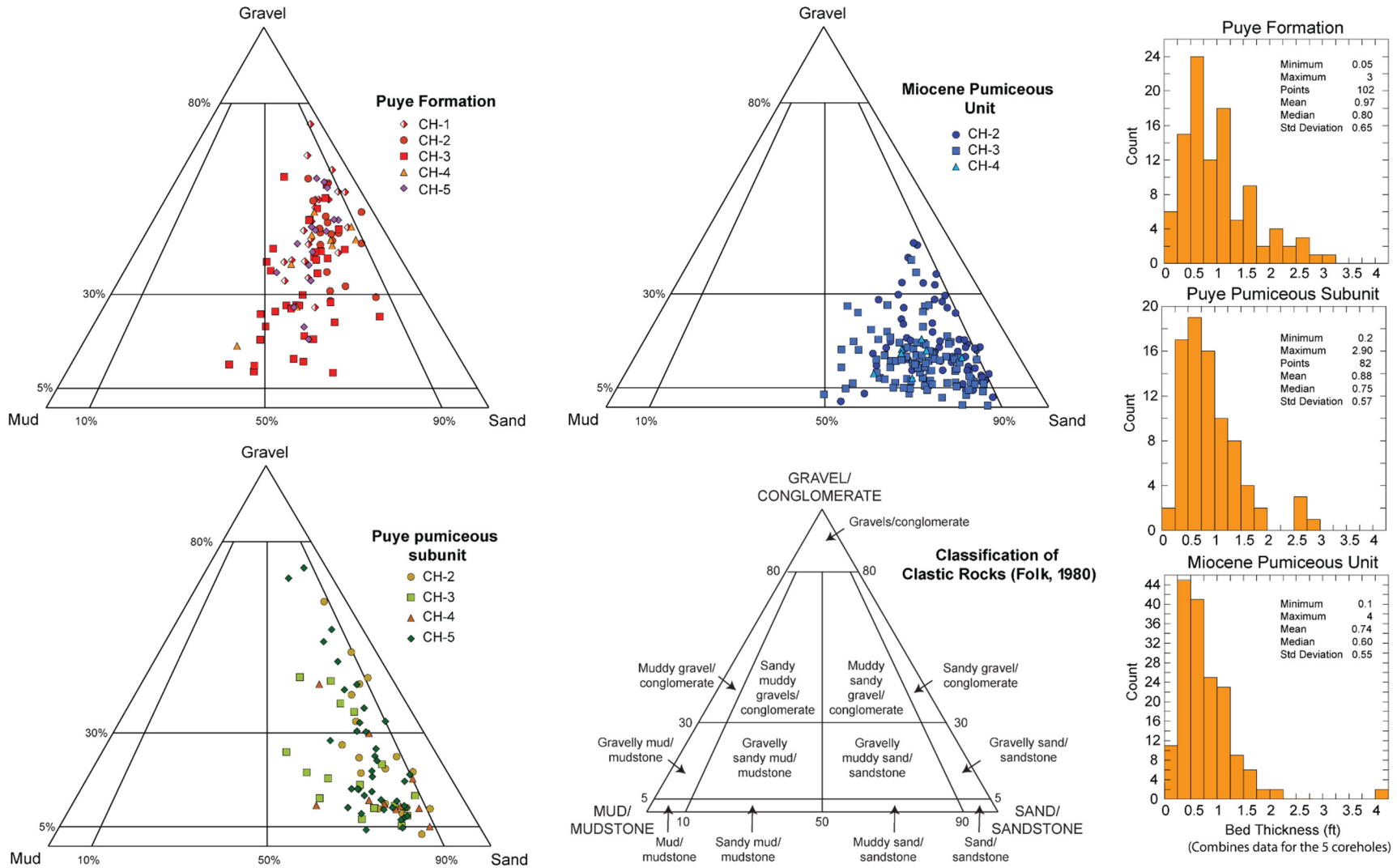


### NW-SE Geologic Cross Section in the Upper Part of the Regional Aquifer



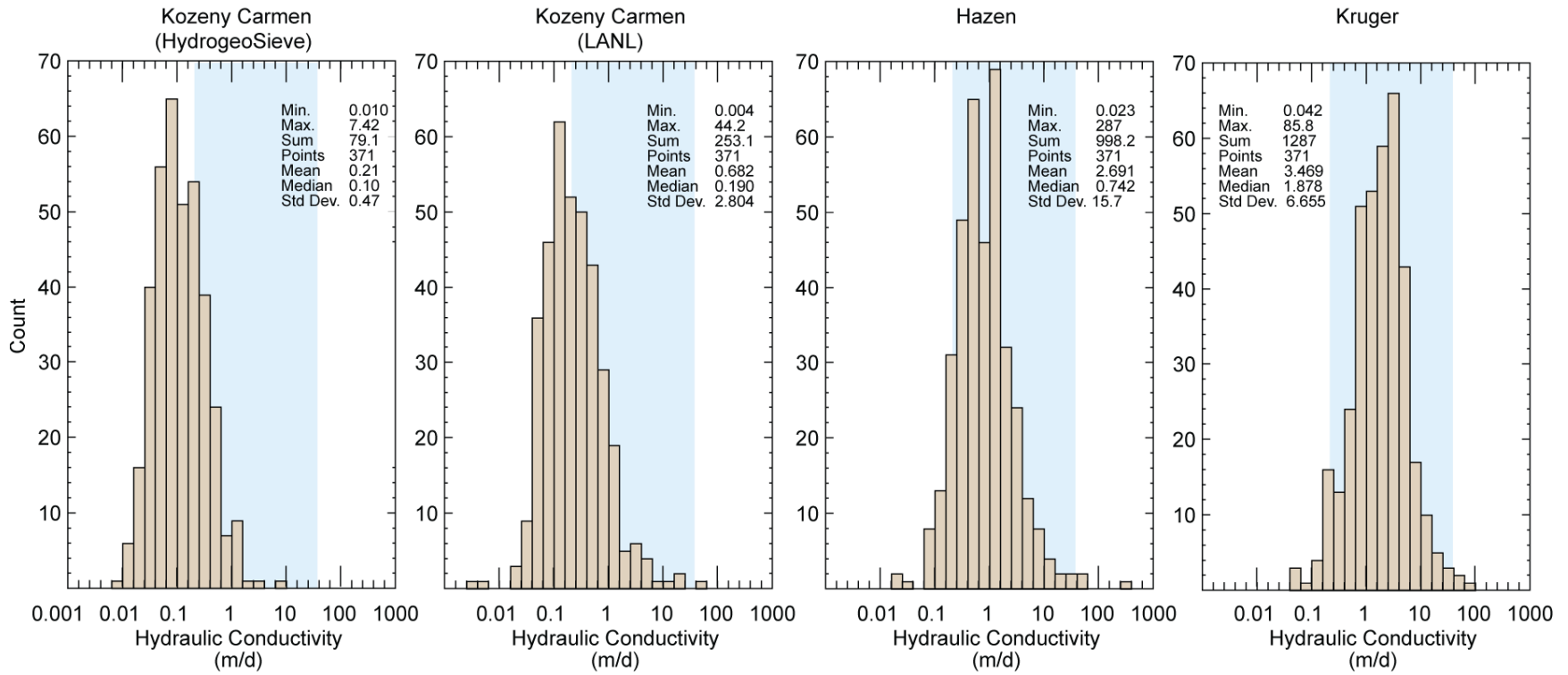
Note: Line of section is shown in upper figure.

**Figure 2.0-1** Geologic map at the top of the regional aquifer and geologic cross-section for the upper part of the regional aquifer in the chromium plume at Los Alamos National Laboratory



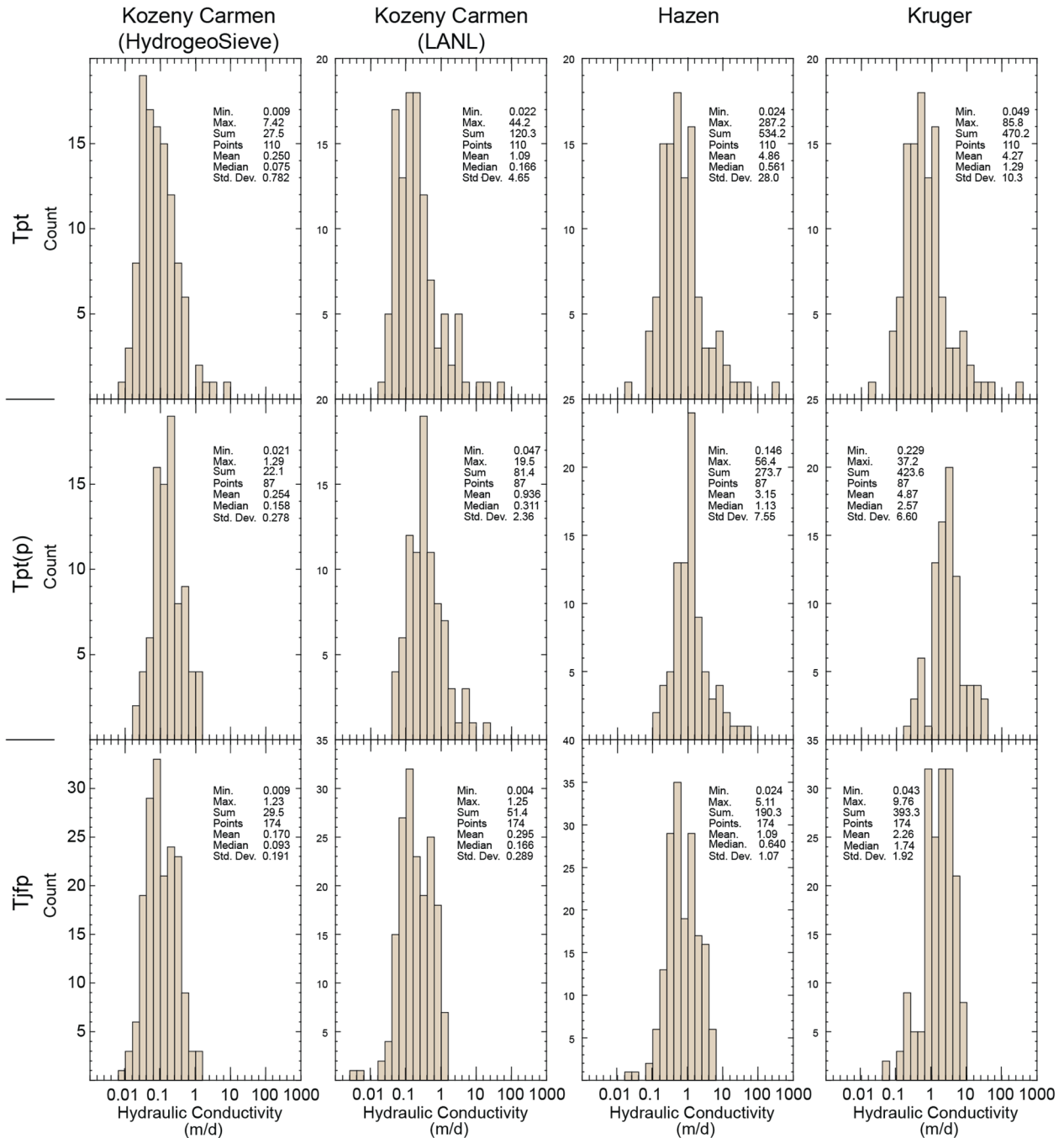
Note: Histograms show bedding thicknesses for the geologic units.

**Figure 2.1-1 Clastic rock classification of Pliocene and Miocene geologic units at the top of the regional aquifer beneath Mortandad Canyon based on particle-size data for cores collected from CrCH-1, CrCH-2, CrCH-3, CrCH-4, and CrCH-5**



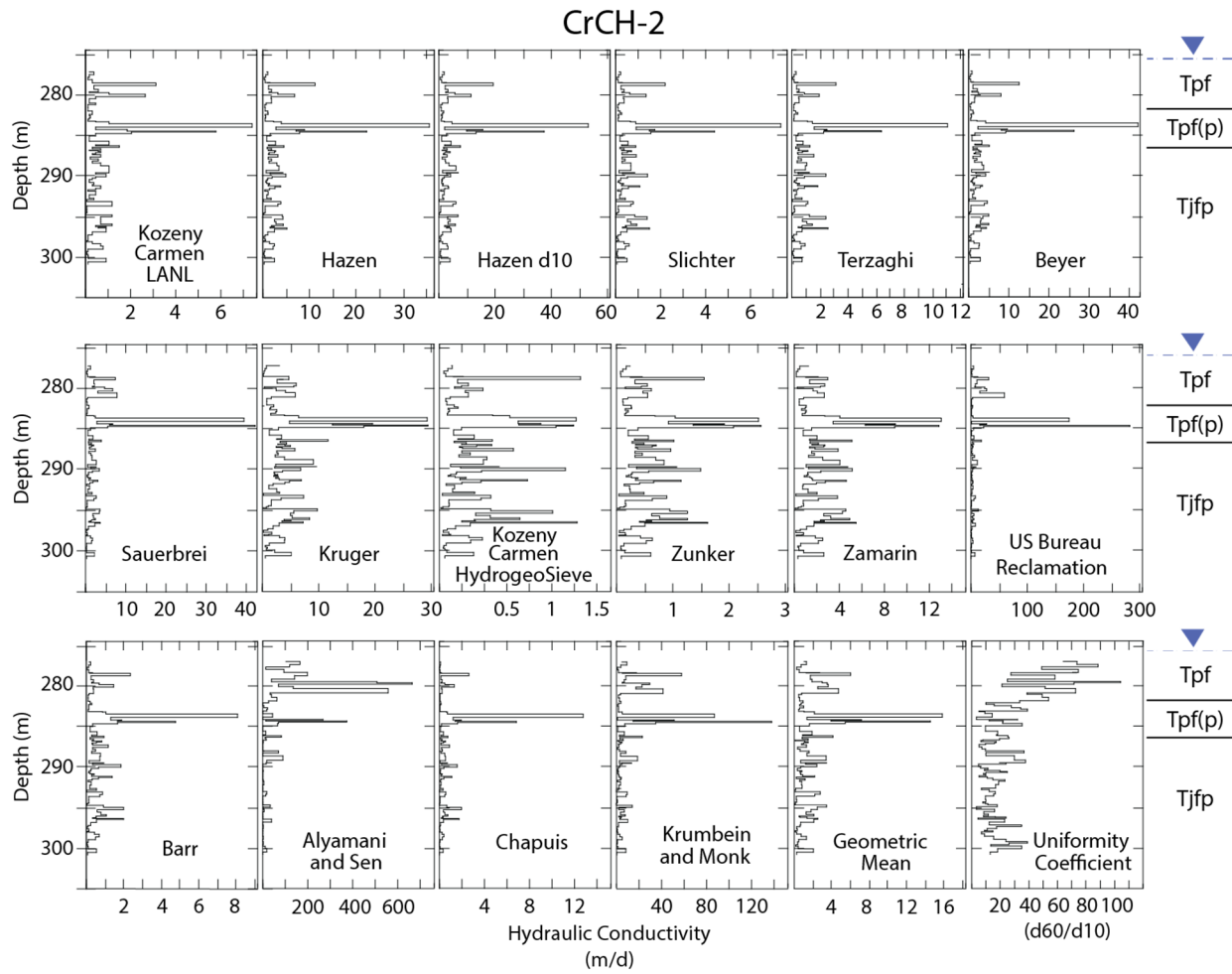
Notes: Ks represent data for all core holes combined. The range of Ks determined by aquifer tests conducted in nearby wells is shown as blue shading for reference.

**Figure 2.2-1 Histograms of K for four of the K estimation methods used in this study**



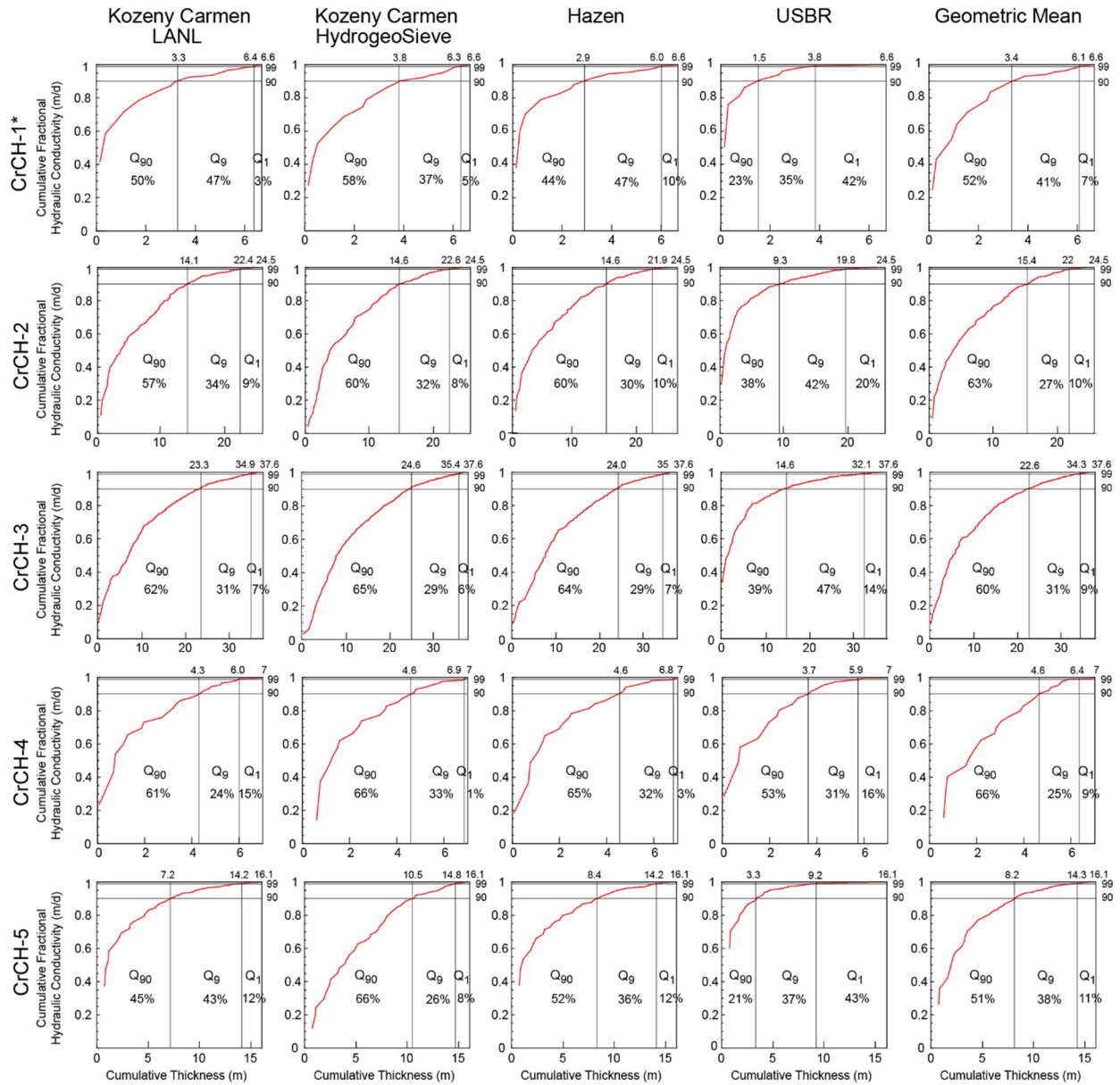
Note: Geologic units are Puye Formation (Tpf), Pumiceous Subunit of the Puye Formation [Tpf(p)], and Miocene Pumiceous Unit (Tjfp).

**Figure 2.2-2** Histograms comparing Ks by geologic unit for four of the K estimation methods



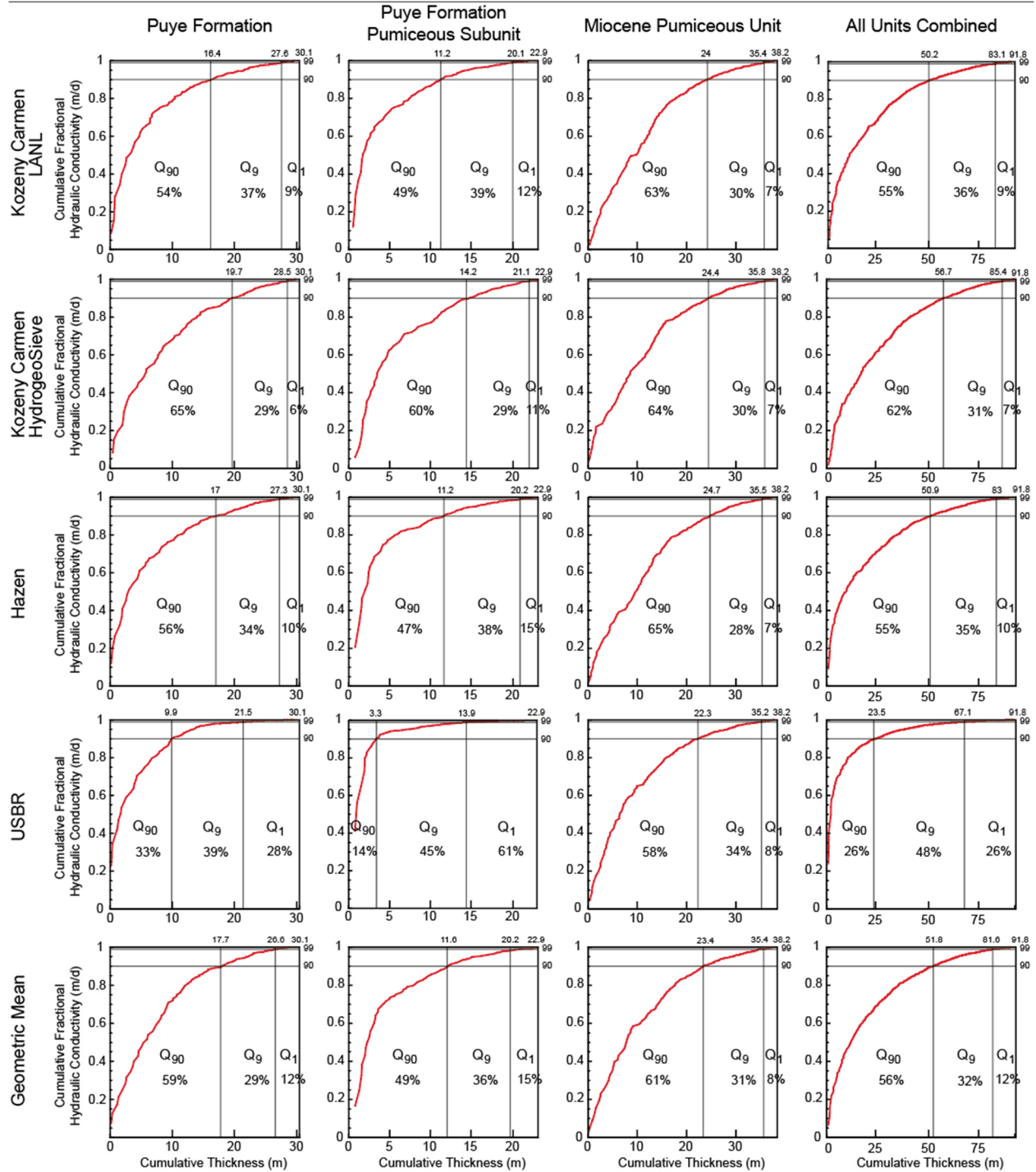
Note: Regional water table shown as inverted triangle, and geologic units are Puye Formation (Tpf), Pumiceous Subunit of the Puye Formation [Tpf(p)], and Miocene Pumiceous Unit (Tjfp).

**Figure 2.2-3 High-resolution vertical profiles of Ks in the regional aquifer at core hole CrCH-2 by various K estimation methods**



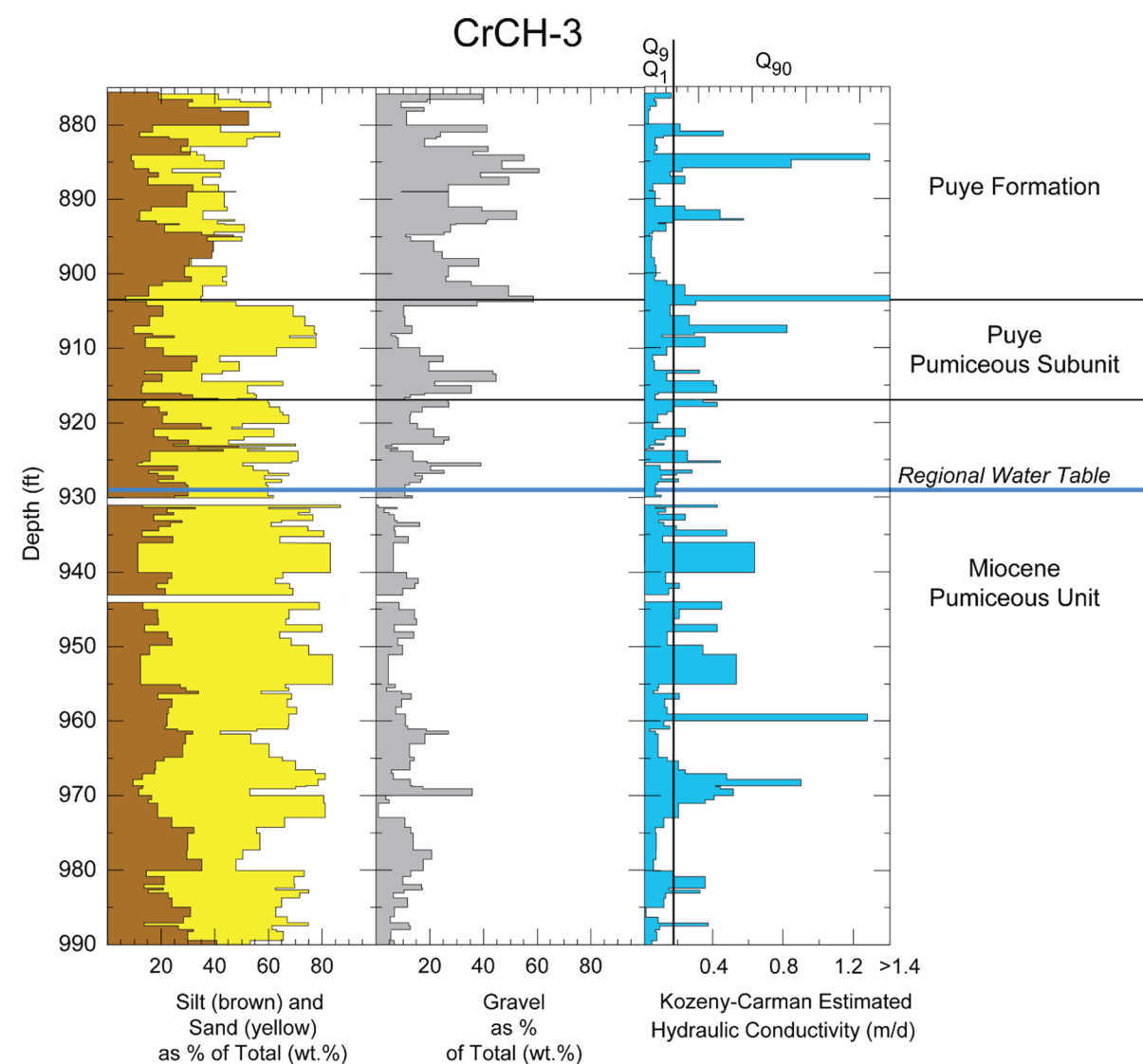
Note: Five methods for estimating Ks are shown.

**Figure 2.3-1 Cumulative flow distribution plots for core holes based on Ks determined from particle-size data**



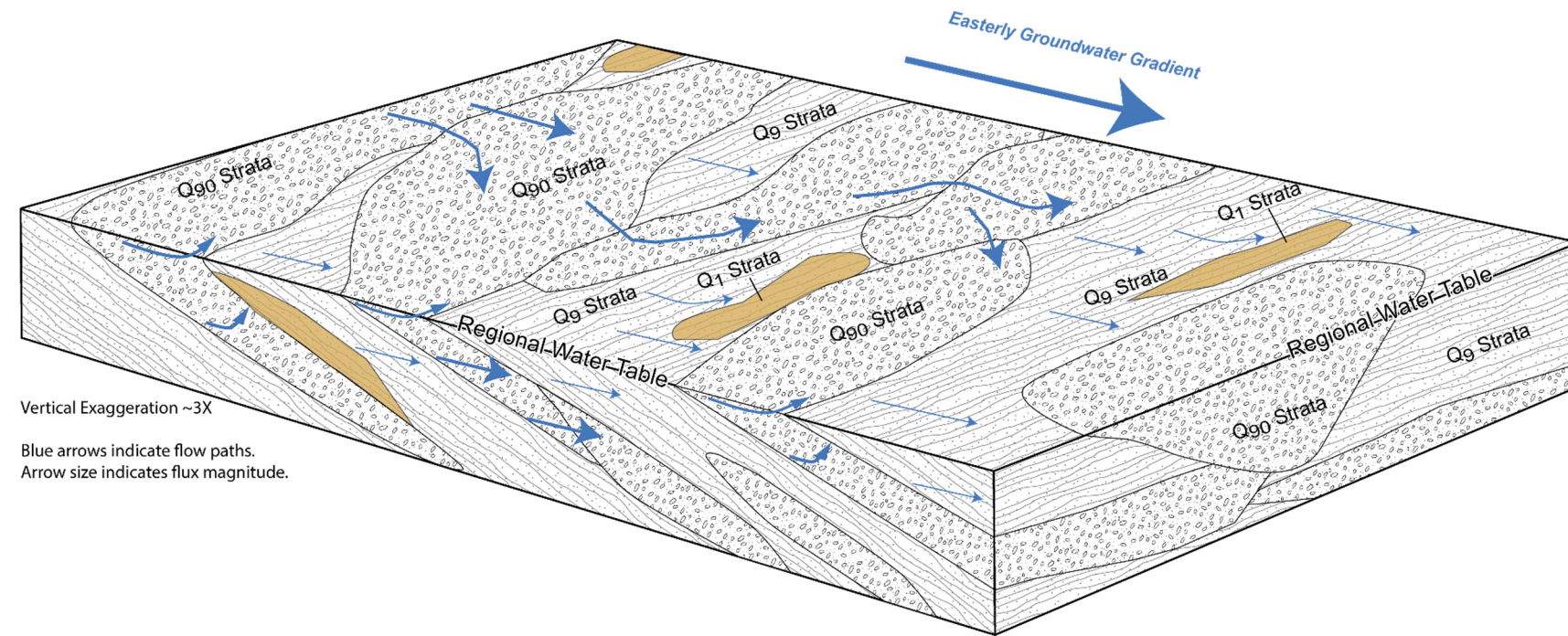
Note: Five methods for estimating Ks are shown.

**Figure 2.3-2 Cumulative flow distribution plots for the Puye Formation (Tpf), pumiceous subunit of the Puye Formation [Tpf(p)], and Miocene pumiceous unit (Tjfp)**



Note: Gaps indicate no core collected.

**Figure 2.3-3 High-resolution stratigraphy for core hole CrCH-3 showing distribution of Q90 beds**



Note: Advective flow (Q90) occur where high permeability beds are juxtaposed by erosional and depositional processes.

Figure 2.4-1 Conceptual geologic block diagram showing potential groundwater flow paths in heterogeneous alluvial fan deposits

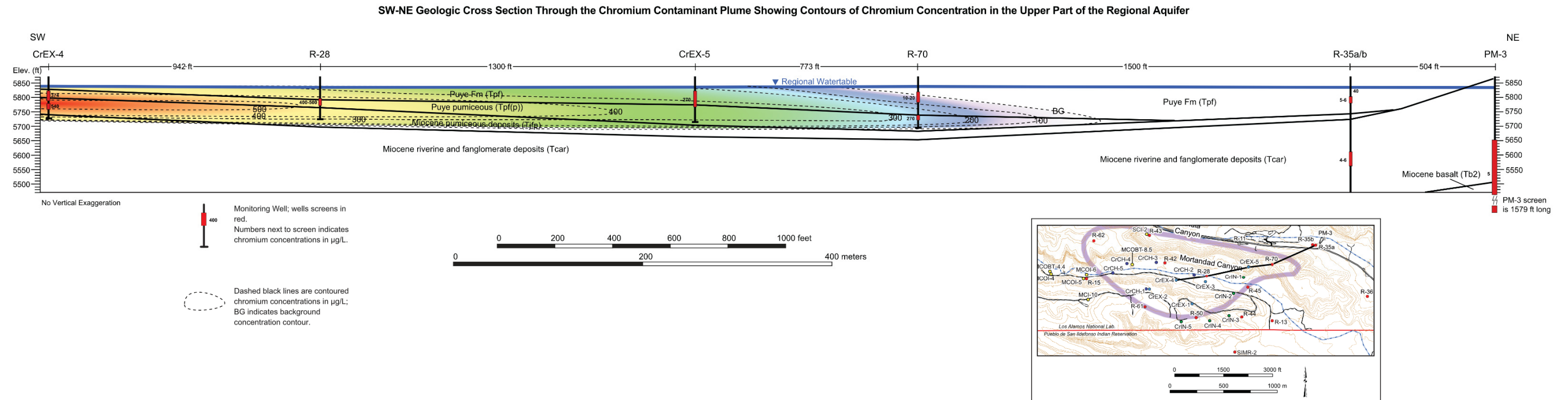


Figure 2.4-2 Geologic cross-section between wells CrEX-4 and PM-3 showing potential groundwater flow paths that cross geologic units

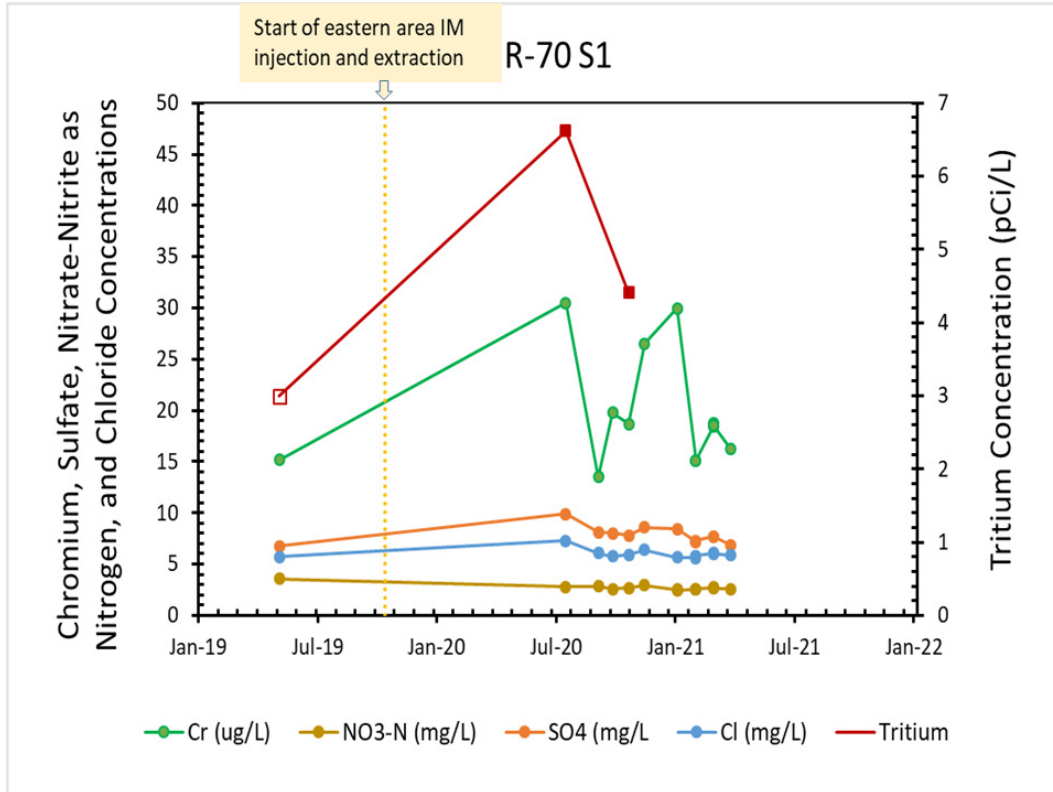


Figure 3.1-1 R-70 screen 1 trends in chromium and other solutes

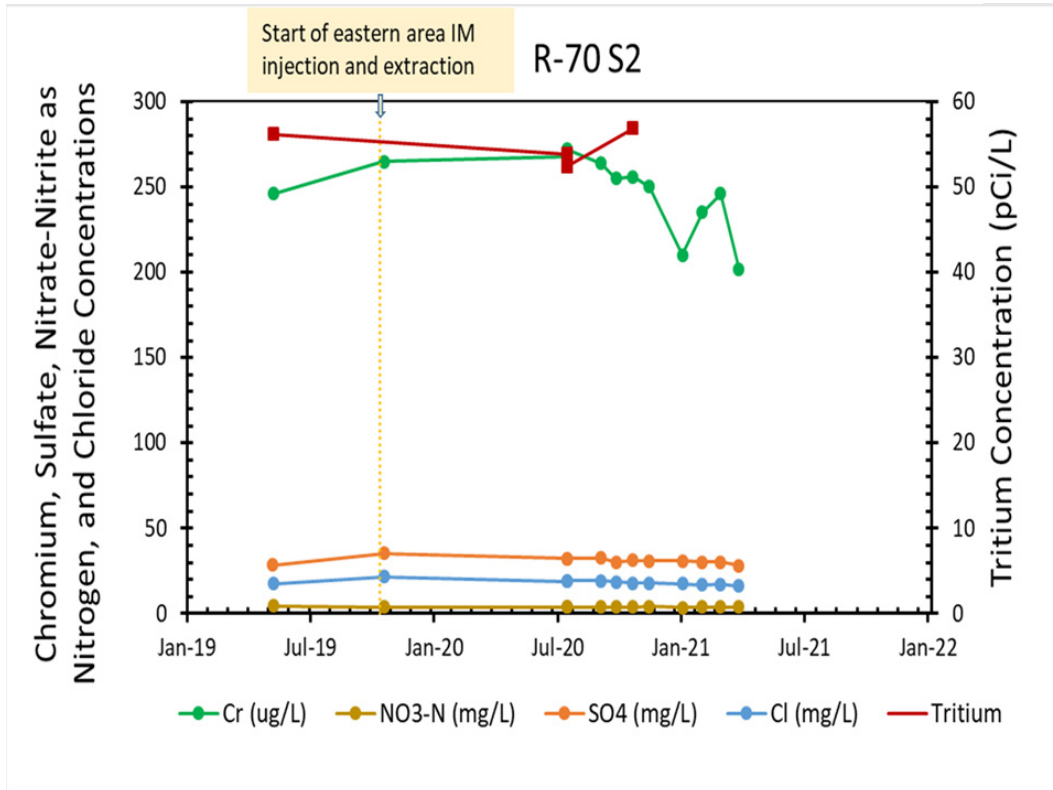


Figure 3.1-2 R-70 screen 2 trends in chromium and other solutes

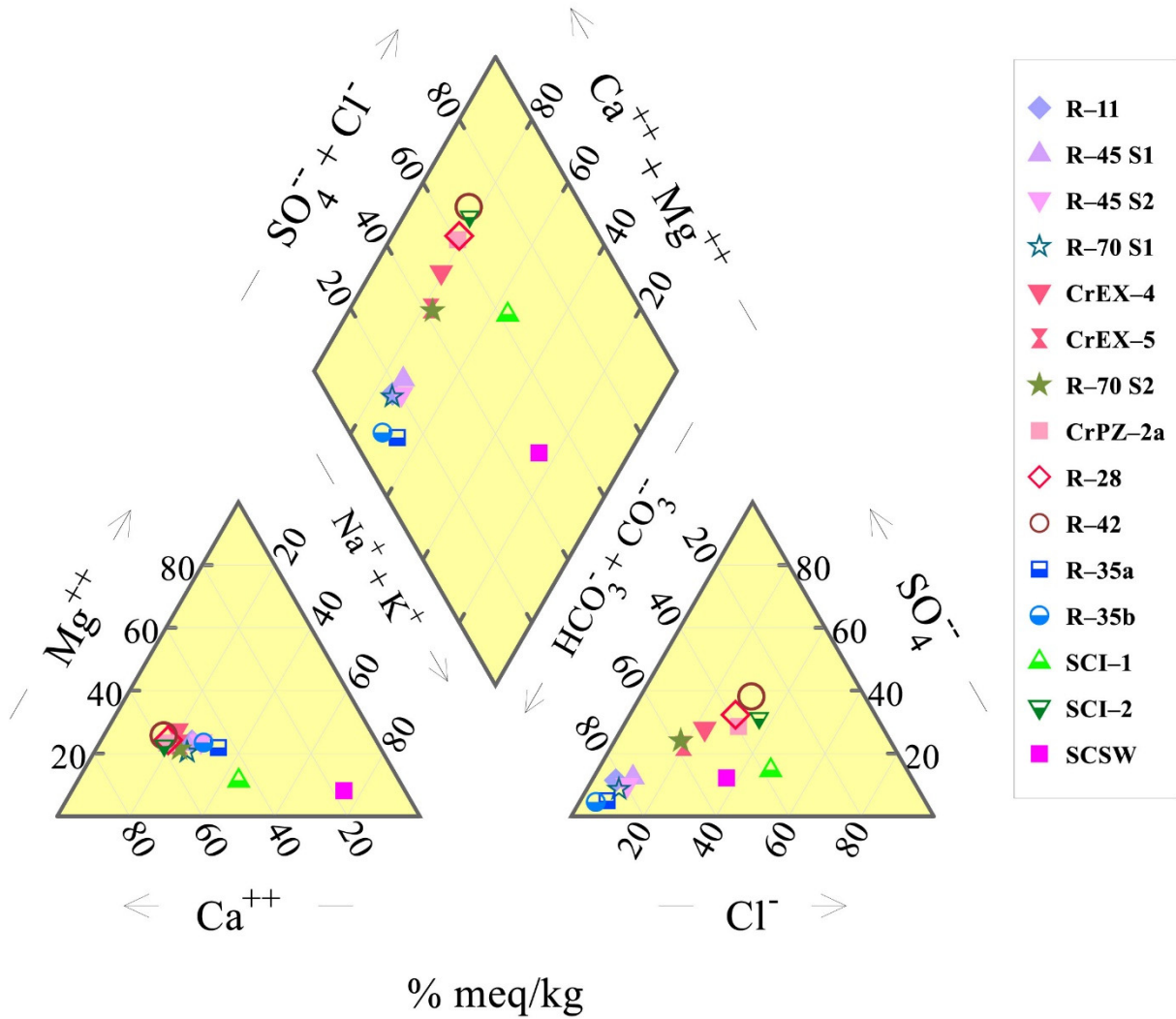


Figure 3.2-1 R-70 screen 1 Piper diagram illustrating the geochemical evolution of plume migration from the plume centroid near R-42 towards R-70 screen 2

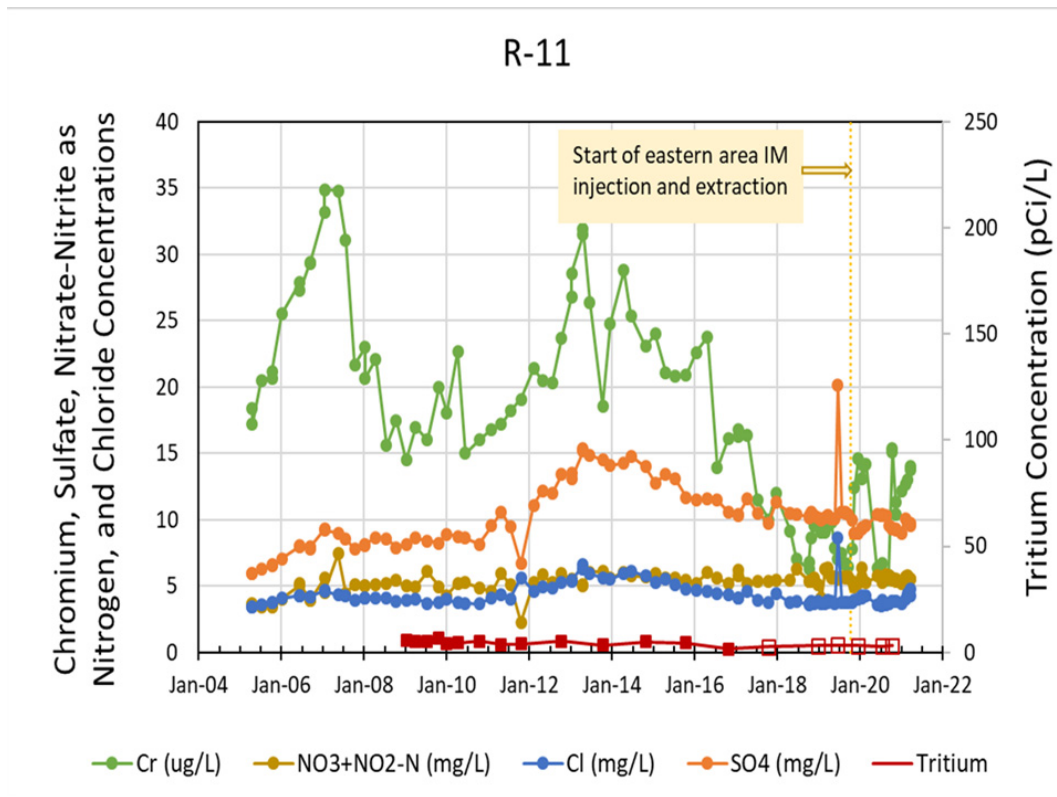


Figure 3.2-2 R-11 trends in chromium and other constituents

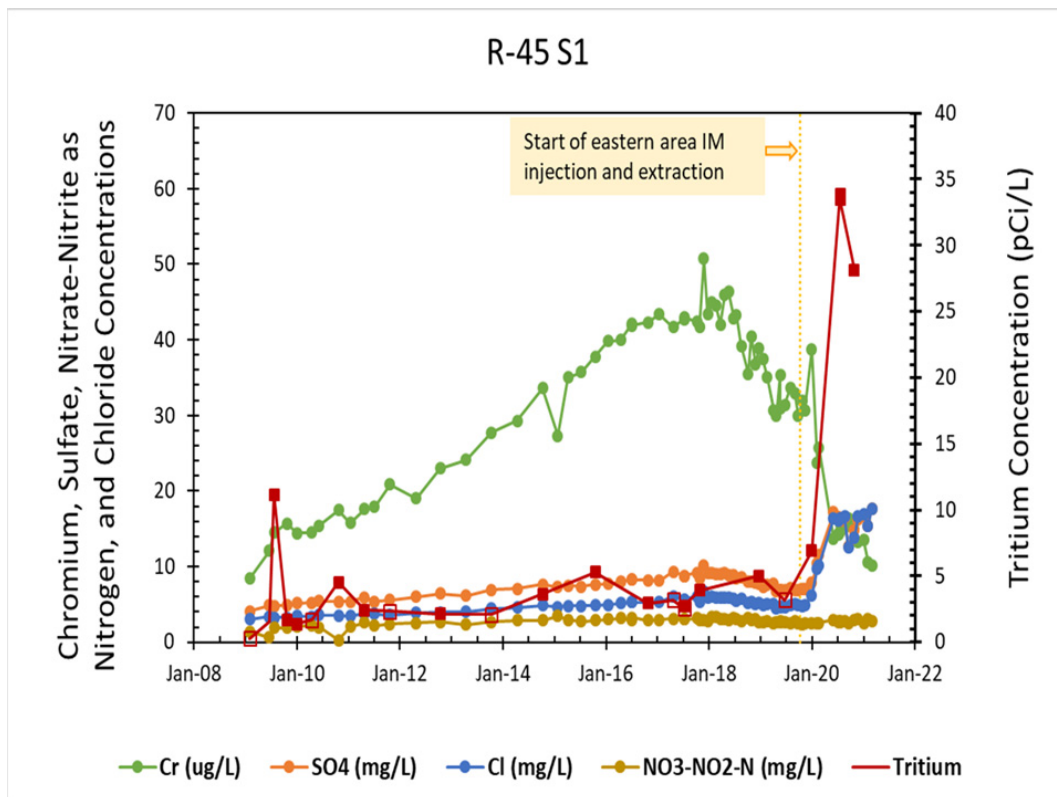
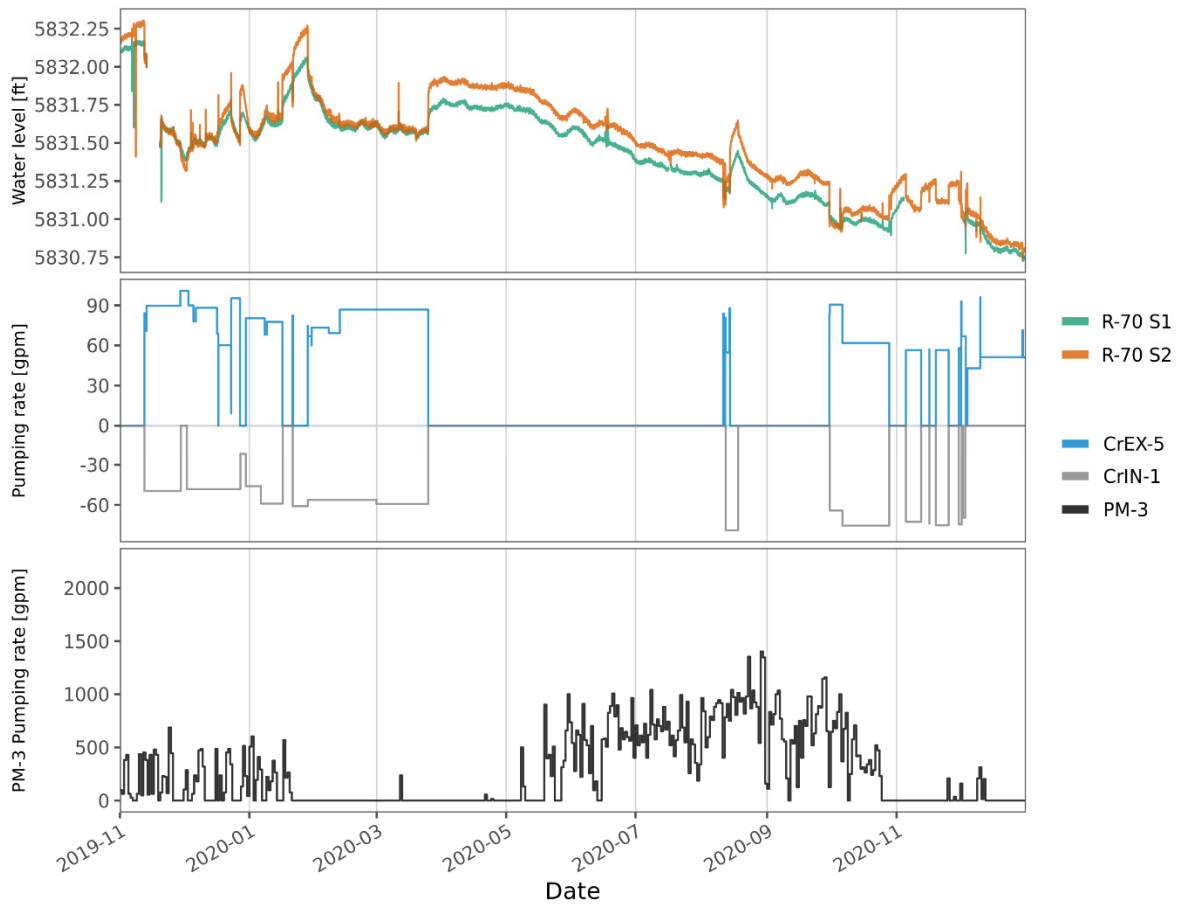
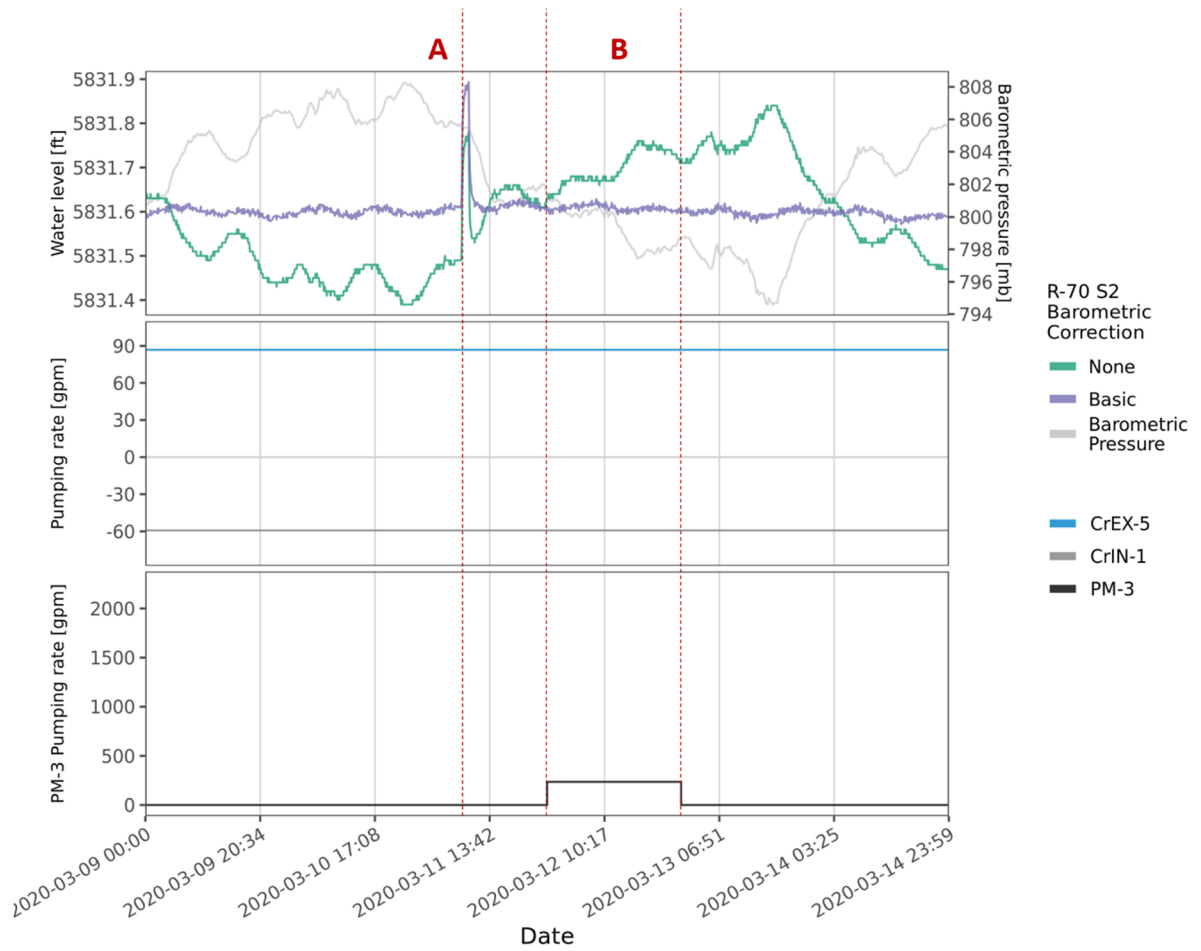


Figure 3.2-3 R-45 screen 1 trends in chromium and other constituents



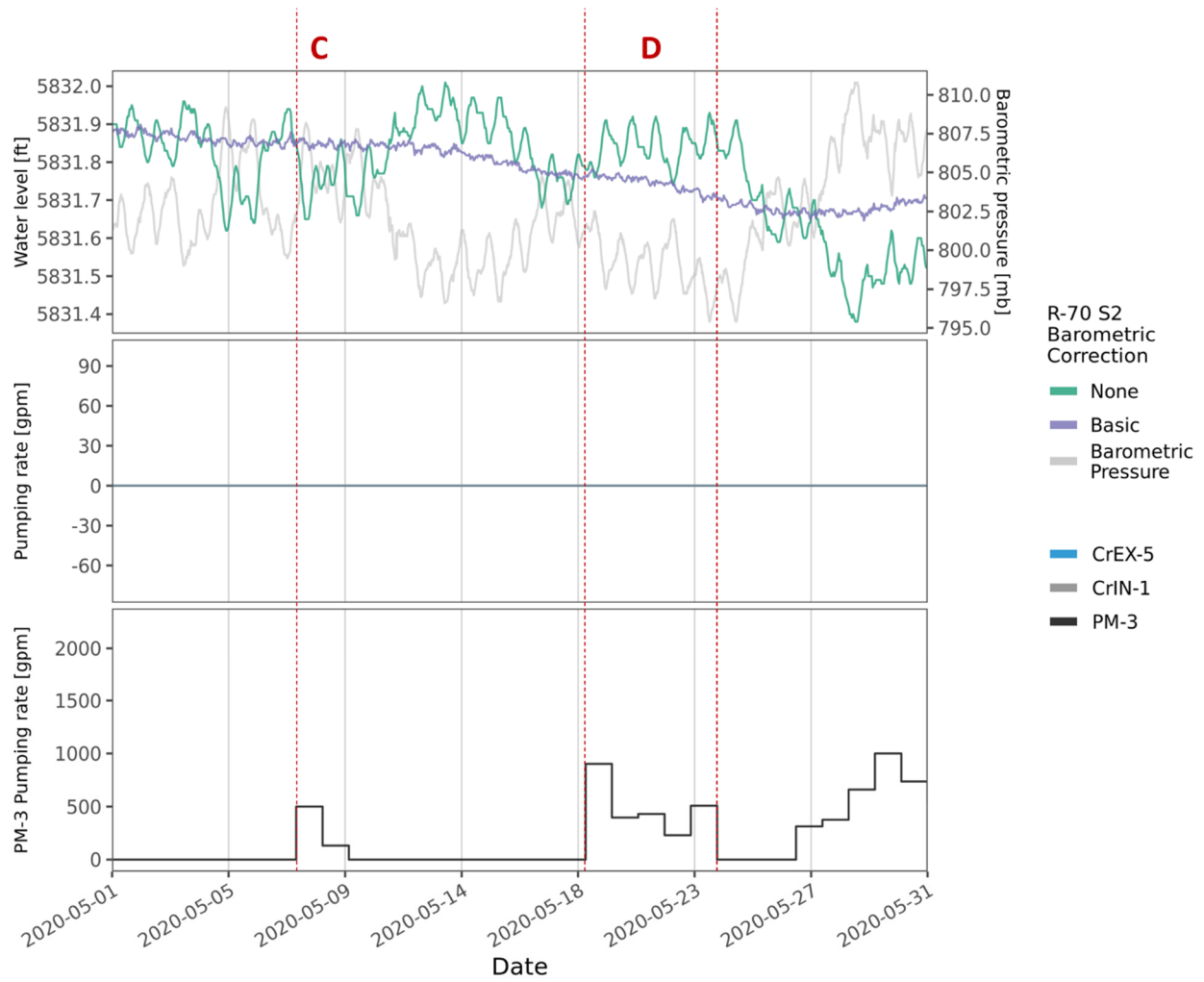
Notes: Top panel shows water-level data with the “basic” correction method described in the text. Middle panel shows CrEX-5 and CrIN-1 pumping rates (negative pumping rates represent injection). Bottom panel shows PM-3 pumping rates.

**Figure 4.1-1 Hydrograph for R-70 screen 1 and screen 2 from installation to December 31, 2020**



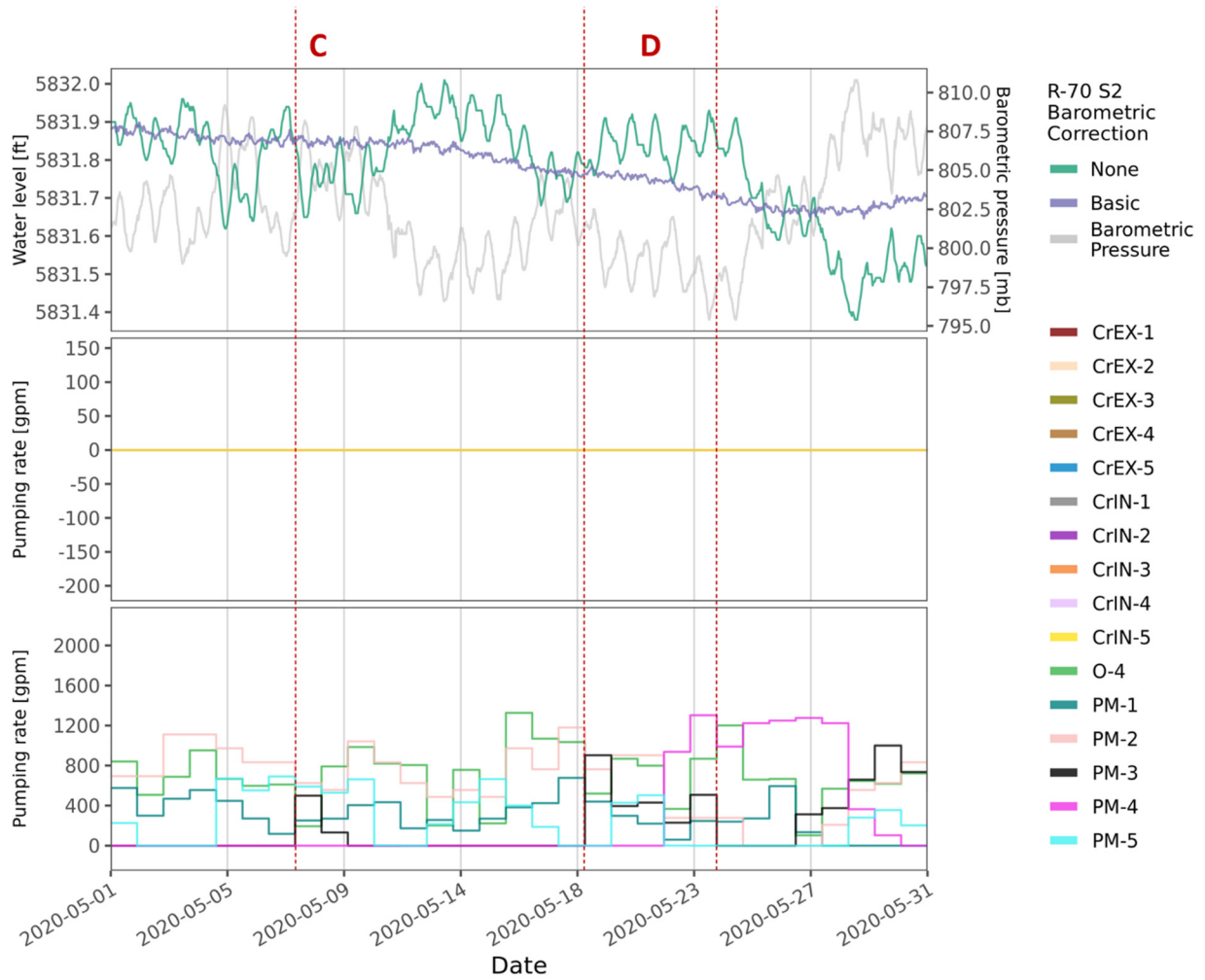
Notes: Top panel shows water-level data with the “basic” correction method described in the text. Middle panel shows CrEX-5 and CrIN-1 pumping rates (negative pumping rates represent injection). Bottom panel shows PM-3 pumping rates.

**Figure 4.1-2 Hydrograph for R-70 screen 2 from March 9 to 14, 2020**



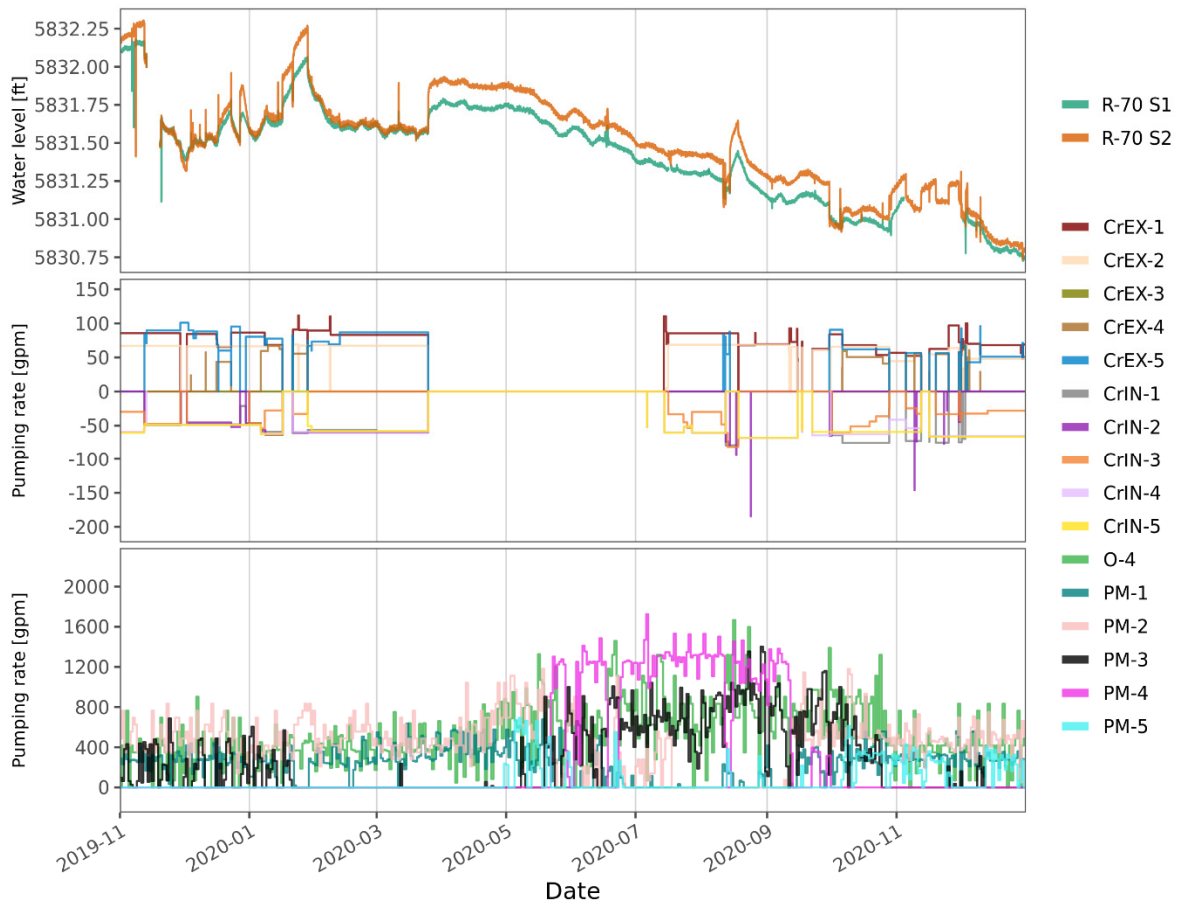
Notes: Top panel shows water-level data with the “basic” correction method described in the text. Middle panel shows CrEX-5 and CrIN-1 pumping rates (negative pumping rates represent injection). Bottom panel shows PM-3 pumping rates.

**Figure 4.1-3 Hydrograph for R-70 screen 2 from May 1 to 31, 2020**



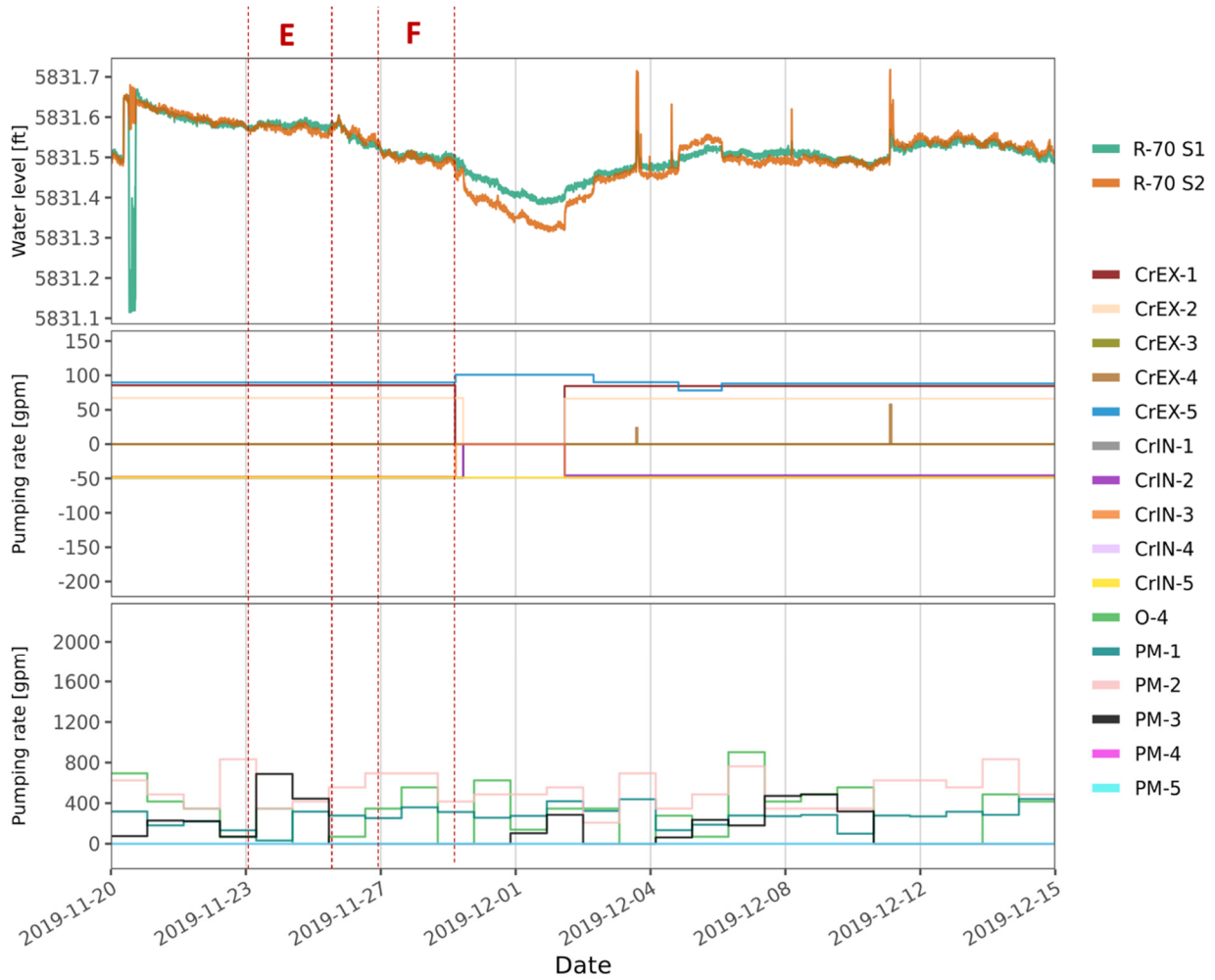
Notes: Top panel shows water-level data with the “basic” correction method described in the text. Middle panel shows CrEX and CrIN pumping rates (negative pumping rates represent injection). Bottom panel shows municipal water-supply pumping rates.

**Figure 4.1-4 Hydrograph for R-70 screen 2 from May 1 to 31, 2020, showing all nearby pumping**



Notes: Top panel shows water-level data with the “basic” correction method described in the text. Middle panel shows CrEX and CrIN pumping rates (negative pumping rates represent injection). Bottom panel shows municipal water-supply pumping rates.

**Figure 4.1-5 Hydrograph for R-70 screen 1 and screen 2 showing all nearby pumping**



Notes: Top panel shows water-level data with the “basic” correction method described in the text. Middle panel shows CrEX and CrIN pumping rates (negative pumping rates represent injection). Bottom panel shows municipal water-supply pumping rates.

**Figure 4.1-6 Hydrograph for R-70 screen 1 and screen 2 showing all nearby pumping from November 20 to December 16, 2020**

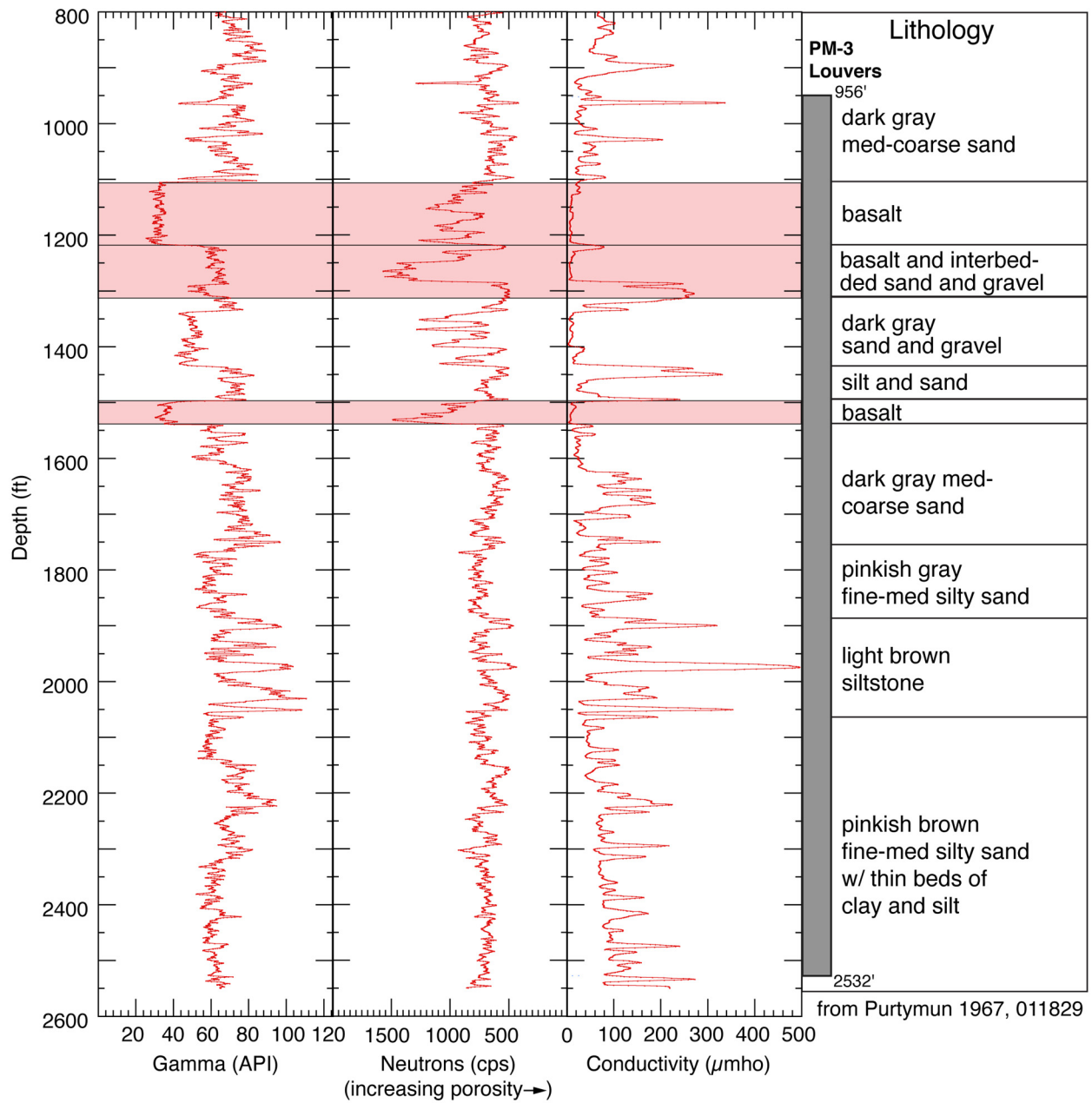


Figure 4.1-7 Geophysical logs for well PM-3

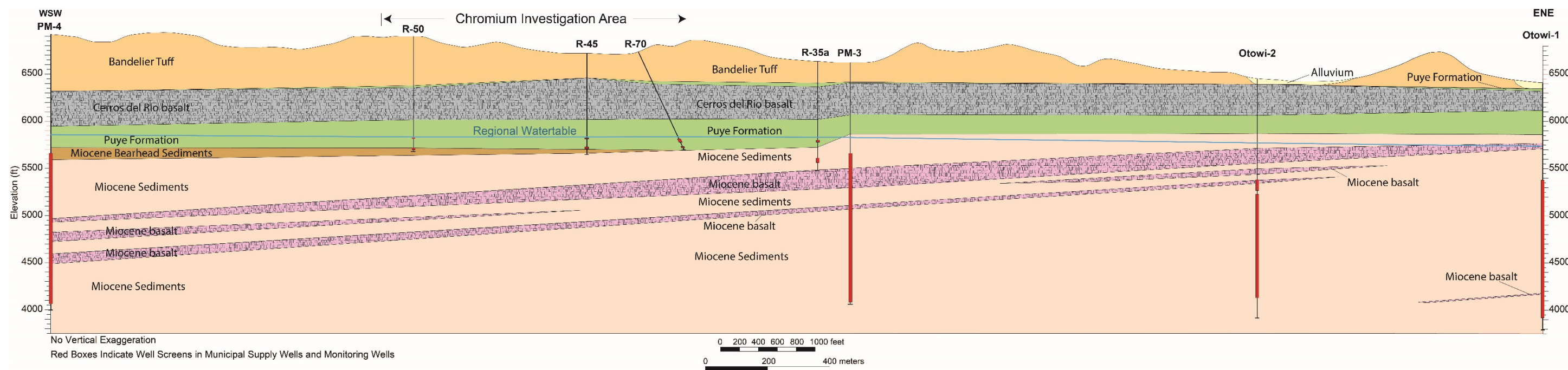
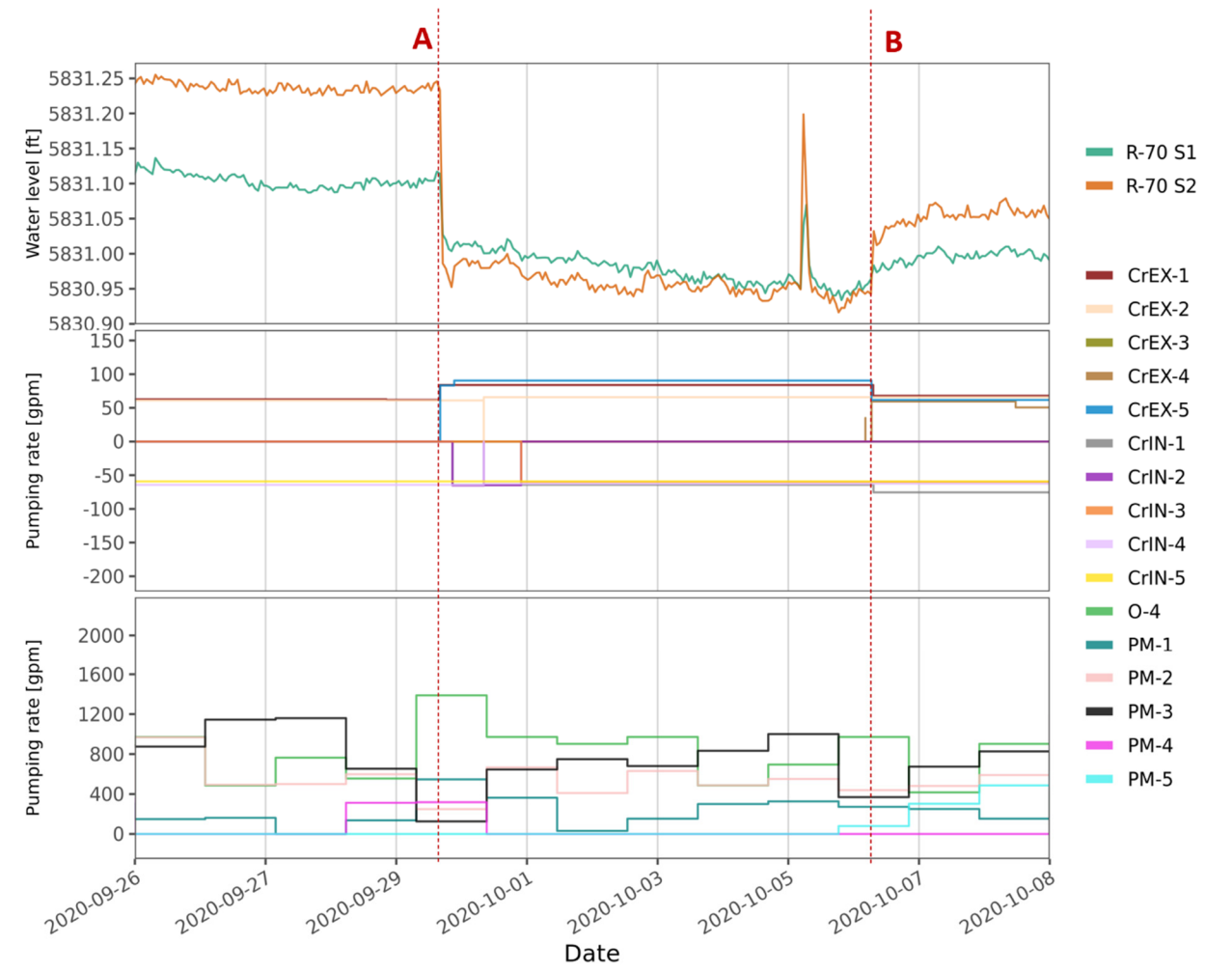
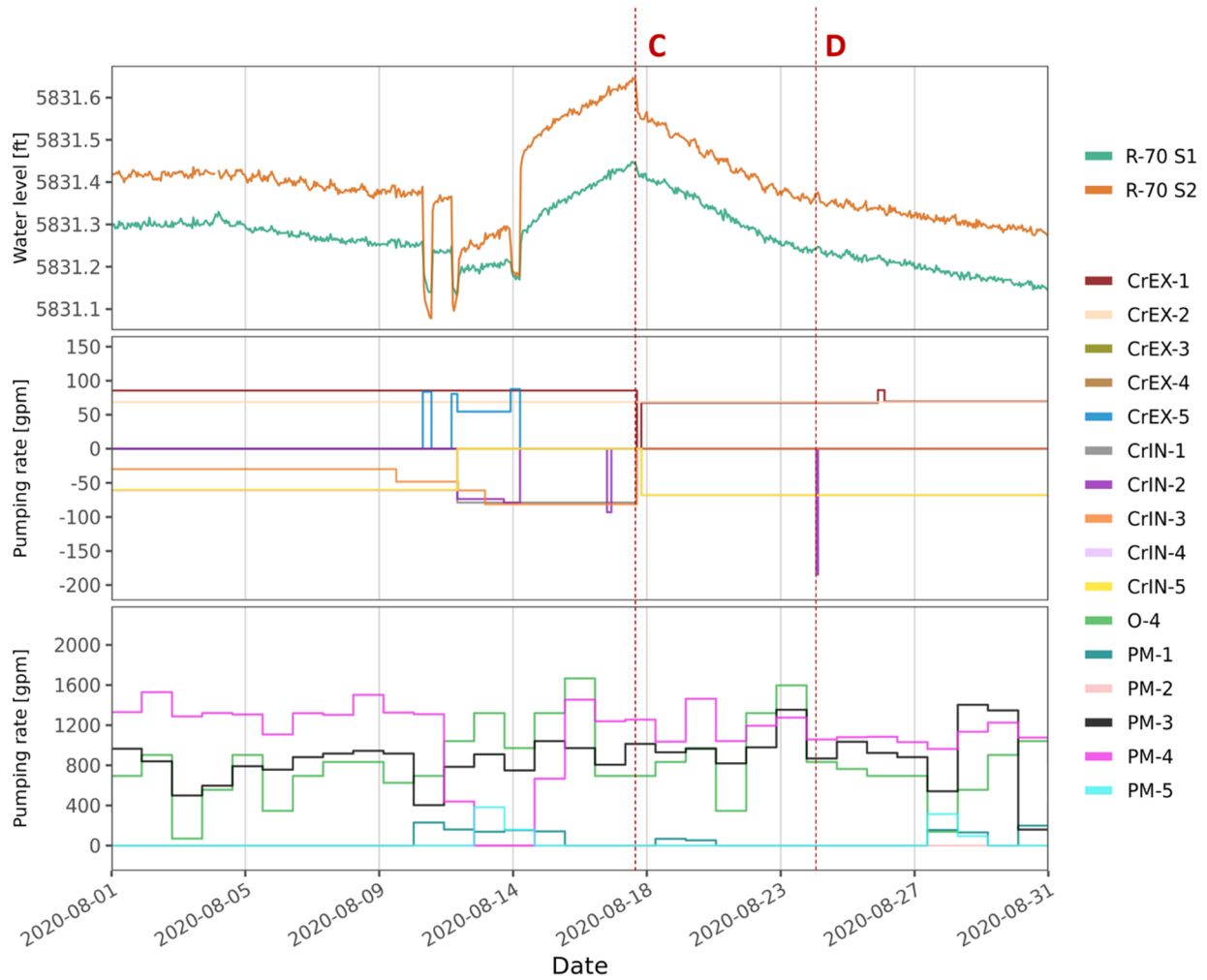


Figure 4.1-8 West-southwest/east-northeast regional geologic cross-section



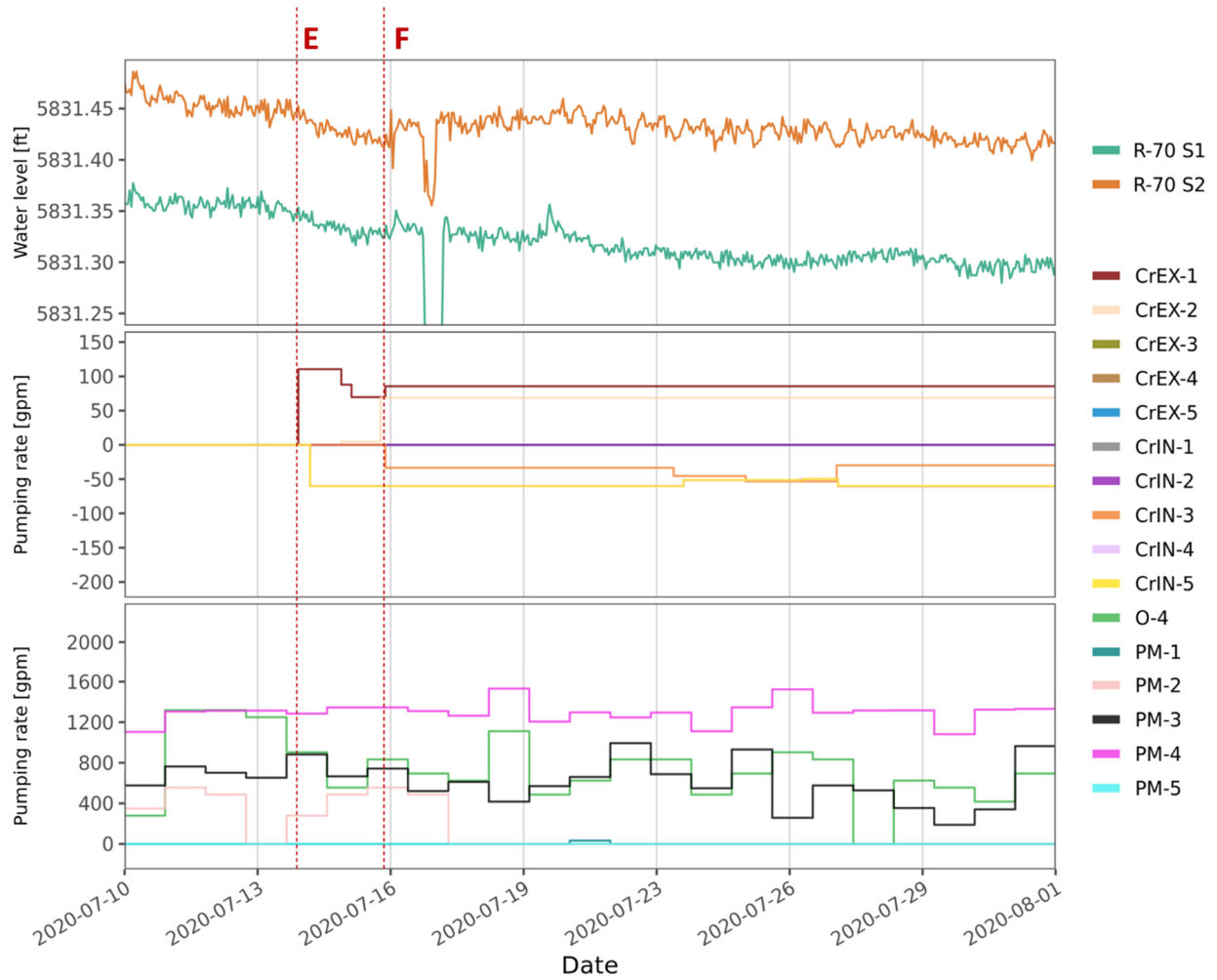
Notes: Top panel shows water-level data with the “basic” correction method described in the text. Middle panel shows CrEX and CrIN pumping rates (negative pumping rates represent injection). Bottom panel shows municipal water-supply pumping rates.

**Figure 4.1-9 Hydrograph for R-70 screen 1 and screen 2 from September 26 to October 8, 2020**



Notes: Top panel shows water-level data with the “basic” correction method described in the text. Middle panel shows CrEX and CrIN pumping rates (negative pumping rates represent injection). Bottom panel shows municipal water-supply pumping rates.

**Figure 4.1-10 Hydrograph for R-70 screen 1 and screen 2 from August 1 to 31, 2020**



Notes: Top panel shows water-level data with the “basic” correction method described in the text. Middle panel shows CrEX and CrIN pumping rates (negative pumping rates represent injection). Bottom panel shows municipal water-supply pumping rates.

**Figure 4.1-11 Hydrograph for R-70 screen 1 and screen 2 from July 10 to August 1, 2020**

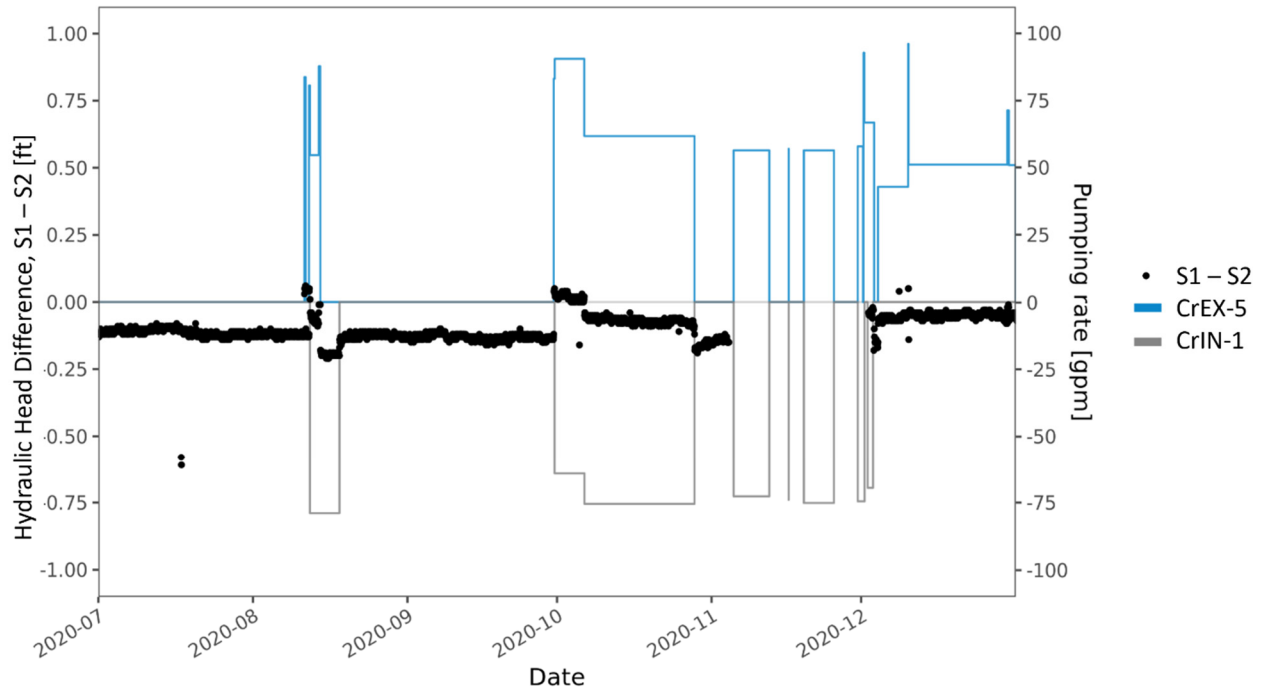
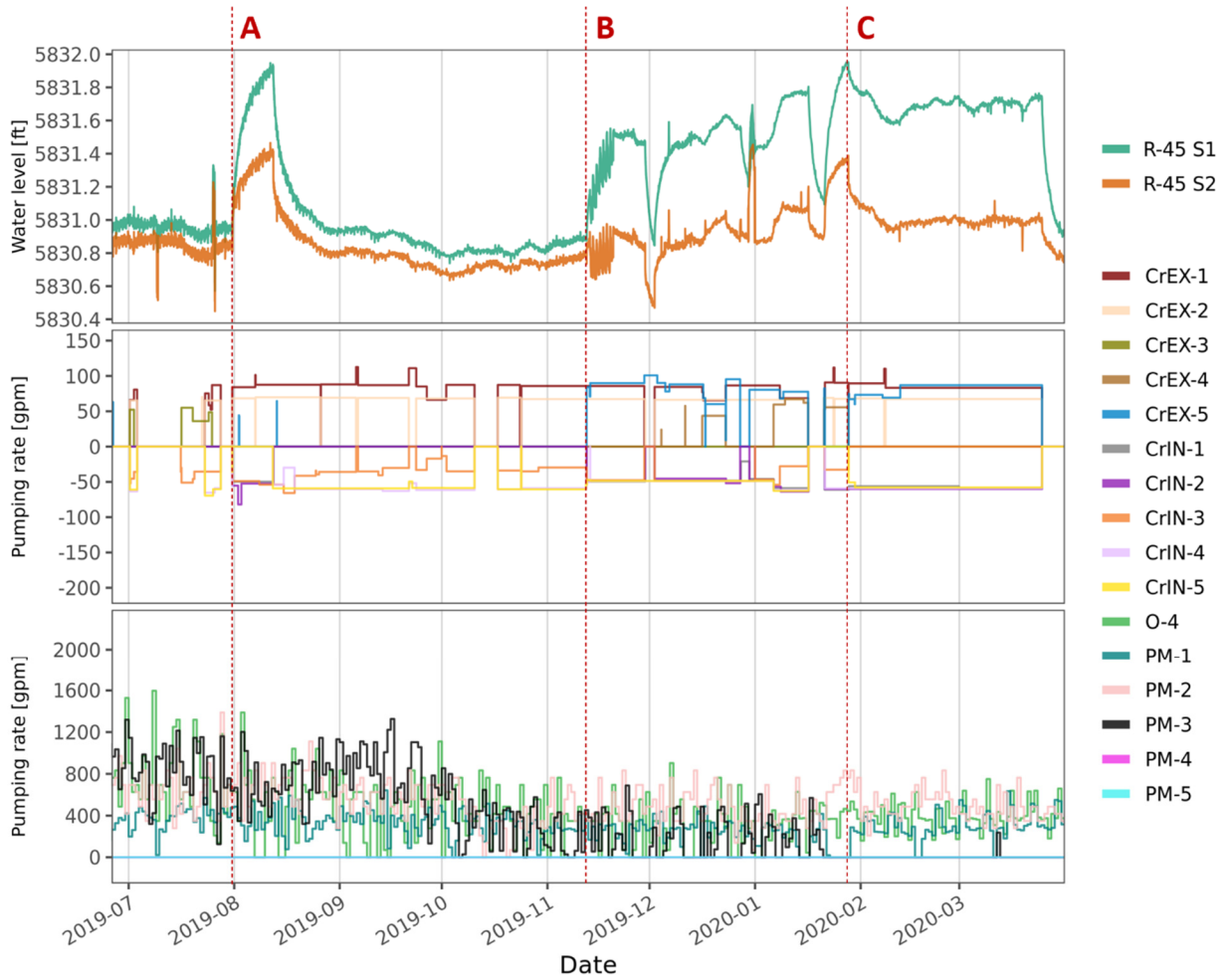


Figure 4.1-12 Hydraulic head difference between R-70 screen 1 and screen 2, along with CrEX-5 and CrIN-1 pumping rates



Notes: Top panel shows water-level data with the “basic” correction method described in the text. Middle panel shows CrEX and CrIN pumping rates (negative pumping rates represent injection). Bottom panel shows municipal water-supply pumping rates.

**Figure 4.1-13 Hydrograph for R-45 screen 1 and screen 2 from June 26, 2019, to March 31, 2020**

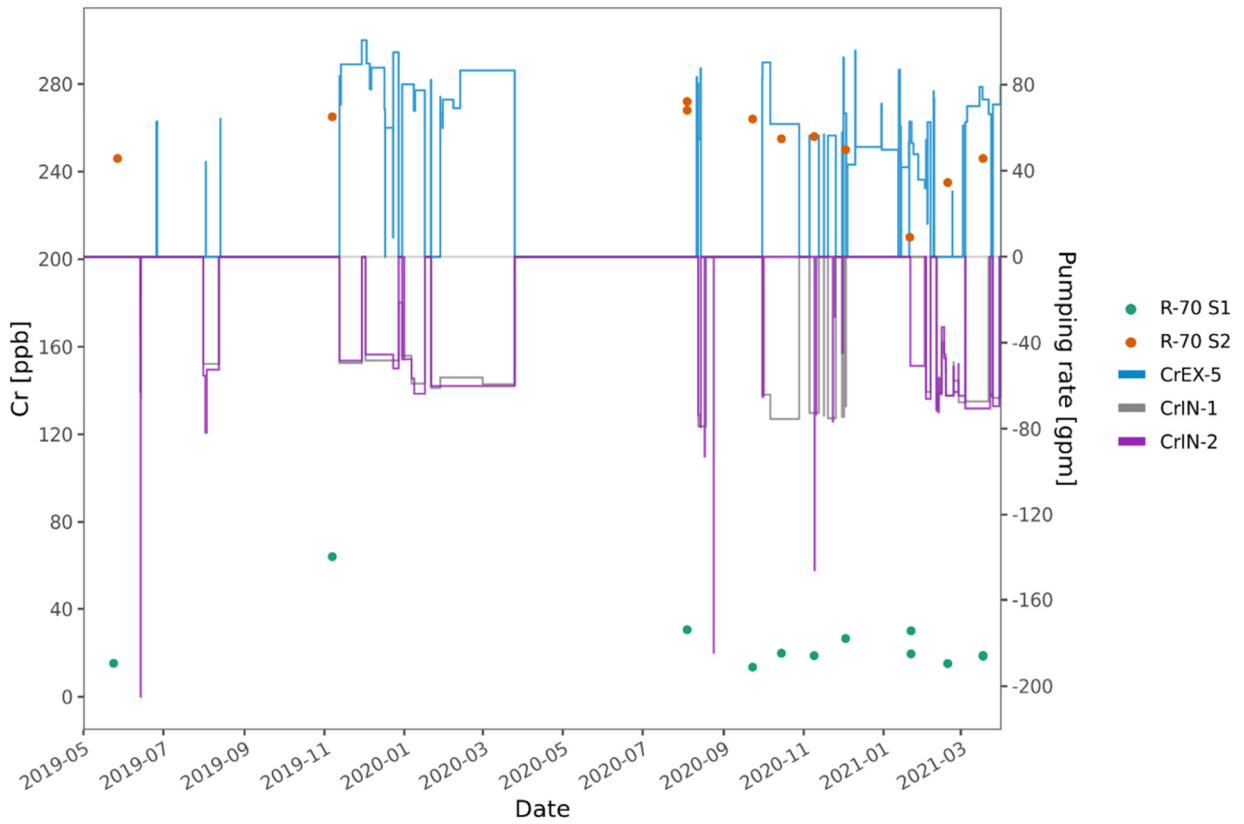
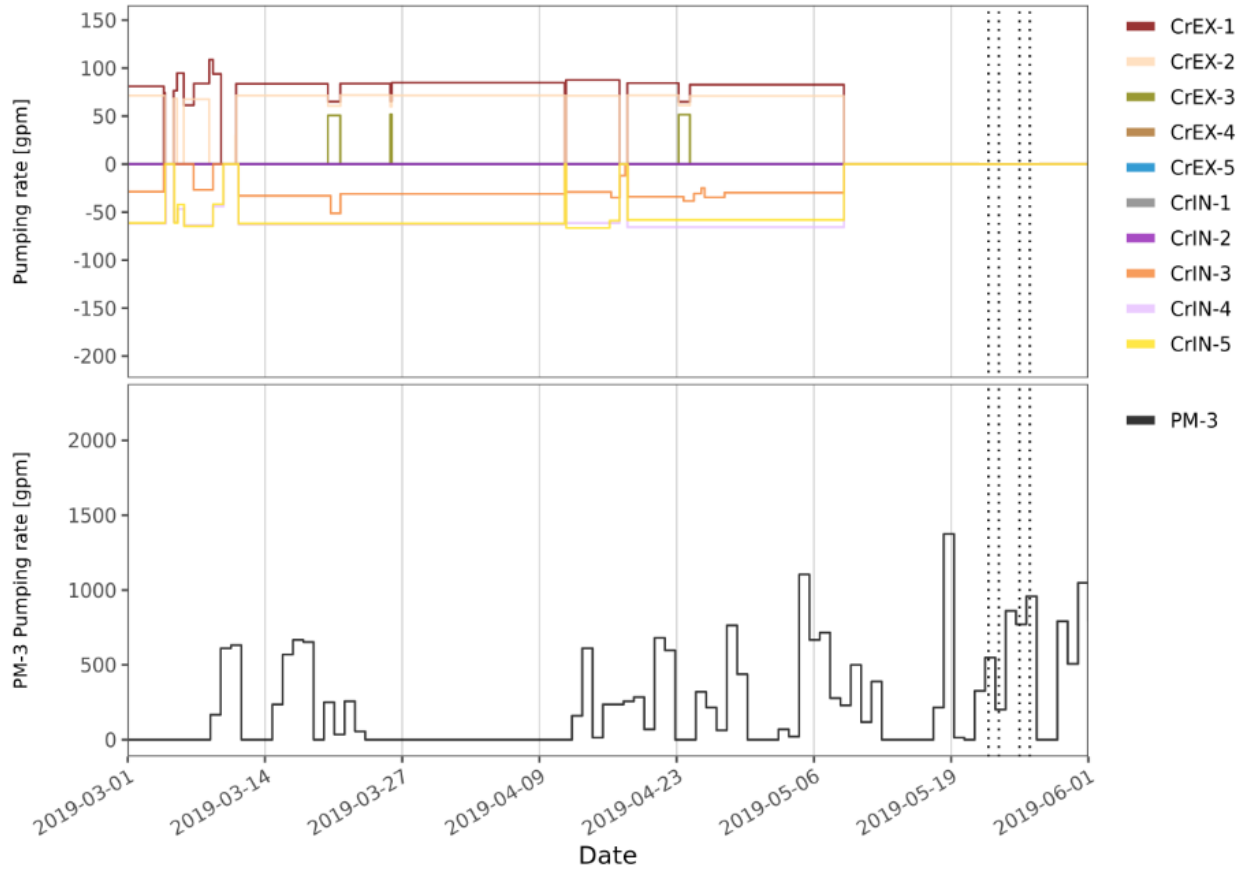


Figure 4.1-14 Chromium concentrations at R-70 screen 1 and screen 2 along with pumping rates at CrEX-5 and CrIN-1 and -2



Notes: Top panel shows CrEX and CrIN pumping rates (negative pumping rates represent injection). Bottom panel shows municipal water-supply pumping rates.

**Figure 4.1-15 IM and PM-3 activity before and during the 24-hr R-70 pumping tests (vertical dashed lines)**

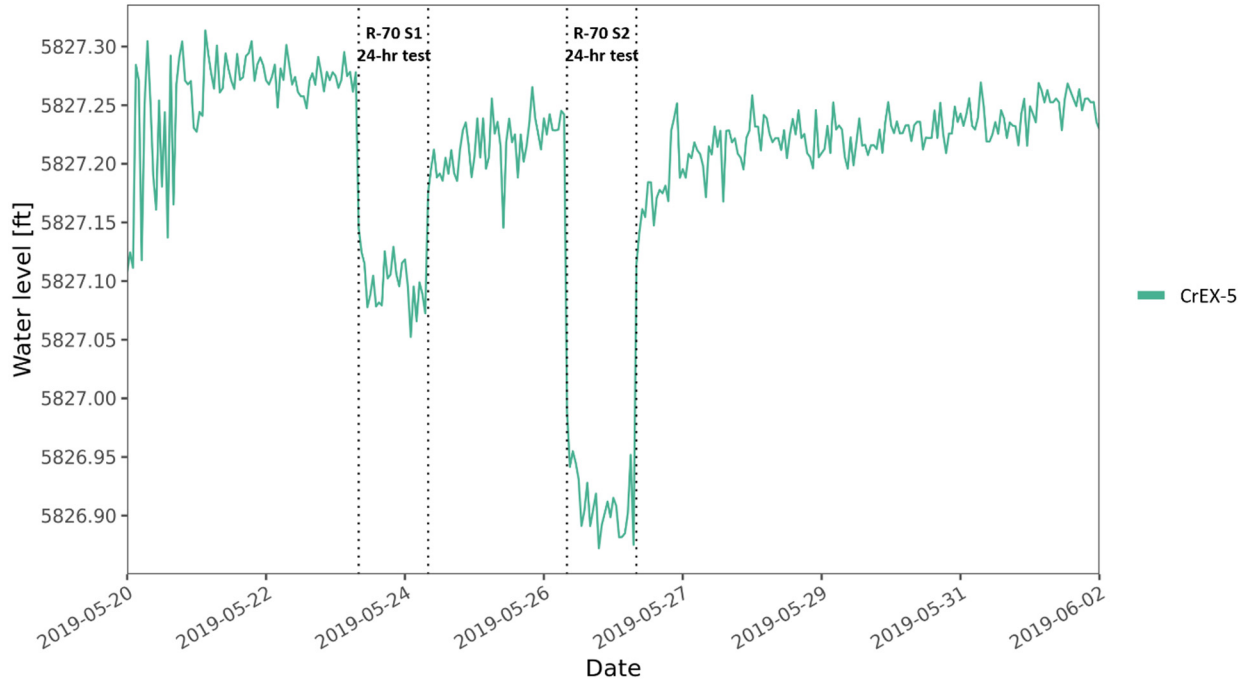


Figure 4.1-16 Hydrograph for CrEX-5 during the R-70 screen 1 and screen 2 pumping tests

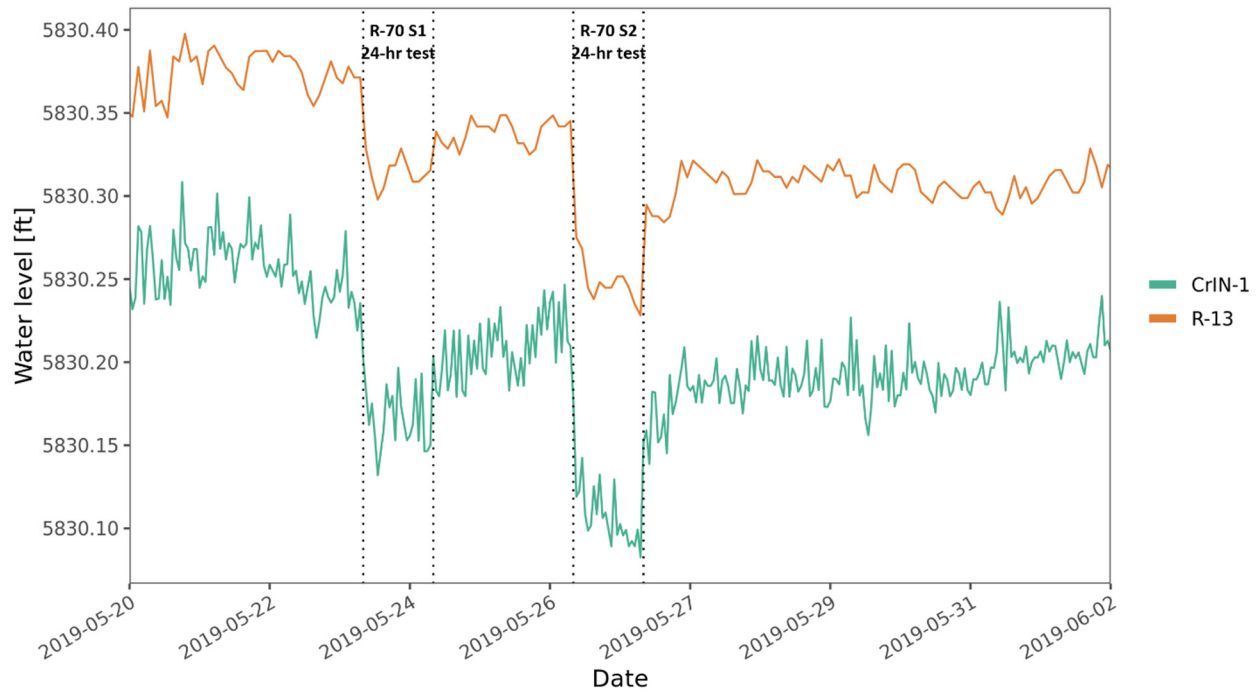
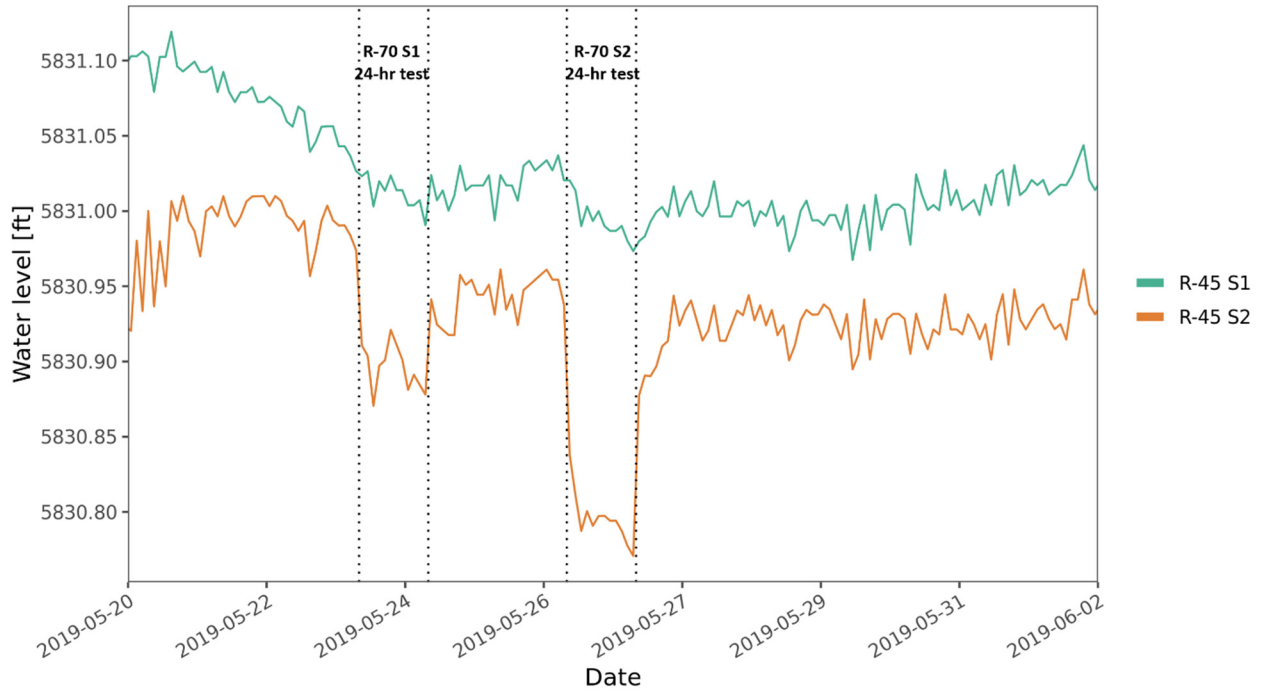
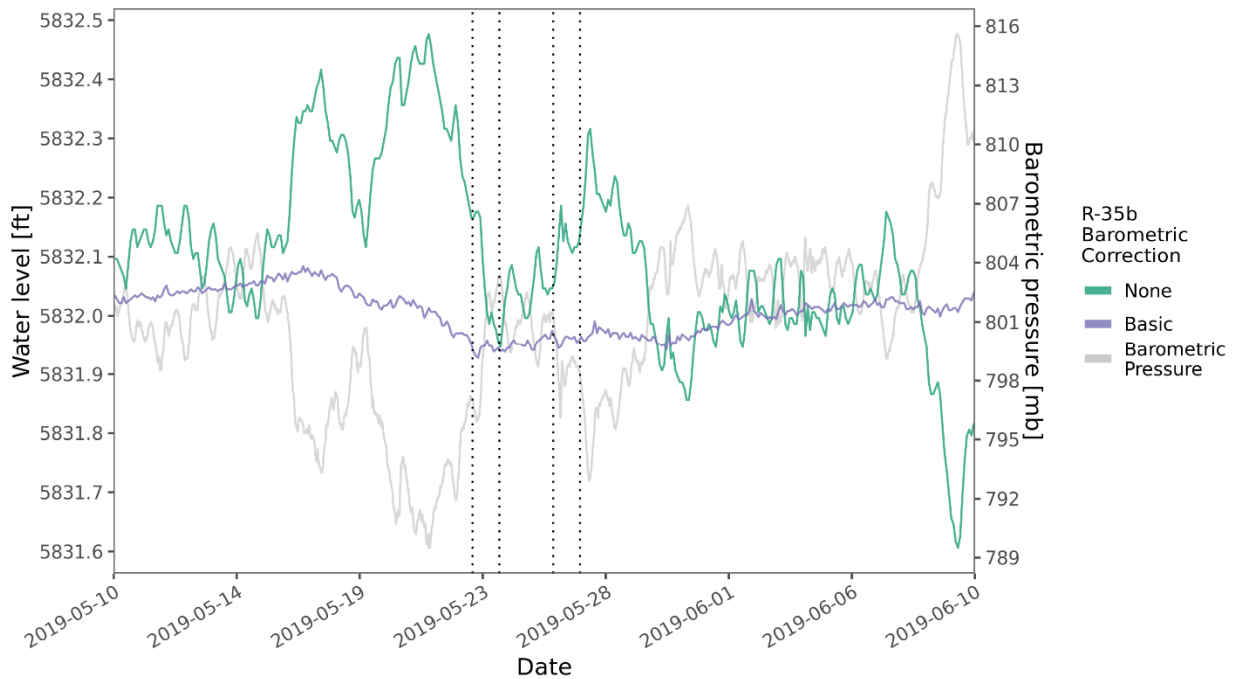


Figure 4.1-17 Hydrographs for CrIN-1 and R-13 during the R-70 screen 1 and screen 2 pumping tests



**Figure 4.1-18 Hydrographs for R-45 screen 1 and screen 2 during the R-70 screen 1 and screen 2 pumping tests**



Notes: The vertical lines indicate the R-70 screen 1 and screen 2 tests, respectively. Water levels are shown with no barometric correction and with the “basic” method applied. Barometric pressure is also shown.

**Figure 4.1-19 Hydrograph for R-35b during the R-70 screen 1 and screen 2 pumping tests**

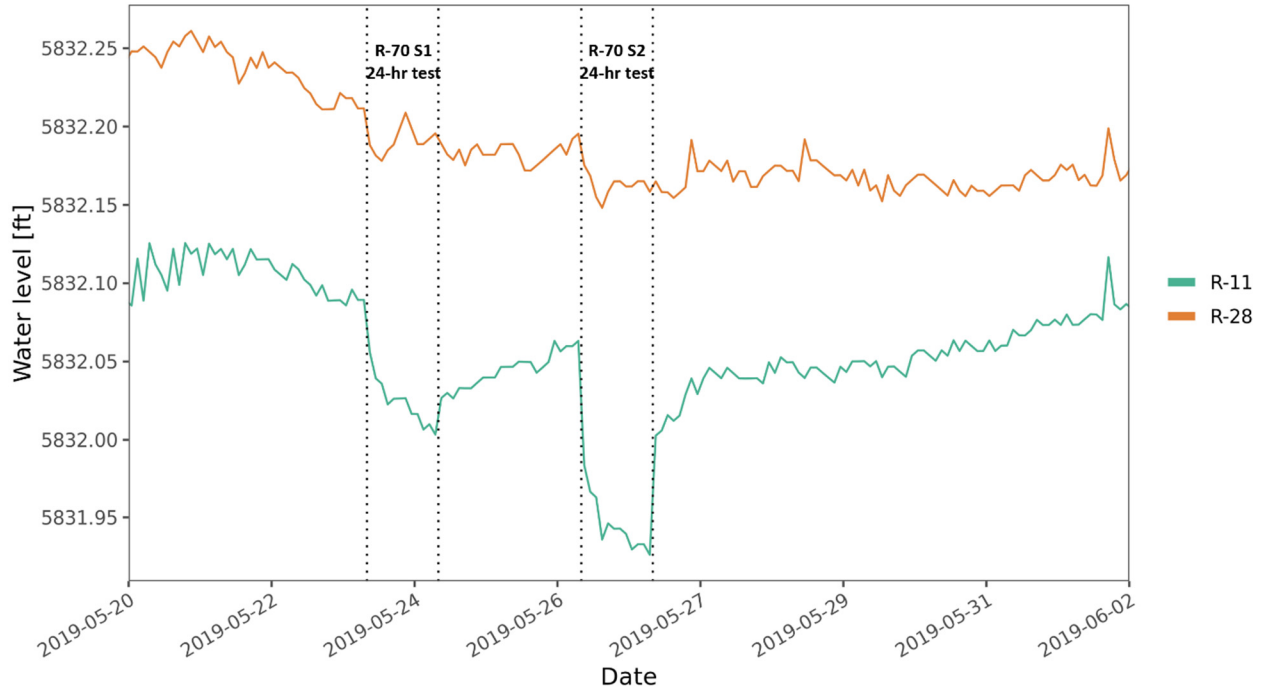


**Figure 4.1-20 Hydrographs for R-11 and R-28 during the R-70 screen 1 and screen 2 pumping tests**

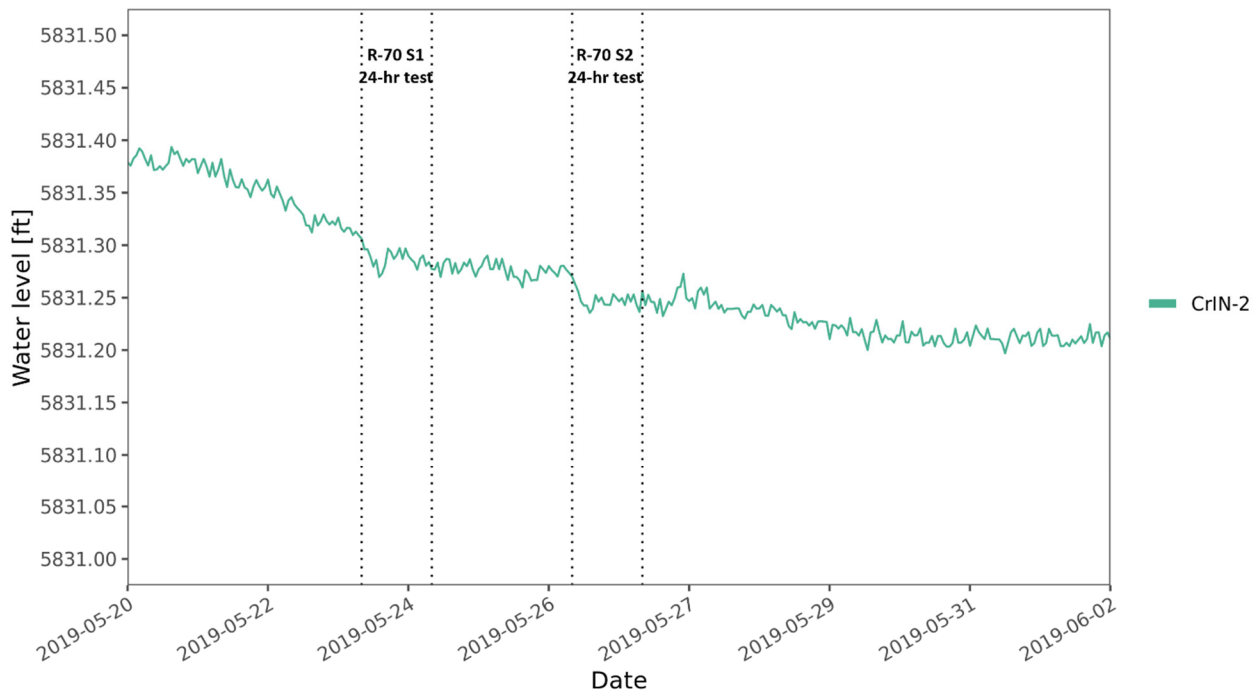


**Figure 4.1-21 Hydrograph for CrIN-2 during the R-70 screen 1 and screen 2 pumping tests**

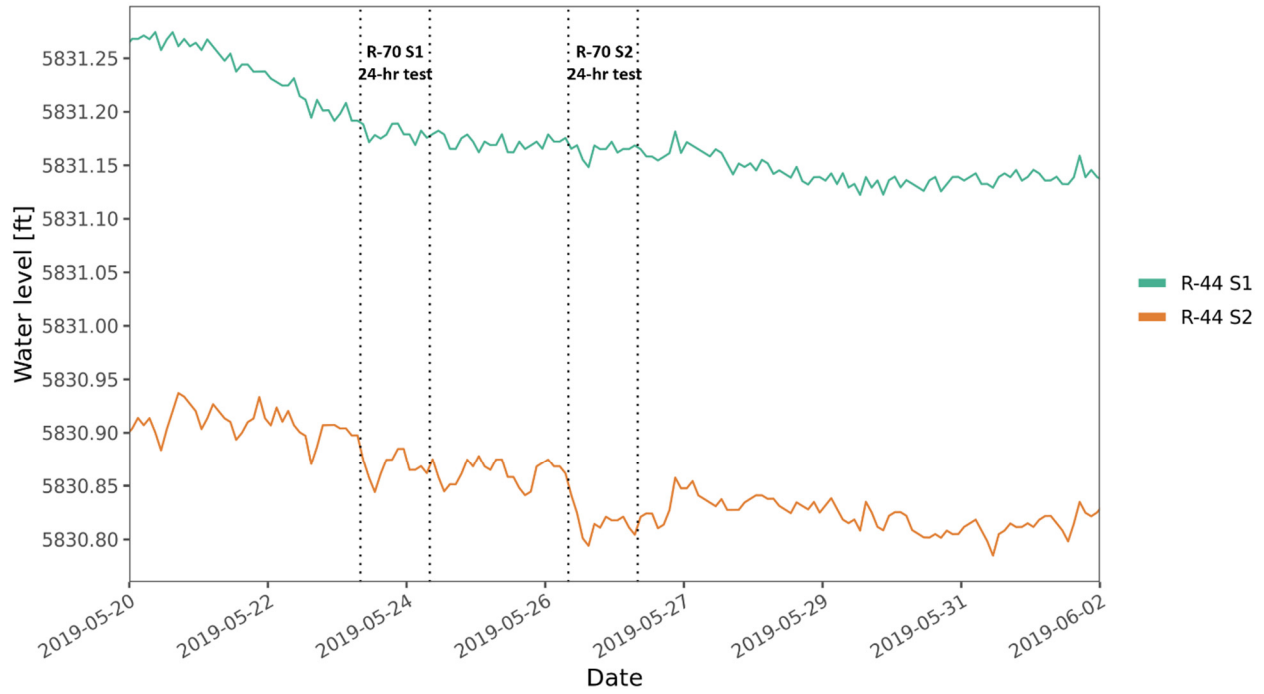


**Figure 4.1-22 Hydrographs for R-44 screen 1 and screen 2 during the R-70 screen 1 and screen 2 pumping tests**

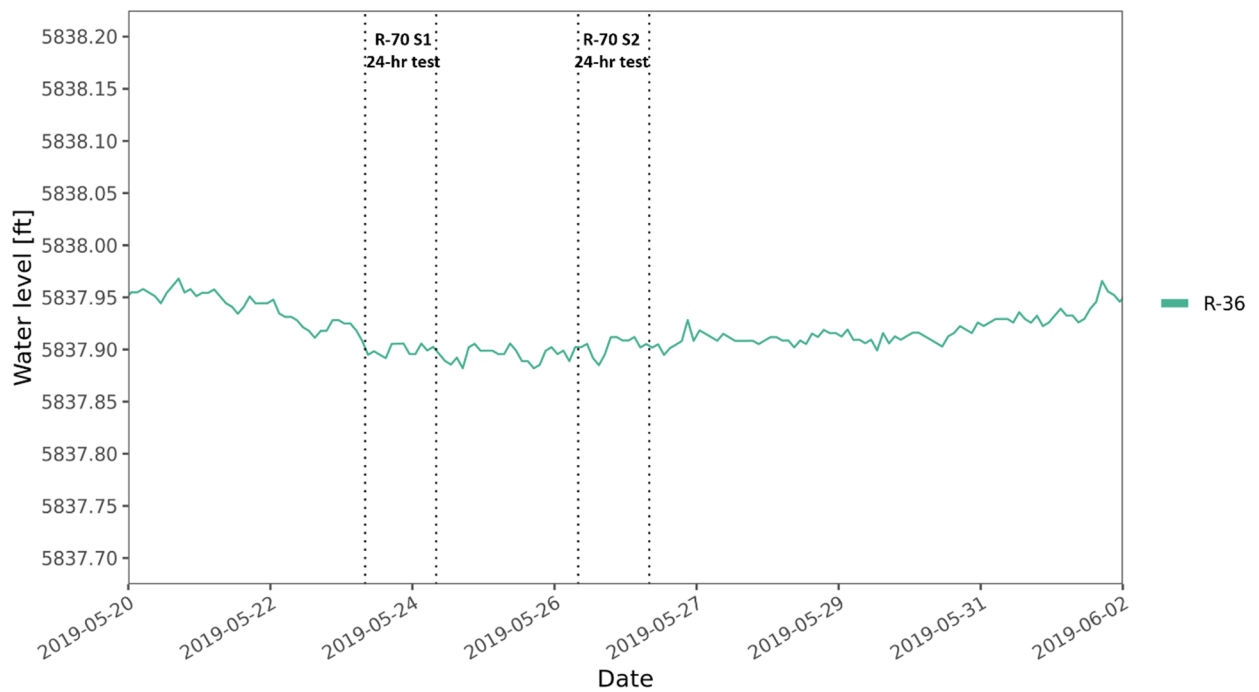


**Figure 4.1-23 Hydrograph for R-36 during the R-70 screen 1 and screen 2 pumping tests**

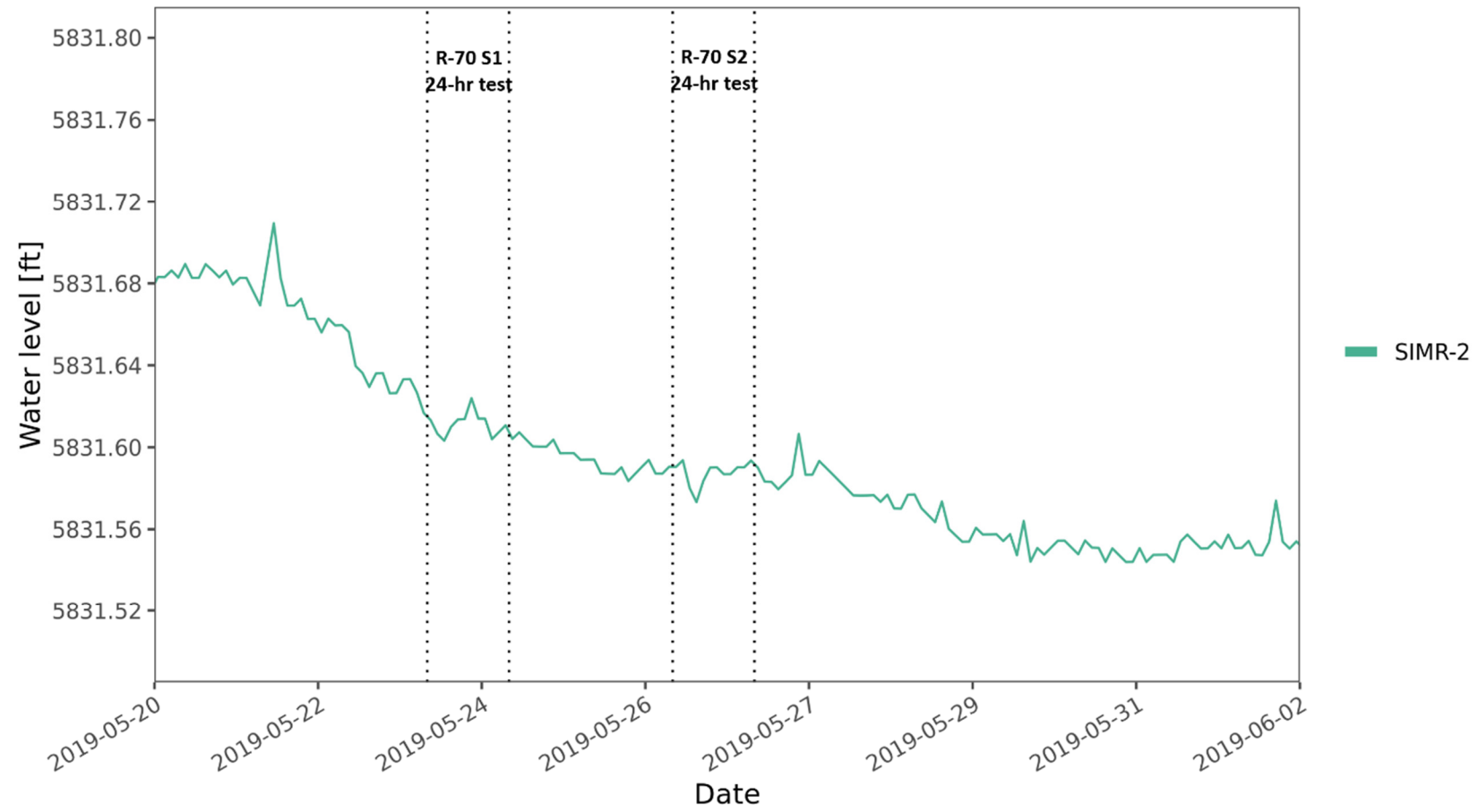


Figure 4.1-24 Hydrograph for SIMR-2 during the R-70 screen 1 and screen 2 pumping tests

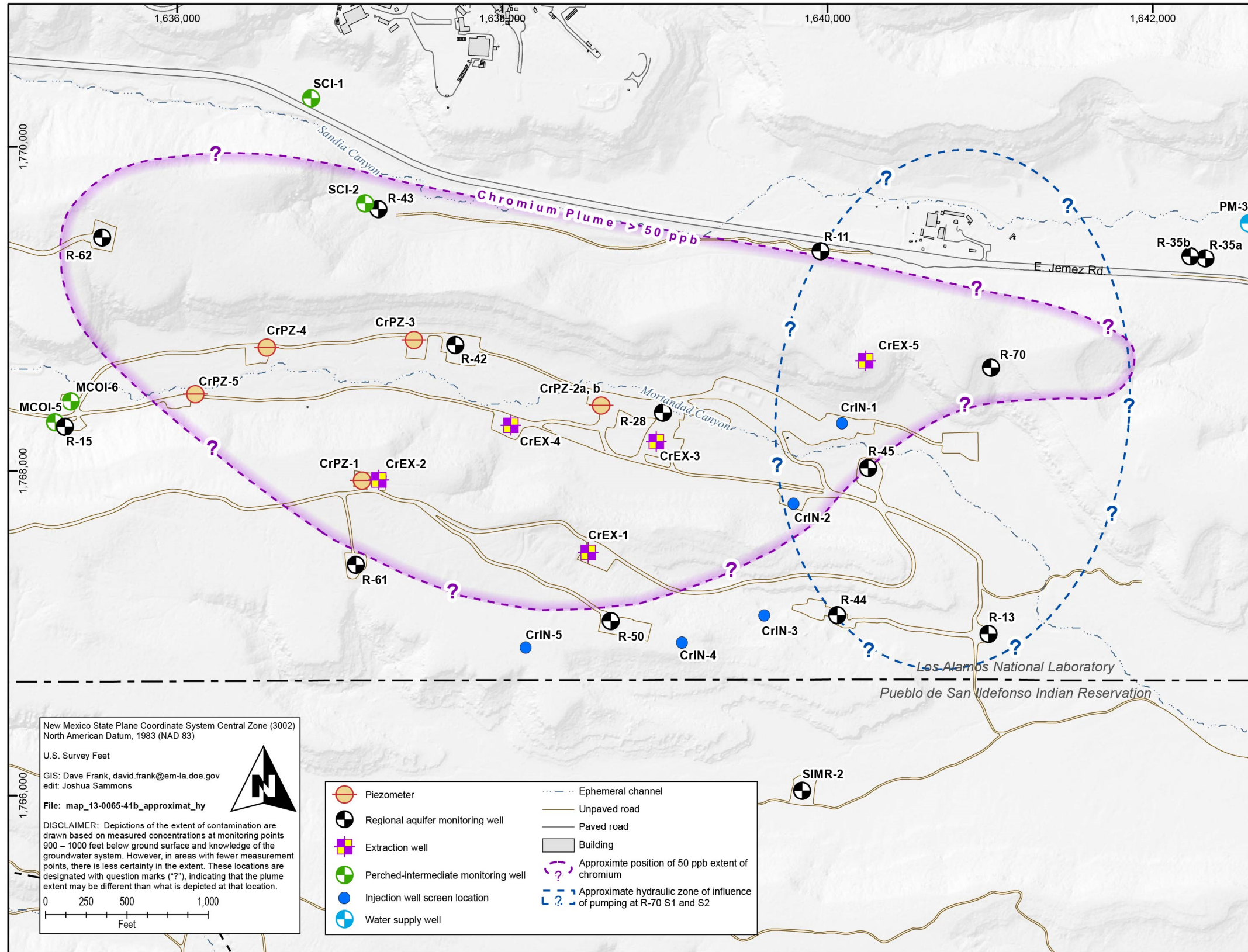


Figure 4.1-25 Approximate hydraulic zone of influence of pumping at R-70 S1 and S2

**Table 2.0-1  
Sieve Mesh-Sizes, Particle Size Distributions, and  
Particle-Size Classification for Analysis of Cores from CrCH-1 through CrCH-5**

U.S. Standard Sieve Mesh #	Fraction	Particle Size (mm)	Phi Size	Particle Size Classification
5/16 in.	1	≥8	≤-3	Pebbles and cobbles
12-5/16 in.	2	1.7-8	-0.8--3	Very coarse sand to pebbles
45-12	3	0.355-1.7	1.5--0.8	Medium to very coarse sand
80-45	4	0.177-0.355	2.5-1.5	Fine to medium sand
230-80	5	0.063-0.177	4-2.5	Very fine to fine sand
≤230	6	≤0.063	≥4	Silt
>>24 hr gravity settling	7	≤2 μm	≥9	Clay

